

AMALGAMATION IN TOTALLY NON-NEGATIVE GRASSMANNIANS AND REAL REGULAR KP DIVISORS ON M-CURVES

SIMONETTA ABENDA AND PETR G. GRINEVICH

ABSTRACT. In this paper we use the fact that every Postnikov planar bicolored (plabic) trivalent graph representing a given irreducible positroid cell $\mathcal{S}_{\mathcal{M}}^{\text{TNN}}$ in the totally non-negative Grassmannian $Gr^{\text{TNN}}(k, n)$ is dual to a rationally degenerate M-curve Γ , to provide parametrizations of $\mathcal{S}_{\mathcal{M}}^{\text{TNN}}$ in terms of real regular KP divisors in the ovals of Γ in agreement with the characterization of real regular finite-gap solutions of the Kadomtsev-Petviashvili (KP) II equation in [22]. Our construction is based on the connection established in [3, 5] between real regular finite-gap KP solutions [22] and real regular multi-line KP solitons which are known to be parametrized by points in $Gr^{\text{TNN}}(k, n)$ [16, 41]. In [3, 5] we studied such connection for Le-graphs with a fixed orientation and were not able to prove the invariance of the KP divisor with respect to the many geometric gauge freedoms on the network. Here we both extend the previous construction to any trivalent plabic graph representing the given positroid cell to which the soliton data belong to and we prove the invariance of the divisor on the choice of gauges using the space of totally non-negative relations studied in [7]. Such systems of relations were proposed in [50] in connection with the computation of scattering amplitudes on on-shell diagrams $N = 4$ SYM [10] and govern the totally non-negative amalgamation of the little positive Grassmannians, $Gr^{\text{TP}}(1, 3)$ and $Gr^{\text{TP}}(2, 3)$, into any given positroid cell $\mathcal{S}_{\mathcal{M}}^{\text{TNN}} \subset Gr^{\text{TNN}}(k, n)$. In our setting they rule the reality and regularity properties of the KP divisor.

Finally, we explain the transformation of both the curve and the divisor under Postnikov moves and reductions and apply our construction to some examples.

2010 MSC. 37K40; 37K20, 14H50, 14H70.

KEYWORDS. Totally non-negative Grassmannians, amalgamation of positroid varieties, M-curves, KP hierarchy, real soliton and finite-gap solutions, positroid cells, planar bicolored networks in the disk, moves and reductions, Baker-Akhiezer function.

CONTENTS

1. Introduction	2
2. Systems of edge vectors on PBDTP networks	7
2.1. Planar bicolored directed trivalent perfect networks in the disk (PBDTP networks)	7
2.2. Systems of edge vectors on PBDTP networks: definition and explicit representation	9
2.3. The dependence of the edge vectors on the gauge freedoms and the orientation of the network	14
2.4. Systems of relations on PBDTP networks	16
2.5. Topological characterization of the total signatures on the faces of PBDTP graphs	20
3. KP multi-line solitons in the Sato Grassmannian and in finite-gap theory	23
4. Algebraic-geometric approach for irreducible KP soliton data in $Gr^{\text{TNN}}(k, n)$	26
4.1. The reducible rational curve $\Gamma = \Gamma(\mathcal{G})$	27

This research has been partially supported by GNFM-INDAM and RFO University of Bologna, by the Russian Foundation for Basic Research, grant 17-01-00366, by the program “Fundamental problems of nonlinear dynamics”, Presidium of RAS. Partially this research was fulfilled during the visit of the second author (P.G.) to IHES, Universit Paris-Saclay, France in November 2017.

4.2. The KP divisor on $\Gamma(\mathcal{G})$ for the soliton data $(\mathcal{K}, [A])$	30
5. Construction of the KP divisor on $\Gamma(\mathcal{G})$	33
5.1. The dressed edge wave function	34
5.2. The dressed network divisor	35
6. Construction of the KP wave function $\hat{\psi}$ and characterization of the KP divisor $\mathcal{D}_{\text{KP},\Gamma}$ on Γ .	38
6.1. The KP wave function and its pole divisor	38
6.2. Combinatorial characterization of the regularity of $\mathcal{D}_{\text{KP},\Gamma}$	41
7. Amalgamation of positroid cells and divisor structure	42
8. Effect of moves and reductions on curves and divisors	46
9. Plane curves and divisors for soliton data in $\mathcal{S}_{34}^{\text{TNN}} \subset Gr^{\text{TNN}}(2, 4)$	52
9.1. Spectral curves for the reduced Le-network and their desingularizations	53
9.2. The KP divisor on $\Gamma_{T,\text{red}}$	54
9.3. The effect of Postnikov moves and reductions on the KP divisor	54
10. Effect of the square move on the KP divisor for soliton data in $Gr^{\text{TP}}(2, 4)$	56
11. Generalizations and open problems	57
11.1. Global parametrization of positroid cells via KP divisors: the case $Gr^{\text{TP}}(1, 3)$	58
11.2. Construction of the divisor in the case of zero edge vectors	59
References	61

1. INTRODUCTION

Totally non-negative Grassmannians $Gr^{\text{TNN}}(k, n)$ are a special case of the generalization to reductive Lie groups by Lusztig [52, 53] of the classical notion of total positivity [30, 31, 65, 39]. As for classical total positivity, $Gr^{\text{TNN}}(k, n)$ naturally arise in relevant problems in different areas of mathematics and physics [10, 11, 12, 15, 17, 26, 49, 60, 62, 66]. In particular, the deep connection of the combinatorial structure of $Gr^{\text{TNN}}(k, n)$ with KP real soliton theory was unveiled in a series of papers by Chakravarthy, Kodama and Williams (see [16, 40, 41] and references therein). In [40] it was proven that multi-line soliton solutions of the Kadomtsev-Petviashvili 2 (KP) equation are real and regular in space-time if and only if their soliton data correspond to points in the irreducible part of totally non-negative Grassmannians, whereas the combinatorial structure of the latter was used in [16, 41] to classify the asymptotic behavior in space-time of such solutions.

In [3, 5] we started to investigate a connection of different nature between this family of KP solutions and total positivity in the framework of the finite-gap approach, using the fact that any such solution may also be interpreted as a potential in a degenerate spectral problem for the KP hierarchy. In particular in [5], for any positroid cell $\mathcal{S}_{\mathcal{M}}^{\text{TNN}} \subset Gr^{\text{TNN}}(k, n)$, we used the fact that its Le-graph [61] is dual to an M-curve Γ of genus g equal to the dimension of $\mathcal{S}_{\mathcal{M}}^{\text{TNN}}$ to associate a degree g real regular divisor on Γ to any real regular multi-line KP soliton solution whose soliton data belong to $\mathcal{S}_{\mathcal{M}}^{\text{TNN}}$. In that paper we left open the problem of proving the invariance of the KP divisor with respect to the many gauge freedoms on the network.

Here we positively answer the question of the invariance of the KP divisor and extend such construction to the whole class of trivalent planar bicolored graphs in the disk representing $\mathcal{S}_{\mathcal{M}}^{\text{TNN}}$. We remark that our construction of real regular KP divisors on M-curves is completely explicit. At this aim we use the edge vectors solving the full rank system of relations on the network introduced in [7]. In that paper we have shown that such system of relations provides an explicit geometric representation of the amalgamation of several copies of $Gr^{\text{TP}}(1, 3)$ and $Gr^{\text{TP}}(2, 3)$ in

such a way that the total non-negativity property is preserved at each step, *i.e.* for any choice of positive edge weights the solution to the system of relations is the value of Postnikov boundary measurement map for such choice of weights. We remark that our construction of real regular KP divisors provides a new application of the amalgamation of cluster varieties introduced by Fock and Goncharov in [24] in the special case of totally non-negative Grassmannians. The connection of the system of relation to the amalgamation of cluster varieties suggests that a purely cluster algebraic approach should be possible for the characterization of the KP divisor.

Before continuing, let us briefly recall that the finite-gap approach to soliton systems was first suggested by Novikov [59] for the Korteweg-de Vries equation, and extended to the 2+1 KP equation by Krichever in [43, 44], where it was shown that finite-gap KP solutions correspond to non special divisors on arbitrary algebraic curves. Dubrovin and Natanzon [22] then proved that real regular KP finite gap solutions correspond to divisors on smooth M-curves satisfying natural reality and regularity conditions. In [46] Krichever developed, in particular, the direct scattering transform for the real regular parabolic operators associated with KP and proved that the corresponding spectral curves are always M-curves, and divisor points are located in the ovals as in [22]. In [45, 48] finite gap theory was extended to reducible curves in the case of degenerate solutions. Applications of singular curves to the finite-gap integration are reviewed in [67].

In our setting the degenerate solutions are the real regular multiline KP solitons studied in [14, 16, 40, 41]: the real regular KP soliton data correspond to a well defined reduction of the Sato Grassmannian [64], and they are parametrized by pairs $(\mathcal{K}, [A])$, *i.e.* n ordered phases $\mathcal{K} = \{\kappa_1 < \kappa_2 < \dots < \kappa_n\}$ and a point in an irreducible positroid cell $[A] \in \mathcal{S}_M^{\text{TNN}} \subset Gr^{\text{TNN}}(k, n)$. We recall that the irreducible part of $Gr^{\text{TNN}}(k, n)$ is the natural setting for the minimal parametrization of such solitons [16, 41].

Following [54], to the soliton data $(\mathcal{K}, [A])$ there is associated a rational spectral curve Γ_0 (Sato component), with a marked point P_0 (essential singularity of the wave function), and k simple real poles $\mathcal{D}_{S, \Gamma_0} = \{\gamma_{S, r}, r \in [k]\}$, such that $\gamma_{S, r} \in [\kappa_1, \kappa_n]$ (Sato divisor). However, due to a mismatch between the dimension of $Gr^{\text{TNN}}(k, n)$ and that of the variety of Sato divisors, generically the Sato divisor is not sufficient to determine the corresponding KP solution.

In [3, 5] we proposed a completion of the Sato algebraic-geometric data based on the degenerate finite gap theory of [45] and constructed divisors on reducible curves for the real regular multiline KP solitons. In our setting, the data $(\Gamma, P_0, \mathcal{D})$, where Γ is a reducible curve with a marked point P_0 , and $\mathcal{D} \subset \Gamma$ is a divisor, correspond to the soliton data $(\mathcal{K}, [A])$ if

- (1) Γ contains Γ_0 as a rational component and $\mathcal{D}_{S, \Gamma_0}$ coincides with the restriction of \mathcal{D} to Γ_0 and different rational components of Γ are connected at double points;
- (2) The data $(\Gamma, P_0, \mathcal{D})$ uniquely define the wave function $\hat{\psi}$ as a meromorphic function on $\Gamma \setminus P_0$ with divisor \mathcal{D} , having an essential singularity at P_0 . Moreover, at double points the values of the wave function coincide on both components for all times.

In degenerate cases, the construction of the components of the curve and of the divisor is obviously not unique and, as pointed out by S.P. Novikov, an untrivial question is whether **real regular** soliton solutions can be obtained as rational degenerations of **real regular** finite-gap solutions. In the case of the real regular KP multisolitons this imposes the following additional requirements:

- (1) Γ is the rational degeneration of an M-curve;
- (2) The divisor is contained in the union of the ovals.

In [3] we provided an optimal answer to the above problem for the real regular soliton data in the totally positive part of the Grassmannian, $Gr^{\text{TP}}(k, n)$. We proved that Γ_0 is a component of a reducible curve $\Gamma(\xi)$ arising as a rational degeneration of some smooth M-curve of genus

equal to the dimension of the positive Grassmannian, $k(n-k)$. We also proved that this class of real regular KP multisoliton solutions may be obtained from real regular finite-gap KP solutions, since soliton data in $Gr^{\text{TP}}(k, n)$ can be parametrized by real regular divisors on $\Gamma(\xi)$, i.e. one divisor point in each oval of $\Gamma(\xi)$ but the one containing the essential singularity of the wave function. In [3], we used classical total positivity for the algebraic part of the construction and computed explicitly the divisor positions in the ovals at leading order in ξ .

In [5] we extended the construction of [3] to the whole totally non-negative Grassmannian $Gr^{\text{TNN}}(k, n)$ using the Le-graphs introduced by Postnikov [61]. In particular, we made explicit the relation between the degenerate spectral problem associated to such family of solutions and the stratification of $Gr^{\text{TNN}}(k, n)$, by proving that the Le-graph associated to the soliton data $[A]$ is dual to a reducible spectral curve, and that the linear relations at the vertices of the Le-network uniquely identify the divisor satisfying the reality and regularity conditions established in [22]. Again our approach was constructive and in [4] we applied it to obtain real regular finite gap solutions parametrized by real regular non special divisors on a genus 4 M-curve obtained from the desingularization of spectral problem for the soliton solutions in $Gr^{\text{TP}}(2, 4)$.

In [5], we chose a specific acyclic orientation of the Le-graph in the construction and left open the question of the invariance of the construction with respect to changes of orientation and to the several gauge freedoms in the construction. Moreover, any positroid cell in a totally non-negative Grassmannian is represented by an equivalence class of plabic graphs in the disc with respect to a well-defined set of moves and reductions [61]. Therefore another set of natural questions left open in [5] was how to associate a real regular KP divisor on a curve constructed starting from a generic plabic network in the disk and to explain the transformation of such algebraic geometric data with respect to Postnikov moves and reductions.

In this paper we answer positively all such questions under some genericity assumptions. Below we outline the construction and the main results of this paper. We remark that a preliminary version of the present paper was published as a preprint [6] using systems of relations on the vertices instead than on the edges of the graph.

Main results. Let the soliton data $(\mathcal{K}, [A])$ be fixed, with $[A] \in \mathcal{S}_{\mathcal{M}}^{\text{TNN}} \subset Gr^{\text{TNN}}(k, n)$ and $\mathcal{S}_{\mathcal{M}}^{\text{TNN}}$ an irreducible positroid cell of dimension $|D|$, and let \mathcal{G} be a connected planar bicolored directed trivalent perfect (PBDTP) graph in the disk representing $\mathcal{S}_{\mathcal{M}}^{\text{TNN}}$ (Definition 2.1.3). In our setting boundary vertices are all univalent, internal sources or sinks are not allowed, internal vertices may be either bivalent or trivalent and \mathcal{G} may be either reducible or irreducible in Postnikov sense [61]. \mathcal{G} has $g+1$ faces where $g = |D|$ if the graph is reduced, otherwise $g > |D|$.

The construction of the curve Γ (Section 4.1) is analogous to that in [5] where we treated the case of Le-graphs. \mathcal{G} is the dual graph of a reducible curve Γ which is the connected union of rational components: the boundary of the disk and all internal vertices of \mathcal{G} are copies of \mathbb{CP}^1 , the edges represent the double points where two such components are glued to each other and the faces are the ovals of the real part of the resulting reducible curve. We identify the boundary of the disk with the Sato component Γ_0 , and the n boundary vertices b_1, \dots, b_n counted clockwise correspond to the ordered marked points, $\mathcal{K} = \{\kappa_1 < \kappa_2 < \dots < \kappa_n\}$. It is easy to check that Γ is a rational reduction of a smooth genus g M-curve.

To extend the wave-function from Γ_0 to Γ , we first rule its values for all times \vec{t} at the double points of the curve. Since the latter correspond to the edges of the graph, we use the full-rank system of linear relations at the vertices of \mathcal{G} introduced in [7]. As proven in [7], the requirement that the system of relations has full rank and provides the value of the boundary measurement map on $\mathcal{S}_{\mathcal{M}}^{\text{TNN}}$ fixes the system uniquely up to a simple gauge freedom which accounts for the possible choices of perfect orientations of the graph and of the gauge ray directions. Such

properties imply that, for any given soliton data and upon normalization, there is a unique edge wave function $\hat{\Psi}_e(\vec{t})$ satisfying the Sato constraints at the boundary of the disk.

In particular, thanks to the gauge invariance, it is possible to fix the geometric gauge by fixing both the orientation of the graph and the gauge ray direction and explicitly solve the system of relations in terms of edge and of conservative flows [68, 7] so to compute explicitly also the KP divisor in the coordinates associated to such orientation. In Section 6 we assign the value $\hat{\Psi}_e(\vec{t})$ to the corresponding double points $P_e, Q_e \in \Gamma$ and then extend the wave function to the component $\Gamma_V \subset \Gamma$ corresponding to the internal vertex V as follows. If V is a black vertex or bivalent white vertex then, for any fixed \vec{t} , $\hat{\Psi}$ takes the same value at all edges at V ; therefore it is natural to extend the wave function on Γ_V to a function $\hat{\psi}(P, \vec{t})$ constant with respect to the spectral parameter P in such case. On the contrary, $\hat{\Psi}(\vec{t})$ generically takes real distinct values at the edges at a trivalent white vertex V ; therefore we may extend it to a degree one meromorphic function $\hat{\psi}(P, \vec{t})$, $P \in \Gamma_V$ such that its pole P_V has real coordinate γ_V .

The KP divisor on Γ is then $\mathcal{D}_{\text{KP}, \Gamma} = \mathcal{D}_{\text{S}, \Gamma_0} \cup \{P_V, V \text{ white trivalent vertex in } \mathcal{G}\}$, where $\mathcal{D}_{\text{S}, \Gamma_0}$ is the degree k Sato divisor. Since the number of trivalent white vertices of a PBDTP graph is $g - k$, $\mathcal{D}_{\text{KP}, \Gamma}$ has degree g and by construction it is contained in the union of the ovals of Γ . $\hat{\psi}(P, \vec{t})$ is the unique meromorphic function on $\Gamma \setminus \{P_0\}$ and divisor $\mathcal{D}_{\text{KP}, \Gamma}$, that is $(\hat{\psi}(\cdot, \vec{t})) + \mathcal{D}_{\text{KP}, \Gamma} \geq 0$, for all \vec{t} , therefore $\hat{\psi}$ is the wave function on Γ for the soliton data $(\mathcal{K}, [A])$ (Theorem 6.1.3).

By construction $\mathcal{D}_{\text{KP}, \Gamma}$ is invariant with respect to changes of orientation and of the choice of gauge ray, weight and vertex gauges (Theorem 6.1.2). In Lemma 6.1.1 we use the half-edge wave function to detect the oval to which each divisor point P_V belongs to, whereas in Section 6.2 we use the topological characterization of signatures of faces (Theorem 2.5.1) to prove that each finite oval contains exactly one divisor point, i.e. $\mathcal{D}_{\text{KP}, \Gamma}$ satisfies the reality and regularity conditions established in [22]. As a consequence, we obtain a direct relation between the total non-negativity property encoded in the geometrical setting [7] and the reality and regularity condition of the divisor studied in this paper.

Since the system of relations has a geometric interpretation as amalgamation of the little positive Grassmannians, in Section 7 we explain the effect of the direct summation and defrosting of positroid cells on the corresponding admissible real and regular divisors.

In Section 8 we give the explicit transformation rules of the curve, the edge vectors and the divisor with respect to Postnikov moves and reductions. We also present some examples. In Section 9 we apply our construction to soliton data in $\mathcal{S}_{34}^{\text{TNN}}$, the 3-dimensional positroid cell in $Gr^{\text{TNN}}(2, 4)$ corresponding to the matroid $\mathcal{M} = \{12, 13, 14, 23, 24\}$. We construct both the reducible rational curve and its desingularization to a genus 3 M-curve and the KP divisor for generic soliton data $\mathcal{K} = \{\kappa_1 < \kappa_2 < \kappa_3 < \kappa_4\}$ and $[A] \in \mathcal{S}_{34}^{\text{TNN}}$. We then apply a parallel edge unredution and a flip move and compute the divisor on the transformed curve. We also show the effect of the square move on the divisor for soliton data $(\mathcal{K}, [A])$ with $[A] \in Gr^{\text{TP}}(2, 4)$ in Section 10.

Remarks and open questions. In Section 11 we briefly address the following open questions, leaving their thorough discussion to a future publication. If the graph \mathcal{G} is reduced, as a byproduct, we get a local parametrization of positroid cells in terms of non-special divisors. We remark that the map from the weights - parametrizing the cell - to the divisor is birational for any fixed time, and loses maximal rank and injectivity along certain subvarieties of the positroid cell where the divisor becomes special. We plan to discuss the question of the global parametrization of positroid cells via KP real regular KP divisors in a future work and we present the resolution of singularities for the case $Gr^{\text{TP}}(1, 3)$ in Section 11.1 as a starting example.

In the case of reducible graphs, the divisor depends on extra freedom in the assignment of the edge weights (see Remark 11.2.1 for an example) and the appearance of null edge vectors in the solution to the system of relations imposes a modification to the construction of both the curve and of the divisor briefly outlined in Section 11.2.

Below we list few more open questions.

Our construction may be considered as a tropicalization of the spectral problem (smooth M -curves and divisors) associated to real regular finite-gap KP solutions (potentials) in the rational degeneration of such curves. An interesting open question is whether all smooth M -curves may be obtained starting from our construction.

The tropical limit studied in [41] (see also [19] for a special case) has a different nature: reconstruct the soliton data from the asymptotic contour plots. In our setting, that would be equivalent to tropicalize the reducible rational spectral problem connecting the asymptotic behavior of the potential (KP solution) to the asymptotic behavior in \bar{t} of the zero divisor of the KP wave function (see [2] for some preliminary results concerning soliton data in $Gr^{\text{TP}}(2, 4)$). Relations between integrability and cluster algebras were demonstrated in [23, 35], and the cluster algebras were essentially motivated by total positivity [27, 28]. In [41] cluster algebras have appeared in connection with KP solitons asymptotic behavior. We expect that they should also appear in our construction in connection with the tropicalization of the zero divisor. Moreover a deep relation of (degenerate) KP solutions with cluster algebras is also suggested by the fact that the geometric systems of relations which encode the position of the divisor have a natural interpretation as amalgamation of small positive Grassmannians respecting total non-negativity [24, 50, 7].

For a fixed reducible curve the Jacobian may contain more than one connected component associated to real regular solutions. Therefore, in contrast with the smooth case, different connected components may correspond to different Grassmannians. Some of these components may correspond not to full positroid cells, but to special subvarieties. For generic curves the problem of describing these subvarieties is completely open. For a rational degeneration of genus $(n - 1)$ hyperelliptic M -curves this problem was studied in [1] and it was shown that the corresponding soliton data in $Gr^{\text{TP}}(k, n)$ formed $(n - 1)$ -dimensional varieties known in literature [13] to be related to the finite open Toda system. The same KP soliton family has been recently re-obtained in [57] in the framework of the Sato Grassmannian, whereas the spectral data for the finite Toda was studied earlier in [48].

Moreover, all results valid in the KP hierarchy also go through for its reductions such as the KdV and the Boussinesq hierarchies. Therefore a natural question is to classify the subvarieties in $Gr^{\text{TP}}(k, n)$ associated to such relevant reductions. At this aim it could be fruitful to establish a connection with the approach in [42] for complex KP soliton solutions.

In [4] we studied in details the transition from multiline soliton solutions to finite-gap solutions associated to almost degenerate M -curves in the first non-trivial case, and in [5] we provided a generic construction. We expect that the coordinates on the moduli space, compatible with M -structure, introduced in [47], may be useful in this study.

It is an open problem whether all real and regular divisor positions in the ovals are realizable as the soliton data vary in $\mathcal{S}_{\mathcal{M}}^{\text{TP}}$ for a given normalizing time \bar{t}_0 . The latter problem is naturally connected to the classification of realizable asymptotic soliton graphs studied in [41].

Finally, similar gluing problems of little Grassmannians expressed as compatibility of linear systems at vertices respecting the total positivity property appear also in several different problems, such as the momentum-helicity conservation relations in the on-shell amplituhedron problem for the $N = \text{SYM}$ in [10, 11, 50] and the geometry of polyhedral subdivisions [62, 63]. It is unclear to us whether and how our approach for KP may be related to these questions.

Plan of the paper: We did our best to make the paper self-contained. In Section 2 we briefly summarize the properties of the systems of edge vectors on PBDTP networks following [7], whereas in Section 3, we briefly present some results of KP soliton theory necessary in the rest of the paper. Section 4 contains the main construction and the statements of the principal theorems. Sections 5 and 6 contain the proofs of the main theorems together with the explicit construction of the wave function and of the real regular divisor on the reducible regular curve. In particular, in Section 7 we discuss how the admissible divisor structure changes due to amalgamation. In Section 8 we explain how edge vectors depend on Postnikov moves and reductions and characterize the dependence of the divisors on moves and reductions. Sections 9 and 10 contain several examples and applications from the previous sections.

Notations: We use the following notations throughout the paper:

- (1) k and n are positive integers such that $k < n$;
- (2) For $s \in \mathbb{N}$ let $[s] = \{1, 2, \dots, s\}$; if $s, j \in \mathbb{N}$, $s < j$, then $[s, j] = \{s, s+1, s+2, \dots, j-1, j\}$;
- (3) $\vec{t} = (t_1, t_2, t_3, \dots)$ is the infinite vector of real KP times where $t_1 = x$, $t_2 = y$, $t_3 = t$, and we assume that only a finite number of components are different from zero;
- (4) We denote $\theta(\zeta, \vec{t}) = \sum_{s=1}^{\infty} \zeta^s t_s$, due to the previous remark $\theta(\zeta, \vec{t})$ is well-defined for any complex ζ ;
- (5) We denote the real KP phases $\kappa_1 < \kappa_2 < \dots < \kappa_n$ and $\theta_j \equiv \theta(\kappa_j, \vec{t})$.

2. SYSTEMS OF EDGE VECTORS ON PBDTP NETWORKS

In this Section we define the class of graphs \mathcal{G} used throughout the text and recall the definition and properties of the systems of edge vectors following [7]. In Section 2.5 we provide a topological characterization of the edge signatures introduced in [7].

The results of this Section are used throughout the paper. Indeed, the KP soliton data are points of irreducible positroid cells $\mathcal{S}_{\mathcal{M}}^{\text{TNN}} \subset Gr^{\text{TNN}}(k, n)$. In our construction, the plabic graph \mathcal{G} representing $\mathcal{S}_{\mathcal{M}}^{\text{TNN}}$ is dual to a reducible M-curve. A necessary requirement for the regularity of the KP wave function is that it takes equal values at pairs of glued points in Γ for all times. Using the correspondence of double points on Γ to edges of \mathcal{G} , we use the n -edge vectors constructed in this Section to rule the values of the KP wave-function at such points and then extend it to a meromorphic function on the whole Γ . The system of relations satisfied by the edge vectors rules the position of the KP divisor in the ovals, and the combinatorial proof of the reality and regularity properties of the KP divisor follows from the topological characterization of the geometric signature in Section 2.5.

2.1. Planar bicolored directed trivalent perfect networks in the disk (PBDTP networks).

Definition 2.1.1. Totally non-negative Grassmannian [61]. Let $Mat_{k,n}^{\text{TNN}}$ denote the set of real $k \times n$ matrices of maximal rank k with non-negative maximal minors $\Delta_I(A)$. Let GL_k^+ be the group of $k \times k$ matrices with positive determinants. Then the totally non-negative Grassmannian $Gr^{\text{TNN}}(k, n)$ is

$$Gr^{\text{TNN}}(k, n) = GL_k^+ \backslash Mat_{k,n}^{\text{TNN}}.$$

In the theory of totally non-negative Grassmannians an important role is played by the positroid stratification. Each cell in this stratification is defined as the intersection of a Gelfand-Serganova stratum [34, 33] with the totally non-negative part of the Grassmannian. More precisely:

Definition 2.1.2. Positroid stratification [61]. Let \mathcal{M} be a matroid i.e. a collection of k -element ordered subsets I in $[n]$, satisfying the exchange axiom (see, for example [34, 33]). Then the positroid cell $\mathcal{S}_{\mathcal{M}}^{TNN}$ is defined as

$$\mathcal{S}_{\mathcal{M}}^{TNN} = \{[A] \in Gr^{TNN}(k, n) \mid \Delta_I(A) > 0 \text{ if } I \in \mathcal{M} \text{ and } \Delta_I(A) = 0 \text{ if } I \notin \mathcal{M}\}.$$

A positroid cell is irreducible if, for any $j \in [n]$, there exist $I, J \in \mathcal{M}$ such that $j \in I$ (absence of isolated boundary sinks) and $j \notin J$ (absence of isolated boundary sources).

The combinatorial classification of all non-empty positroid cells and their rational parametrizations were obtained in [61], [68]. In our construction we use the classification of positroid cells via directed planar networks in the disk in [61]. Irreducible positroid cells play the relevant role in the applications to real regular KP soliton solutions, since they provide the minimal realization of such solutions in totally non-negative Grassmannians [16, 41] (see also Section 3).

In the following we restrict ourselves to **irreducible positroid cells** $\mathcal{S}_{\mathcal{M}}^{TNN}$ and we consider planar bicolored directed trivalent perfect graphs in the disk (PBDTP graphs) representing $\mathcal{S}_{\mathcal{M}}^{TNN}$ which satisfy the following additional assumption (Item 7 in the definition below): for any internal edge e there exists a directed path containing e and starting at a boundary source and ending at a boundary sink. Such assumption is essential to guarantee that amalgamation of the little positive Grassmannians $Gr^{TP}(1, 3)$ and $Gr^{TP}(2, 3)$ preserving the total non-negativity is fully controlled by geometric signatures and that all signatures compatible with the total non-negative property are of geometric type.

More precisely, we consider the following class of graphs \mathcal{G} :

Definition 2.1.3. Planar bicolored directed trivalent perfect graphs in the disk (PBDTP graphs). A graph \mathcal{G} is called PBDTP if:

- (1) \mathcal{G} is planar, directed and lies inside a disk. Moreover \mathcal{G} is connected in the sense that it does not possess components isolated from the boundary;
- (2) It has finitely many vertices and edges;
- (3) It has n boundary vertices on the boundary of the disk labeled b_1, \dots, b_n clockwise. Each boundary vertex has degree 1. We call a boundary vertex b_i a source (respectively sink) if its edge is outgoing (respectively incoming);
- (4) The remaining vertices are called internal and are located strictly inside the disk. They are either bivalent or trivalent;
- (5) \mathcal{G} is a perfect graph, that is each internal vertex in \mathcal{G} is incident to exactly one incoming edge or to one outgoing edge;
- (6) Each vertex is colored black or white. If a trivalent vertex has only one incoming edge, it is colored white, otherwise, it is colored black. Bivalent vertices are assigned either white or black color. Finally each internal face possesses trivalent vertices of both colors;
- (7) For any internal edge e there exists a directed path containing e and starting at a boundary source and ending at a boundary sink.

Moreover, to simplify the overall construction we further assume that the boundary vertices b_j , $j \in [n]$, lie on a common interval in the boundary of the disk and that each boundary vertex b_i is joined by its edge to an internal bivalent white vertex which we denote V_i , $i \in [n]$.

Remark 2.1.1. In our paper we use different orientations on the same bicolored graph \mathcal{G} , but we always assume that these orientations respect properties (5), (6), i.e. they respect perfectness of \mathcal{G} .

Remark 2.1.2. The assumption that the boundary vertices b_j , $j \in [n]$ lie on a common interval in the boundary of the disk simplifies the computations.

In our construction only the bivalent vertices joined by edges to two boundary vertices have to be kept. All other bivalent vertices may be eliminated using Postnikov moves and are irrelevant in the construction of the KP divisor.

In Figure 1 we present an example of a PBDTP graph satisfying Definition 2.1.3 and representing a 10-dimensional positroid cell in $Gr^{\text{TNN}}(4, 9)$.

The graph is of type (k, n) if it has n boundary vertices and k of them are boundary sources. Any choice of perfect orientation preserves the type of \mathcal{G} . To any perfect orientation \mathcal{O} of \mathcal{G} one assigns the base $I_{\mathcal{O}} \subset [n]$ of the k -element source set for \mathcal{O} . Following [61] the matroid of \mathcal{G} is the set of k -subsets $I_{\mathcal{O}}$ for all perfect orientations:

$$\mathcal{M}_{\mathcal{G}} := \{I_{\mathcal{O}} | \mathcal{O} \text{ is a perfect orientation of } \mathcal{G}\}.$$

In [61] it is proven that $\mathcal{M}_{\mathcal{G}}$ is a totally non-negative matroid $\mathcal{S}_{\mathcal{M}_{\mathcal{G}}}^{\text{TNN}} \subset Gr^{\text{TNN}}(k, n)$: for any choice of real positive weights on the edges of \mathcal{G} the image of Postnikov boundary measurement map on the directed network \mathcal{N} of graph \mathcal{G} is a point in $\mathcal{S}_{\mathcal{M}_{\mathcal{G}}}^{\text{TNN}}$ and, vice versa, for any point $[A] \in \mathcal{S}_{\mathcal{M}_{\mathcal{G}}}^{\text{TNN}}$ there is a choice of positive weights so that the resulting network of graph \mathcal{G} represents $[A]$.

PBDTP graphs \mathcal{G} representing the same positroid cell $\mathcal{S}_{\mathcal{M}}^{\text{TNN}}$ are equivalent via a finite sequence of moves and reductions [61]. More precisely, a PBDTP graph \mathcal{G} can be transformed into a PBDTP graph \mathcal{G}' via a finite sequence of Postnikov moves and reductions if and only if $\mathcal{M}_{\mathcal{G}} = \mathcal{M}_{\mathcal{G}'}$.

A graph \mathcal{G} is reduced if there is no other graph in its move reduction equivalence class which can be obtained from \mathcal{G} applying a sequence of transformations containing at least one reduction. Each positroid cell $\mathcal{S}_{\mathcal{M}}^{\text{TNN}}$ is represented by at least one reduced graph, the so called Le-graph, associated to the Le-diagram representing $\mathcal{S}_{\mathcal{M}}^{\text{TNN}}$ and it is possible to assign weights to such graphs in order to obtain a global parametrization of $\mathcal{S}_{\mathcal{M}}^{\text{TNN}}$ [61].

Each Le-graph is reduced and may be transformed into a reduced PBDTP Le-graph. If \mathcal{G} is a reduced PBDTP graph, then the dimension of $\mathcal{S}_{\mathcal{M}_{\mathcal{G}}}^{\text{TNN}}$ is equal to the number of faces of \mathcal{G} minus 1. The PBDTP graph in Figure 1 is a PBDTP Le-graph.

2.2. Systems of edge vectors on PBDTP networks: definition and explicit representation. For any given $[A] \in \mathcal{S}_{\mathcal{M}_{\mathcal{G}}}^{\text{TNN}}$, there exists a choice of positive edge weights w_e such that the weighted network \mathcal{N} of graph \mathcal{G} represents $[A]$ [61]. In [61], for any given oriented planar network in the disk it is defined the formal boundary measurement map

$$M_{ij} := \sum_{P: b_i \rightarrow b_j} (-1)^{\text{wind}(P)} w(P),$$

where the sum is over all directed walks from the source b_i to the sink b_j , $w(P)$ is the product of the edge weights of P and $\text{wind}(P)$ is its topological winding index. These formal power series sum up to subtraction free rational expressions in the weights [61] and explicit expressions in function of flows and conservative flows in the network is provided in [68]. Let I be the base inducing the orientation of \mathcal{N} used in the computation of the boundary measurement map. Then the point $\text{Meas}(\mathcal{N}) \in Gr(k, n)$ is represented by the boundary measurement matrix A such that:

- The submatrix A_I in the column set I is the identity matrix;
- The remaining entries $A_j^r = (-1)^{\sigma(i_r, j)} M_{ij}$, $r \in [k]$, $j \in \bar{I}$, where $\sigma(i_r, j)$ is the number of elements of I strictly between i_r and j .

In [7] (see also [6]), we have constructed row edge vectors in \mathbb{R}^n on each perfectly oriented PBDTP network in such a way that, if we assign the j -th vector of the canonical basis, E_j , to the boundary sink b_j , $j \in \bar{I}$, then, at e_r , the edge at a boundary source $i_r \in I$, the edge vector is $E_{e_r} = A[r] - E_{i_r}$. We have then provided an explicit representation of the components of the edge

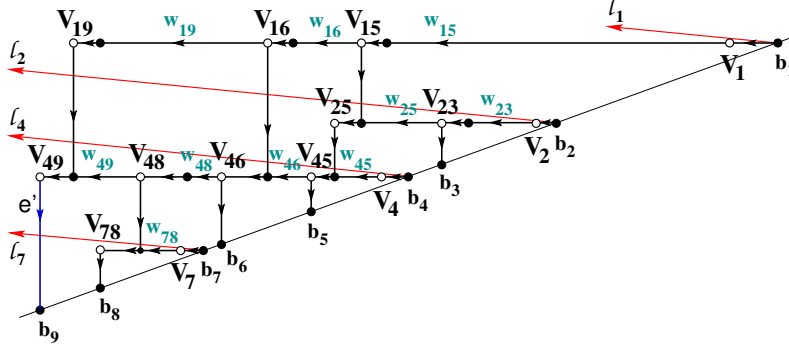


FIGURE 1. The rays starting at the boundary sources for a given orientation of the network uniquely fix the edge vectors.

vectors and shown that they solve a full rank system of linear relations at the internal vertices. To be compatible with the total non-negativity at the boundary, these linear relations must contain some non-trivial signs. In [7] we have defined and characterized these signs (signature) using the orientation and gauge ray direction on the graph. More precisely, in [7]:

- (1) We have assigned a geometric edge signature to each choice of orientation and gauge ray direction on a given PBDTP graph \mathcal{G} ;
- (2) We have shown that all geometric signatures on \mathcal{G} are equivalent with respect to a simple gauge transformation at its vertices;
- (3) We have proven that a system of relations on a PBDTP network has full rank for any choice of positive edge weights if and only if its signature is geometric and in such case the image is the full positroid cell $\mathcal{S}_{\mathcal{M}}^{\text{TN}}$ associated to the given graph;
- (4) We have proven that the solution to the system of relations are the edge vectors defined as signed summations over all directed paths from the given edge to the boundary. Moreover, the components of such vectors are rational in the edge weights with subtraction-free denominators and are expressible in term of the edge and conservative flows introduced in [68].

Finally in Theorem 2.5.1 we provide the topological meaning of the edge signature for trivalent bicolored graphs.

The starting point in the definition of geometric signature and in the explicit construction of the system of edge vectors associated to it for the given choice of positive weights, is the notion of gauge ray direction. The latter measures the local winding between consecutive edges in the path and counts the number of boundary sources passed by a path starting at an internal edge as the number of intersections of gauge rays starting at the boundary sources with it.

Remark 2.2.1. *Gauge ray directions were used in [32] to measure the local winding number. In [7] we introduce the intersections of gauge rays with a given path as an analog of the index $\sigma(i_r, j)$ for internal edges.*

Definition 2.2.1. *The gauge ray direction \mathfrak{l} . A gauge ray direction is an oriented direction \mathfrak{l} with the following properties:*

- (1) *The ray with the direction \mathfrak{l} starting at a boundary vertex points inside the disk;*
- (2) *No internal edge is parallel to this direction;*
- (3) *All rays starting at boundary vertices do not contain internal vertices.*

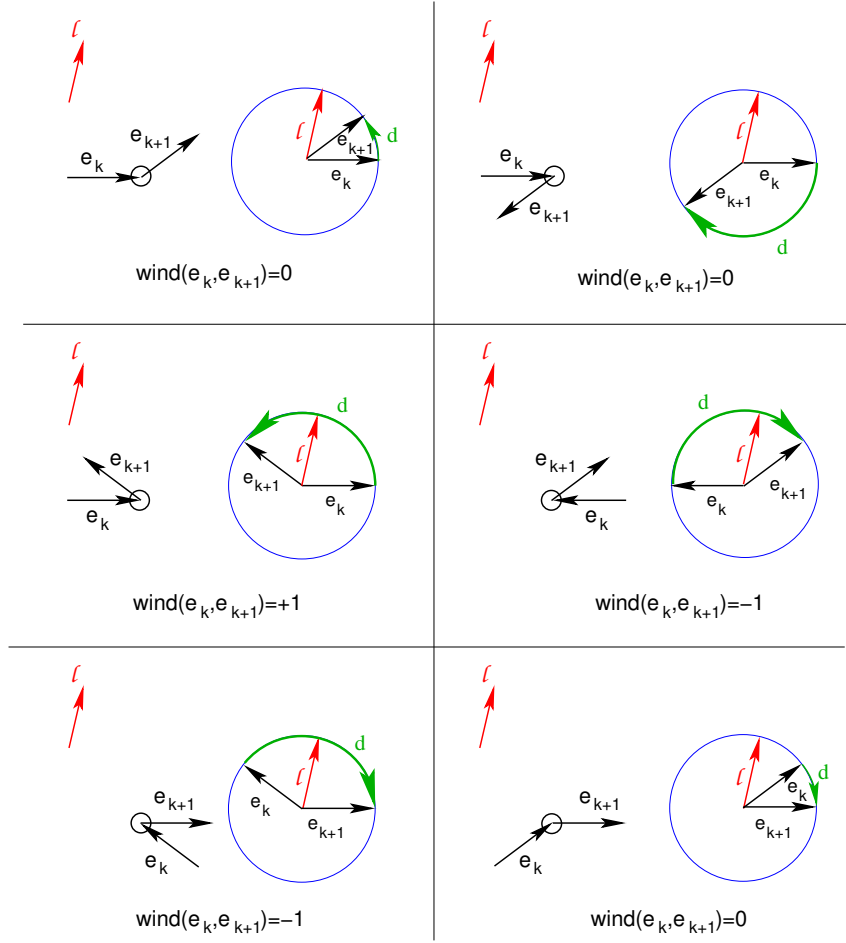


FIGURE 2. The local rule to compute the winding number.

We remark that the first property may always be satisfied since all boundary vertices lie at a common straight interval in the boundary of \mathcal{N} . The local winding number between a pair of consecutive edges e_k, e_{k+1} is then defined as follows (see also Figure 2).

Definition 2.2.2. *The local winding number at an ordered pair of oriented edges* For an ordered pair (e_k, e_{k+1}) of oriented edges, define

$$(2.1) \quad s(e_k, e_{k+1}) = \begin{cases} +1 & \text{if the ordered pair is positively oriented} \\ 0 & \text{if } e_k \text{ and } e_{k+1} \text{ are parallel} \\ -1 & \text{if the ordered pair is negatively oriented} \end{cases}$$

Then the winding number of the ordered pair (e_k, e_{k+1}) with respect to the gauge ray direction l is

$$(2.2) \quad \text{wind}(e_k, e_{k+1}) = \begin{cases} +1 & \text{if } s(e_k, e_{k+1}) = s(e_k, l) = s(l, e_{k+1}) = 1 \\ -1 & \text{if } s(e_k, e_{k+1}) = s(e_k, l) = s(l, e_{k+1}) = -1 \\ 0 & \text{otherwise.} \end{cases}$$

Then draw the rays l_r , $r \in [k]$, starting at b_{i_r} associated with the pivot columns of the given orientation (see Figure 1 for an example).

Let now $\mathcal{P} = \{e = e_1, e_2, \dots, e_m\}$ be a directed path starting at a vertex V_1 (either a boundary source or internal vertex) and ending at a boundary sink b_j , where $e_1 = (V_1, V_2)$, $e_2 = (V_2, V_3)$, \dots , $e_m = (V_m, b_j)$. At each edge the orientation of the path coincides with the orientation of this edge in the graph. Let b_{i_r} , $r \in [k]$, b_{j_l} , $l \in [n - k]$, respectively be the set of boundary sources and boundary sinks associated to the given orientation. We assign three numbers to \mathcal{P} [7]:

- (1) The **weight** $w(\mathcal{P})$ is the product of the weights w_l of all edges e_l in \mathcal{P} , $w(\mathcal{P}) = \prod_{l=1}^m w_l$;
- (2) The **generalized winding number** $\text{wind}(\mathcal{P})$ is the sum of the local winding numbers in Definition 2.2.2 at each ordered pair of its edges

$$\text{wind}(\mathcal{P}) = \sum_{k=1}^{m-1} \text{wind}(e_k, e_{k+1});$$

- (3) $\text{int}(\mathcal{P})$ is the **number of intersections** between the path and the rays \mathfrak{l}_{i_r} , $r \in [k]$:
 $\text{int}(\mathcal{P}) = \sum_{s=1}^m \text{int}(e_s)$, where $\text{int}(e_s)$ is the number of intersections of gauge rays \mathfrak{l}_{i_r} with e_s .

The generalized winding of the path \mathcal{P} depends on the gauge ray direction \mathfrak{l} since it counts how many times the tangent vector to the path is parallel and has the same orientation as \mathfrak{l} .

Definition 2.2.3. *The edge vector E_e [7]. For any edge e , let us consider all possible directed paths $\mathcal{P} : e \rightarrow b_j$, in $(\mathcal{N}, \mathcal{O}, \mathfrak{l})$ such that the first edge is e and the end point is the boundary vertex b_j , $j \in [n]$. Then the j -th component of E_e is defined as:*

$$(2.3) \quad (E_e)_j = \sum_{\mathcal{P}: e \rightarrow b_j} (-1)^{\text{wind}(\mathcal{P}) + \text{int}(\mathcal{P})} w(\mathcal{P}).$$

If there is no path from e to b_j , the j -th component of E_e is assigned to be zero. By definition, at the edge e at the boundary sink b_l , the edge vector E_e is

$$(2.4) \quad (E_e)_j = (-1)^{\text{int}(e)} w(e) \delta_{jl}.$$

By definition, for any e , all components of E_e corresponding to the boundary sources in the given orientation are equal to zero. If the number of paths starting at e and ending at a given b_j , $j \in \bar{I}$, is finite, the component $(E_e)_j$ in (2.3) is a polynomial in the edge weights. If the number of paths starting at e and ending at b_j is infinite and the weights are sufficiently small, it is easy to check that the right hand side in (2.3) converges.

In [7] we have adapted the summation procedures of [61] and [68] to prove that the edge vector components are explicit rational expressions in the edge weights with subtraction-free denominators.

Definition 2.2.4. Conservative flows [68]. *A collection C of distinct edges in a PBDTP graph \mathcal{G} is called a conservative flow if*

- (1) *For each interior vertex V_d in \mathcal{G} the number of edges of C that arrive at V_d is equal to the number of edges of C that leave from V_d ;*
- (2) *C does not contain edges incident to the boundary.*

$\mathcal{C}(\mathcal{G})$ denotes the set of all conservative flows C in \mathcal{G} . $w(C)$ is the product of the weights of all edges in $C \in \mathcal{C}(\mathcal{G})$. The trivial flow with no edges is assigned unit weight.

Following [25, 51], in [7] we have adapted the notion of loop-erased walk to our situation, since our walks start at an edge, not at a vertex.

Definition 2.2.5. Edge loop-erased walks [7]. *Let \mathcal{P} be a walk (directed path) given by*

$$V_e \xrightarrow{e} V_1 \xrightarrow{e_1} V_2 \rightarrow \dots \rightarrow b_j,$$

where V_e is the initial vertex of the edge e . The edge loop-erased part of \mathcal{P} , denoted $LE(\mathcal{P})$, is defined recursively as follows. If \mathcal{P} does not pass any edge twice (i.e., all edges e_i are distinct), then $LE(\mathcal{P}) = \mathcal{P}$. Otherwise, set $LE(\mathcal{P}) = LE(\mathcal{P}_0)$, where \mathcal{P}_0 is obtained from \mathcal{P} , by removing the first edge loop it makes; more precisely, find all pairs l, s with $s > l$ and $e_l = e_s$, choose the one with the smallest value of l and s and remove the cycle

$$V_l \xrightarrow{e_l} V_{l+1} \xrightarrow{e_{l+1}} V_{l+2} \rightarrow \dots \xrightarrow{e_{s-1}} V_s,$$

from \mathcal{P} .

Definition 2.2.6. Edge flow at e [7]. A collection F_e of distinct edges in a PBDTP graph \mathcal{G} is called edge flow starting at the edge $e = e_1 = (V_1, V_2)$ if

- (1) $e \in F_e$;
- (2) For each interior vertex $V_d \neq V_1$ in \mathcal{G} the number of edges of F_e that arrive at V_d is equal to the number of edges of F_e that leave from V_d ;
- (3) At V_1 the number of edges of F_e that arrive at V_1 is equal to the number of edges of F_e that leave from V_1 minus 1.

$\mathcal{F}_{e,b_j}(\mathcal{G})$ denotes the set of all edge flows F starting at an edge e and ending at a boundary sink b_j in \mathcal{G} .

Due to the trivalency property of the graphs in our setting, an edge flow F_{e,b_j} is either an edge loop-erased walk P_{e,b_j} or the union of P_{e,b_j} with a conservative flow with no common edges with P_{e,b_j} .

Definition 2.2.7. [7] Let $F_{e,b_j} \in \mathcal{F}_{e,b_j}(\mathcal{G})$ be the union of the edge loop-erased walk P_{e,b_j} with a conservative flow with no common edges with P_{e,b_j} (this conservative flow may be the trivial one). We assign three numbers to F_{e,b_j} :

- (1) The **weight** $w(F_{e,b_j})$ is the product of the weights of all edges in F_{e,b_j} .
- (2) The **winding number** $wind(F_{e,b_j})$: $wind(F_{e,b_j}) = wind(P_{e,b_j})$;
- (3) The **intersection number** $int(F_{e,b_j})$: $int(F_{e,b_j}) = int(P_{e,b_j})$.

Remark 2.2.2. Let us point out that in the definition above we associate neither winding number nor intersection numbers to the conservative flows. This rule turns out to be technically convenient.

Theorem 2.2.1. Rational representation of the vector components [7] Let $(\mathcal{N}, \mathcal{O}, \mathfrak{l})$ be a PBDTP network representing a point $[A] \in \mathcal{S}_{\mathcal{M}}^{TNN} \subset Gr^{TNN}(k, n)$ with orientation \mathcal{O} associated to the base $I = \{1 \leq i_1 < i_2 < \dots < i_k \leq n\}$ in the matroid \mathcal{M} and gauge ray direction \mathfrak{l} . Let us assign the j -th vectors of the canonical basis to the boundary sinks b_j , $j \in \bar{I}$. Then the j -th component of the edge vector at e , $(E_e)_j$, defined in (2.3) is a rational expression in the weights on the network with subtraction-free denominator:

$$(2.5) \quad (E_e)_j = \frac{\sum_{F \in \mathcal{F}_{e,b_j}(\mathcal{G})} (-1)^{wind(F)+int(F)} w(F)}{\sum_{C \in \mathcal{C}(\mathcal{G})} w(C)},$$

where notations are as in Definitions 2.2.4, 2.2.6 and 2.2.7.

In particular, if e is the edge starting at the boundary source b_{i_r} , then (2.5) simplifies to

$$(2.6) \quad (E_e)_j = A_j^r,$$

where A_j^r is the entry of the reduced row echelon matrix A with respect to the base $I = \{1 \leq i_1 < i_2 < \dots < i_k \leq n\}$. Therefore the vector on the edge e at b_{i_r} is

$$(2.7) \quad E_e = A[r] - E_{i_r},$$

where E_{i_r} is the i_r -th vector of the canonical basis.

Remark 2.2.3. The proof of Theorem 2.2.1 in [7] is an adaptation of the technique introduced in [68] to compute the boundary measurement map. In particular if e is the edge at the boundary source b_{i_r} , then for any edge loop-erased path $F \in \mathcal{F}_{e,b_j}(\mathcal{G})$

$$(2.8) \quad \text{wind}(F) + \text{int}(F) = \sigma(i_r, j) \pmod{2},$$

where $\sigma(i_r, j)$ is the number of boundary sources in the interval $]i_r, j[$ (if $i_r < j$), respectively $]j, i_r[$ (if $i_r > j$).

2.3. The dependence of the edge vectors on the gauge freedoms and the orientation of the network. In [7], we have also given explicit formulas on the transformation rules of edge vectors with respect to changes of orientation of the network and of the gauge ray direction, the weight gauge and the graph gauge. Below we briefly recall such results since we use them in our construction and characterization of KP divisors. Any given point $[A] \in \mathcal{S}_{\mathcal{M}}^{\text{TNN}}$ has infinitely many representative networks with the same graph \mathcal{G} . If the graph is reduced, then the weights are uniquely chosen up to the weight gauge freedom, otherwise there is extra gauge freedom.

Remark 2.3.1. The weight gauge freedom [61]. Given a point $[A] \in \mathcal{S}_{\mathcal{M}}^{\text{TNN}}$ and a planar directed graph \mathcal{G} in the disk representing $\mathcal{S}_{\mathcal{M}}^{\text{TNN}}$, then $[A]$ is represented by infinitely many gauge equivalent systems of weights w_e on the edges e of \mathcal{G} . Indeed, if a positive number t_V is assigned to each internal vertex V , whereas $t_{b_i} = 1$ for each boundary vertex b_i , then the transformation on each directed edge $e = (U, V)$

$$(2.9) \quad w_e \rightarrow w_e t_U (t_V)^{-1},$$

transforms the given directed network into an equivalent one representing $[A]$.

Lemma 2.3.1. Dependence of edge vectors on the weight gauge [7] Let E_e be the edge vectors on the network $(\mathcal{N}, \mathcal{O}, \mathfrak{l})$, and \tilde{E}_e be the system of edge vectors on $(\tilde{\mathcal{N}}, \mathcal{O}, \mathfrak{l})$, where $\tilde{\mathcal{N}}$ is obtained from \mathcal{N} applying the weight gauge transformation at the internal vertex V . Then $\tilde{E}_e = E_e$ at all edges e except for those ending at V for which $\tilde{E}_e = t_V E_e$.

Remark 2.3.2. The unreduced graph gauge freedom. There is no one-to-one correspondence between the orbits of the gauge weight action (2.9) for a fixed directed unreduced graph and the points in the corresponding positroid cell [61]. In contrast with gauge transformations of the weights (2.9) the unreduced graph gauge freedom affects the system of edge vectors globally.

We next explain the transformation rule of edge vectors with respect to changes of the gauge ray direction.

Proposition 2.3.2. The dependence of the system of vectors on the ray direction \mathfrak{l} [7] Let $(\mathcal{N}, \mathcal{O})$ be an oriented network and consider two gauge directions \mathfrak{l} and \mathfrak{l}' on it. Then

- (1) At any boundary source edge e_{i_r} , the vector $E_{e_{i_r}}$ does not depend on \mathfrak{l} and its components satisfy (2.6);
- (2) For any other edge e ,

$$(2.10) \quad E'_e = (-1)^{\text{int}(V_e) + \text{par}(e)} E_e,$$

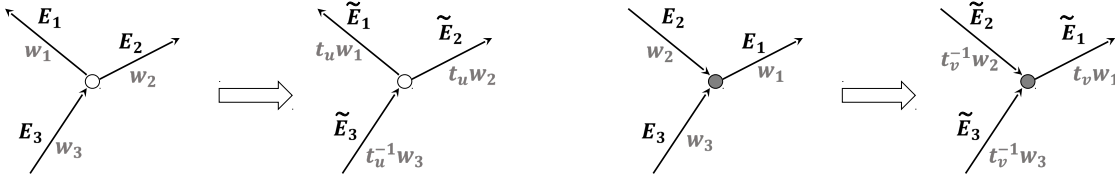


FIGURE 3. The effect of the weight gauge transformation at a white [left] and at a black [right] vertex on the edge vectors.

where E_e and E'_e respectively are the edge vectors for e for the gauge direction \mathfrak{l} and \mathfrak{l}' , $\text{par}(e)$ is 1 if the ray e is crossed in the rotation from \mathfrak{l} to \mathfrak{l}' inside the disk and 0 otherwise, whereas $\text{int}(V_e)$ denotes the number of gauge ray intersections with e which pass the initial vertex V_e of e when we rotate from \mathfrak{l} to \mathfrak{l}' inside the disk.

We now explain how the system of vectors change when the orientation of the graph changes. Here we use the standard rule that we do not change the edge weight if the edge does not change orientation, otherwise we replace the original weight by its reciprocal.

Theorem 2.3.3. The dependence of the system of vectors on the orientation of the network [7] Let \mathcal{N} be a PBDTP network representing a given point $[A] \in S_{\mathcal{M}}^{TNN} \subset Gr^{TNN}(k, n)$ and \mathfrak{l} be a gauge ray direction. Let $\mathcal{O}, \hat{\mathcal{O}}$ be two perfect orientations of \mathcal{N} for the bases $I, I' \in \mathcal{M}$. Let $A[r]$, $r \in [k]$, denote the r -th row of a chosen representative matrix of $[A]$. Let E_e be the system of vectors associated to $(\mathcal{N}, \mathcal{O}, \mathfrak{l})$ and satisfying the boundary conditions $E[j]$ at b_j , $j \in \bar{I}$, whereas \hat{E}_e are those associated to $(\mathcal{N}, \hat{\mathcal{O}}, \mathfrak{l})$ and satisfying the boundary conditions $E[l]$ at b_l , $l \in \bar{I}'$. Then for any $e \in \mathcal{N}$, there exist real constants $\alpha_e \neq 0$, c_e^r , $r \in [k]$ such that

$$(2.11) \quad \hat{E}_e = \alpha_e E_e + \sum_{r=1}^k c_e^r A[r].$$

The graph representing the positroid cell is defined up to vertex shifts transformations. In the following we refer to such class of transformations as vertex gauge freedom of the graph. Any such transformation may be decomposed in a sequence of elementary transformations in which a single vertex is moved whereas all other vertices remain fixed (see also Figure 4). This transformation changes only the sign of the edge vectors incident at the moving vertex.

Lemma 2.3.4. Dependence of edge vectors on the vertex gauge [7] Let E_e and \tilde{E}_e respectively be the system of edge vectors on $(\mathcal{N}, \mathcal{O}, \mathfrak{l})$ and on $(\tilde{\mathcal{N}}, \mathcal{O}, \mathfrak{l})$, where $\tilde{\mathcal{N}}$ is obtained from \mathcal{N} moving one internal vertex V as in Figure 4. Then $\tilde{E}_e = E_e$, for all edges e not incident at V , and

$$(2.12) \quad \tilde{E}_e = \begin{cases} (-1)^{\text{wind}(\tilde{e}, f) - \text{wind}(e, f) + \text{int}(\tilde{e}) - \text{int}(e)} E_e, & \text{if } e \text{ incoming at } V; \\ (-1)^{\text{wind}(f, \tilde{e}) - \text{wind}(f, e)} E_e, & \text{if } e \text{ outgoing at } V, \end{cases}$$

where $(e, f) = (e_i, f_i)$, $i \in [3]$, using the notations of Figure 4.

Remark 2.3.3. Zero edge vectors on reducible networks Since the edge vectors components have no subtraction free enumerators, it may happen that the j -th component of E_e is zero even if there exist directed paths starting at e and ending at b_j . In [7], we prove that all edge vectors are not zero on networks without isolated boundary sources and possessing an acyclic orientation. In particular if \mathcal{N} is either the Le-network representing a point in an irreducible positroid cell,

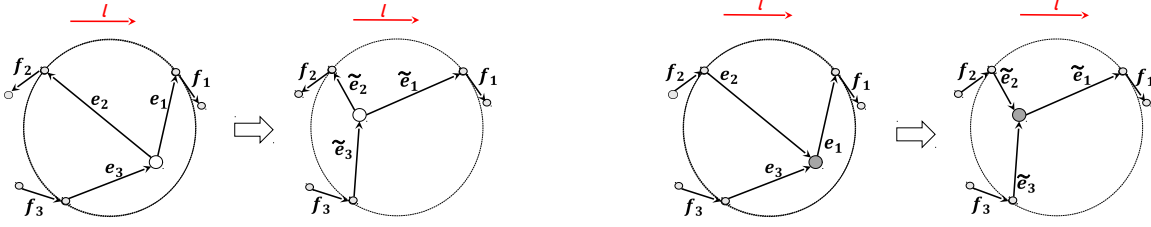


FIGURE 4. The effect of the vertex gauge transformation at a white [left] and at a black [right] vertex on the winding numbers of the edge vectors.

or is equivalent to such *Le-network* via a finite sequence of moves (M1), (M3) and flip moves (M2), then \mathcal{N} does not possess zero edge vectors.

The absence of zero edge vectors for a given network is independent of its orientation and of the choices of the ray direction, of vertex gauge and of weight gauge, because of the transformation rules of edge vectors. In particular, if the edge vector $E_e = 0$ on the PBDTP network $(\mathcal{N}, \mathcal{O}, \mathfrak{l})$ for a given orientation \mathcal{O} , then it is zero in any other orientation of \mathcal{N} .

Finally, in [7] we construct examples of zero edge vectors on reducible PBDTP networks which do not possess an acyclic orientation (see also Section 11.2). Since on reducible networks there is extra freedom in fixing the edge weights (see Remark 2.3.2), we conjecture that we may always choose the weights on reducible networks representing a given point so that all edge vectors are non-zero provided that for each edge there is a path directed to some boundary sink.

2.4. Systems of relations on PBDTP networks. The edge vectors defined in the previous Section satisfy a full rank linear system on the network which is equivalent to the amalgamation of several copies of little Grassmannians $Gr^{\text{TP}}(1, 3)$ and $Gr^{\text{TP}}(2, 3)$. In [7] we have proven that the changes of orientation and the many gauge freedoms act on this geometric system as a simple gauge transformation at the vertices which preserves the full rank and the image of the boundary measurement map in the positroid cell $\mathcal{S}_{\mathcal{M}}^{\text{TNN}}$. Below we recall these results.

Remark 2.4.1. Labeling of edges at trivalent vertices We use the following labeling rule for edges at trivalent vertices: edges are labeled in increasing order counterclockwise and e_3 is the unique incoming edge if the trivalent vertex V is white, whereas e_1 is the unique outgoing edge if V is trivalent black (see Figure 5).

By construction, the edge vectors E_e on $(\mathcal{N}, \mathcal{O}, \mathfrak{l})$ satisfy linear equations at each vertex (see Figure 5 for an example):

- (1) At each bivalent vertex with incoming edge e and outgoing edge f all paths starting at e pass through f first. Therefore:

$$(2.13) \quad E_e = (-1)^{\text{int}(e) + \text{wind}(e, f)} w_e E_f;$$

- (2) At each trivalent black vertex with incoming edges e_2, e_3 and outgoing edge e_1 we have two relations:

$$(2.14) \quad E_2 = (-1)^{\text{int}(e_2) + \text{wind}(e_2, e_1)} w_2 E_1, \quad E_3 = (-1)^{\text{int}(e_3) + \text{wind}(e_3, e_1)} w_3 E_1;$$

- (3) At each trivalent white vertex with incoming edge e_3 and outgoing edges e_1, e_2 :

$$(2.15) \quad E_3 = (-1)^{\text{int}(e_3) + \text{wind}(e_3, e_1)} w_3 E_1 + (-1)^{\text{int}(e_3) + \text{wind}(e_3, e_2)} w_3 E_2,$$

where E_k denotes the vector associated to the edge e_k .



FIGURE 5. An example of linear relations: $E_3 = -w_3(E_1 + E_2)$ [left]; $E_2 = -w_2E_1, E_3 = w_3E_1$ [right].

For any given boundary condition at the boundary sink vertices, the linear system defined by equations (2.13), (2.14) and (2.15) at the internal vertices of $(\mathcal{N}, \mathcal{O}, \mathfrak{l})$ possesses a unique solution.

Theorem 2.4.1. Uniqueness of the system of edge vectors on $(\mathcal{N}, \mathcal{O}, \mathfrak{l})$ [7] *Let $(\mathcal{N}, \mathcal{O}, \mathfrak{l})$ be a given PBDTP network with orientation $\mathcal{O} = (I)$ and gauge ray direction \mathfrak{l} . Then for any set of linearly independent vectors assigned to the boundary sinks b_j , the linear system of equations (2.13), (2.15), (2.14) at all the internal vertices of $(\mathcal{N}, \mathcal{O}, \mathfrak{l})$ has full rank and provides a unique system of edge vectors on $(\mathcal{N}, \mathcal{O}, \mathfrak{l})$.*

In particular, at each edge e the solution E_e of the linear system may be expressed in the form of edge and conservative flows as in Theorem 2.2.1

$$(2.16) \quad E_e = \sum_{j \in \bar{I}} \frac{\sum_{F \in \mathcal{F}_{e, b_j}(\mathcal{G})} (-1)^{\text{wind}(F) + \text{int}(F)} w(F)}{\sum_{C \in \mathcal{C}(\mathcal{G})} w(C)} E_{b_j},$$

where E_{b_j} is the vector assigned to the boundary sink b_j , $j \in \bar{I}$.

The system of relations on \mathcal{N} depends on the geometric indices $\text{wind}(e, f)$ and $\text{int}(e)$, i.e on the choice of orientation and of gauge ray direction. In [7], we have proven that all the geometric systems on the same network are equivalent with respect to a simple gauge transformation at the vertices and that these are the only systems compatible with total non-negativity property of the boundary measurement map for any choice of positive weights. At this aim, we have re-expressed the above system of relations on flags, i.e. as a system on half-edge vectors in the form proposed by [50] where $\epsilon(U, V) \in \{0, 1\}$ is defined in [7] in terms of the winding and the intersection numbers. Such explicit dependence can be read off from Figure 6. Here flags means pairs (e, v) , where v is one of the end points of the edge e .

Theorem 2.4.2. Existence of geometric signature on $(\mathcal{G}, \mathcal{O}, \mathfrak{l})$ parametrizing $\mathcal{S}_{\mathcal{M}}^{\text{TNN}}$ [7] *Let $(\mathcal{G}, \mathcal{O}, \mathfrak{l})$ be a PBDTP graph representing a $|D|$ -dimensional positroid cell $\mathcal{S}_{\mathcal{M}}^{\text{TNN}} \subset \text{Gr}^{\text{TNN}}_{\mathcal{M}}(k, n)$ with perfect orientation \mathcal{O} associated to the base I and gauge ray direction \mathfrak{l} . Let w_e be positive weights at the oriented edges e and let \mathcal{N} be the associated network of graph \mathcal{G} . Then the linear system of relations (2.13)–(2.15) on $(\mathcal{N}, \mathcal{O}, \mathfrak{l})$ may be re-expressed as the following geometric system of relations:*

- (1) *At each black vertex V and for any pair of edges (e_i, e_{i+1}) at V , $z_{V, e_i} = z_{V, e_{i+1}}$, $i \in [3]$;*
- (2) *For any white vertex V , $\sum_{i=1}^3 z_{V, e_i} = 0$, where e_i , $i \in [3]$, are the edges at V ;*
- (3) *$z_{U, e_3} = (-1)^{\epsilon_{U, V}} w_3 z_{V, e_3}$, if $e_3 = (U, V)$ is an internal edge of weight $w_3 = w(U, V)$;*

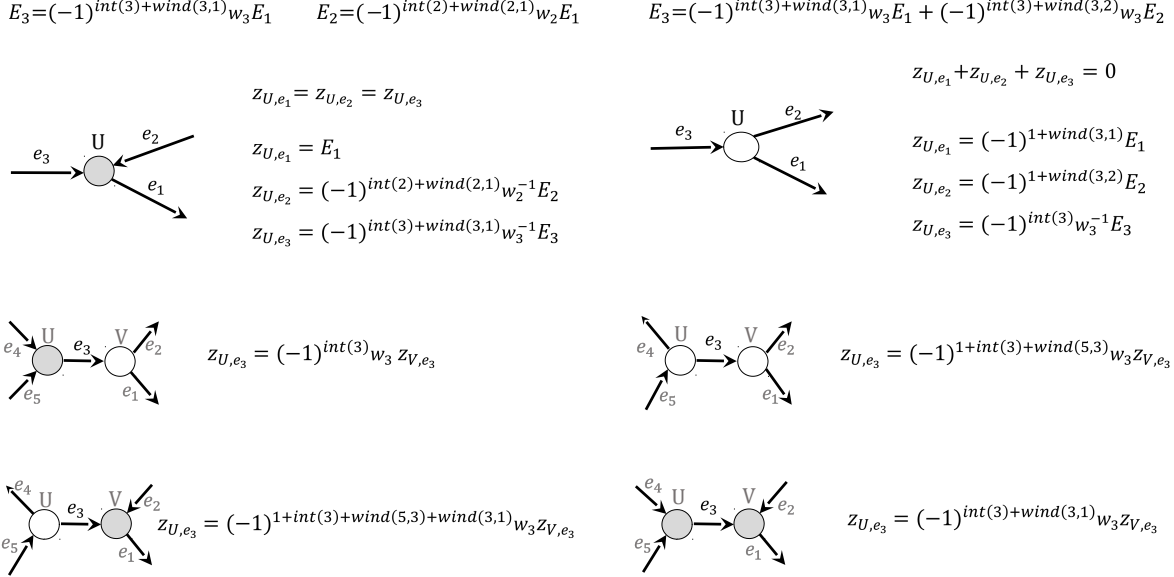


FIGURE 6. The reformulation of the linear relations for the edge vectors as geometric relations for half-edge vectors compatible with Lam [50] approach at the vertices [top] and at edges [bottom]. We use the abridged notations $\text{wind}(i, j) \equiv \text{wind}(e_i, e_j)$ and $\text{int}(i) \equiv \text{int}(e_i)$.

- (4) $z_{b_j, e} = E_j$, $z_{U, e} = (-1)^{\epsilon(U, b_j)} w_{U, b_j} E_j$, if b_j is a boundary sink vertex, $e = (U, b_j)$ its edge and E_j is the j -th vector of the canonical basis, $j \in \bar{I}$;
- (5) If $e = (b_i, V)$ is the edge at the boundary source b_i , $i \in I$, then $z_{b_i, e} = (-1)^{\epsilon_{b_i, U}} w_{b_i, V} z_{V, e}$.

The above system has full rank for any choice of positive weights, its solution at the boundary sources produces the boundary measurement matrix for \mathcal{N} with respect to the base I , and the half-edge vectors $z_{V, e}$ may be expressed as in Theorem 2.2.1.

We have then introduced the following notion of equivalence for edge signatures and defined geometric a signature equivalent to that in Theorem 2.4.2.

Definition 2.4.1. Equivalence between edge signatures [7] Let $\epsilon_{U, V}^{(1)}$ and $\epsilon_{U, V}^{(2)}$ be two signatures on all the edges $e = (U, V)$ of the PBDTP graph \mathcal{G} , included the edges at the boundary. We say that the two signatures are equivalent if there exists an index $\eta(U) \in \{0, 1\}$ at each internal vertex U such that

$$(2.17) \quad \epsilon_{U, V}^{(2)} = \begin{cases} \epsilon_{U, V}^{(1)} + \eta(U) + \eta(V), & \text{if } e = (U, V) \text{ is an internal edge,} \\ \epsilon_{U, V}^{(1)} + \eta(U), & \text{if } e = (U, V) \text{ is the edge at some boundary vertex } V. \end{cases}$$

Definition 2.4.2. Geometric signatures for half-edge vectors [7] Let $(\mathcal{G}, \mathcal{O}, \mathfrak{l})$ be a PBDTP graph representing the positroid cell $\mathcal{S}_{\mathcal{M}}^{TNN} \subset \text{Gr}^{TNN}(k, n)$. A signature $\epsilon_{U, V} \in \{0, 1\}$ is called **geometric** if it is equivalent to the one defined in Theorem 2.4.2.

Lemma 2.4.3. Geometric signatures induce Postnikov boundary measurement map If \mathcal{G} represents the positroid cell $\mathcal{S}_{\mathcal{M}}^{TNN}$ and $\epsilon_{U, V}$ is a geometric signature on it, then the boundary measurement map induced by $\epsilon_{U, V}$ coincides with Postnikov boundary measurement map on $\mathcal{S}_{\mathcal{M}}^{TNN}$.

All geometric signatures on the same graph \mathcal{G} are equivalent. Indeed, all elementary transformations (change of orientation, gauge ray direction or vertex gauge) can be interpreted as special equivalence transformations, explicitly described in [7]:

- (1) The change of orientation along a loop erased directed path \mathcal{P} from a boundary source b_i to a boundary sink b_j can be written the composition of two steps:
 - First the boundary conditions at the old sinks are changed, whereas the system of relations and signature are preserved. The transformed half-edge vectors are denoted by $\tilde{z}^{(1)}$;
 - An equivalence transformation is applied to the signature and the new boundary conditions. The transformed half-edge vectors are denoted by $z^{(2)}$;
- (2) All other transformations, i.e. change of orientation along a closed oriented cycle \mathcal{Q} , change of gauge ray direction, change of vertex gauge, are equivalence transformations between the original half-vectors $z^{(1)}$ and the transformed ones $z^{(2)}$.

All these elementary transformations send a full rank system of edge vectors in the original network into an equivalent full rank system and preserve the point in the Grassmannian. Indeed the following Lemma holds.

Lemma 2.4.4. *The effect of the network transformations on half edge vectors* [7] *Let $\epsilon_{U,V}^{(1)}$ and $\epsilon_{U,V}^{(2)}$ respectively be the edge signatures on $\mathcal{N}^{(1)} \equiv (\mathcal{N}, \mathcal{O}, \mathfrak{l})$ and on $\mathcal{N}^{(2)} \equiv (\hat{\mathcal{N}}, \hat{\mathcal{O}}, \hat{\mathfrak{l}})$, PBDTP networks representing the same point $[A] \in \mathcal{S}_{\mathcal{M}}^{TNN} \subset Gr^{TNN}(k, n)$.*

- (1) *If $\mathcal{N}^{(2)}$ is obtained from $\mathcal{N}^{(1)}$ using one or more of the following transformations:*
 - (a) *\mathcal{O} and $\hat{\mathcal{O}}$ are two orientations on the same graph \mathcal{G} associated to the same base $I \in \mathcal{M}$, i.e. they are obtained from each other reversing the orientation along a closed cycle \mathcal{Q} ;*
 - (b) *\mathfrak{l} and $\hat{\mathfrak{l}}$ are two gauge ray directions for the given oriented graph;*
 - (c) *The graph of $\mathcal{N}^{(2)}$ is vertex gauge equivalent to that of $\mathcal{N}^{(1)}$,**then the signatures $\epsilon_{U,V}^{(i)}$, $i = 1, 2$, are gauge equivalent as in Definition 2.4.1 and the half-edge vectors $z_{U,e}^{(i)}$, $i = 1, 2$, satisfy*

$$(2.18) \quad z_{U,e}^{(2)} = (-1)^{\eta(U)} z_{U,e}^{(1)},$$

where $\eta(U)$ is the gauge equivalence, and both systems of half-edge vectors satisfy the same boundary conditions at the boundary vertices;

- (2) *If $\mathcal{N}^{(2)}$ is obtained from $\mathcal{N}^{(1)}$ reversing the orientation along an edge loop-erased path \mathcal{P} from the boundary source i_0 to the boundary sink j_0 , then $\epsilon_{U,V}^{(i)}$, $i = 1, 2$, are gauge equivalent as in Definition 2.4.1 and at each internal vertex U the transformed system of edge vectors satisfies*

$$(2.19) \quad z_{U,e}^{(2)} = (-1)^{\eta(U)} \tilde{z}_{U,e}^{(1)},$$

where $\eta(U)$ is the gauge transformation for the signatures, $\tilde{z}_{U,e}^{(1)}$ is the system of half-edge vectors on $\mathcal{N}^{(1)}$ associated to the edge vectors \tilde{E}_e satisfying the boundary conditions

$$\tilde{E}_{e_j} = \begin{cases} E_j & \text{if } j \neq j_0; \\ E_{j_0} - \frac{1}{A_{j_0}^{r_0}} A[r_0], & \text{if } j = j_0; \end{cases}$$

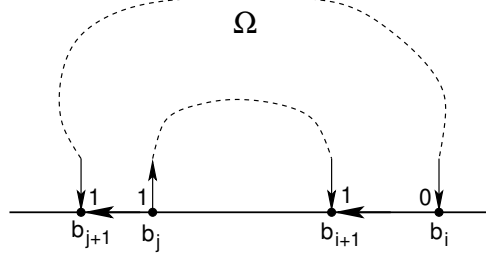


FIGURE 7. We show the index ind_b at the boundary vertices $b \in \partial\Omega$; in this case $i_{b,\Omega} = 3$.

and $z_{U,e}^{(2)}$ is the system of half-edge vectors on $\mathcal{N}^{(2)}$ associated to the edge vectors \hat{E}_e satisfying the boundary conditions

$$\hat{E}_{e_j} = \begin{cases} (-1)^{\text{int}(e_j)'} E_j & \text{if } j \in \bar{I} \setminus \{j_0\} \\ E_{i_0}, & \text{if } j = i_0. \end{cases}$$

Finally, for any graph in our class we have proven the completeness of the geometric signatures.

Theorem 2.4.5. Completeness of the geometric signatures [7] *Let \mathcal{G} be PBDTP graph representing the irreducible positroid $\mathcal{S}_{\mathcal{M}}^{TNN}$. Let $\epsilon_{U,V}$ be a signature on \mathcal{G} . Then, the linear system associated to $\epsilon_{U,V}$ has full rank and its solution is a totally non-negative point for any choice of positive edge weights if and only if $\epsilon_{U,V}$ is geometric. Moreover, in such case, the boundary measurement map induced by $\epsilon_{U,V}$ coincides with Postnikov boundary measurement map on $\mathcal{S}_{\mathcal{M}}^{TNN}$.*

2.5. Topological characterization of the total signatures on the faces of PBDTP graphs. In this Section we provide a topological characterization of the geometric signature on the faces of the oriented PBDTP graph \mathcal{G} which we use in Section 6.2 to prove the reality and regularity properties of KP divisors.

Remark 2.5.1. *In the following we orient the boundary of the disk clockwise.*

Definition 2.5.1. Terminology for faces *A face Ω is internal if its boundary has empty intersection with the boundary of the disk, otherwise it is a boundary face. There is a unique boundary face including the boundary segment from b_n to b_1 clockwise and we call it the infinite face. All other faces are finite faces.*

Let $\epsilon_{U,V}$ be the geometric signature of the network $(\mathcal{N}, \mathcal{O}, \mathfrak{l})$. Let us define ϵ_Ω as the total contribution of the geometric signature at the edges $e = (U, V)$ bounding the face Ω :

$$(2.20) \quad \epsilon_\Omega = \sum_{e \in \partial\Omega} \epsilon_e.$$

In the following $n_{w,\Omega}$ denotes the total number of white vertices in $\partial\Omega$.

We treat the part of the boundary of the disk between two consecutive boundary vertices as an oriented boundary edge. Next we assign index 1 to the boundary vertex $b \in \partial\Omega$ if its edge e and the oriented boundary edge d at b in Ω are either both outgoing or both incoming, otherwise we assign index 0:

$$(2.21) \quad \text{ind}_b = \begin{cases} 1 & \text{if both } e, d \text{ are incoming or outgoing,} \\ 0 & \text{otherwise.} \end{cases}$$

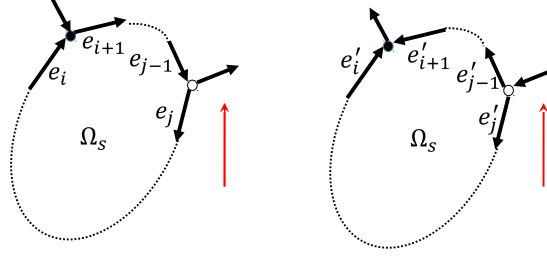


FIGURE 8. The relation between winding and changes of direction.

Next we call $i_{b,\Omega}$ the sum of the contribution of such index for all boundary vertices belonging to Ω

$$(2.22) \quad i_{b,\Omega} \equiv \sum_{b_j \in \partial\Omega} \text{ind}_{b_j}.$$

We show a computation of these indexes in Figure 7. Finally let b_Ω, s_Ω respectively be half the number of boundary vertices bounding Ω and the number of boundary sources belonging to Ω .

The following Theorem provides a topological interpretation of ϵ_Ω for a PBDTP graph \mathcal{G} representing $\mathcal{S}_{\mathcal{M}}^{\text{TNN}}$, and it is used in Section 6.2 to prove that the KP divisor is real and regular, i.e. there is a unique divisor point in each finite oval and no divisor point in the infinite oval of the M-curve dual to \mathcal{G} whenever the soliton data belong to $\mathcal{S}_{\mathcal{M}}^{\text{TNN}}$.

Theorem 2.5.1. The total signature at faces Let \mathcal{G} be a PBDTP graph in the disk representing a positroid cell $\mathcal{S}_{\mathcal{M}}^{\text{TNN}} \subset \text{Gr}^{\text{TNN}}(k, n)$. Let $\epsilon_{U,V}$ be the geometric signature of \mathcal{G} . Let ϵ_Ω , $n_{w,\Omega}$ and s_Ω be as above. Then

(1) If Ω is an internal face,

$$(2.23) \quad \epsilon_\Omega = n_{w,\Omega} - 1 \pmod{2}.$$

(2) If Ω is a boundary face,

$$(2.24) \quad \epsilon_\Omega + n_{w,\Omega} + s_\Omega = \begin{cases} 1 \pmod{2}, & \text{if } \Omega \text{ is a finite face;} \\ k \pmod{2}, & \text{if } \Omega \text{ is the infinite face.} \end{cases}$$

Proof. (2.24) follows immediately from Lemma 2.5.2.

Let us prove (2.23) by induction in the number of trivalent white vertices changing direction.

If there are no changes of directions at the vertices bounding Ω then the statement follows inserting the value of the edge signature in terms of intersection numbers, local winding and number of pair of edges at white vertices bounding the face with one edge incoming and one outgoing (see Figure 6). Indeed, in this case, the number of pair of edges at white vertices bounding the face with one edge incoming and one outgoing (see Figure 6) equals $n_{w,\Omega}$. The total number of intersections is even and the total winding number of the face is odd. Therefore (6.5) is true in this case.

The insertion of a change of direction in Ω along the path $\pi = (e_i, e_{i+1}, \dots, e_{j-1}, e_j)$ which reverts the direction of all the edges e_r , $r \in [i+1, j-1]$ (see Figure 8), changes the winding of Ω by one:

$$\sum_{r=i}^{j-1} (\text{wind}(e_r, e_{r+1}) - \text{wind}(e'_r, e'_{r+1})) = 1 \pmod{2},$$

and diminishes by one the number of pair of edges at white vertices with one edge incoming and one outgoing. Therefore ϵ_Ω keeps the same value and the statement follows. \square

The following Lemma explains the relation between the indices at boundary faces.

Lemma 2.5.2. Relations between indices at boundary faces *Let \mathcal{G} be a PBDTP graph in the disk representing a positroid cell $\mathcal{S}_M^{TNN} \subset Gr^{TNN}(k, n)$. Let $\epsilon_{U,V}$ be the geometric signature of \mathcal{G} . Let ϵ_Ω , $n_{w,\Omega}$, $i_{b,\Omega}$, b_Ω and s_Ω be as above. Then at each boundary face Ω , we have*

$$(2.25) \quad i_{b,\Omega} + b_\Omega + s_\Omega = 0 \pmod{2},$$

$$(2.26) \quad \epsilon_\Omega + n_{w,\Omega} + b_\Omega + i_{b,\Omega} = \begin{cases} 1 & \pmod{2}, & \text{if } \Omega \text{ is a finite face;} \\ k & \pmod{2}, & \text{if } \Omega \text{ is the infinite face.} \end{cases}$$

Proof. (2.25) follows from the definition of $i_{b,\Omega}$. Indeed, if Ω is oriented clockwise, then $i_{b,\Omega} = 0$, and $b_\Omega = s_\Omega$. If we change the orientation at one boundary vertex, we change by ± 1 both $i_{b,\Omega}$ and s_Ω .

Let us prove (2.26) when Ω is a finite face, using Figure 6 to compute ϵ_Ω . In the simplest case $\partial\Omega$ contains two consecutive boundary vertices, of which one is a source and the other a sink, and no change of direction at its internal vertices. In such case (2.26) holds since $i_{b,\Omega} = 0 \pmod{2}$, whereas $\epsilon_\Omega = n_{w,\Omega}$ since the sum of the local winding and intersection numbers along Ω equals the number of boundary sources inside it which is 0 (see (2.8)).

Similarly the statement holds also in the case when $\partial\Omega$ contains $2b_\Omega$ boundary vertices and each component of the boundary inside the network contains a boundary source, a boundary sink and no white vertices with half edges changing of direction. Indeed $i_{b,\Omega} = 0 \pmod{2}$, whereas $\epsilon_\Omega = n_{w,\Omega} + b_\Omega - 1$.

The insertion of a change of direction between two internal vertices changes the winding of Ω by one and diminishes by one the number of pair of edges at white vertices with one edge incoming and one outgoing. Therefore ϵ_Ω keeps the same value and the statement follows.

The transformation of a source into sink (leaving all other boundary vertices unchanged) necessarily involves the insertion of a change of direction at an internal white vertex, whereas the transformation of a sink into source (leaving all other boundary vertices unchanged) necessarily involves the insertion of a change of direction at an internal black vertex. In both cases, both $i_{b,\Omega}$ and ϵ_Ω change their parity leaving the left hand side of (2.26) invariant.

If Ω is the infinite face, in the simplest case $\partial\Omega$ contains two consecutive boundary vertices, of which one is a source and the other a sink, and no change of direction at its internal vertices. In such case (2.26) holds since $i_{b,\Omega} = 0 \pmod{2}$, whereas $\epsilon_\Omega = n_{w,\Omega} + k - b_\Omega \pmod{2}$ again as a consequence of (2.8). \square

Remark 2.5.2. The topological interpretation of ϵ_Ω *Theorem 2.5.1 shows that at each internal face Ω the sum of the geometric signature over all edges bounding Ω has opposite parity from the number of white vertices bounding Ω .*

If the face Ω intersects the boundary of the disk, ϵ_Ω changes when we change the base I ruling the orientation of the graph. Indeed in such case it is the sum of the face signature and of the number of sources bounding Ω , $\epsilon_\Omega + s_\Omega$, to be invariant. The fact that the number of sources plays a role on boundary faces is natural since the geometric signature is constructed so to return the boundary measurement matrix for any given choice of positive weights on the oriented graph.

We remark that the geometric signature has the same properties as the Kasteleyn signature introduced in [8] on bipartite graphs at internal faces, whereas (2.24) has no direct relation to the condition on finite boundary faces in [8] since in their case the graphs are undirected.

3. KP MULTI-LINE SOLITONS IN THE SATO GRASSMANNIAN AND IN FINITE-GAP THEORY

Kadomtsev-Petviashvili-II (KP) equation [38]

$$(3.1) \quad (-4u_t + 6uu_x + u_{xxx})_x + 3u_{yy} = 0,$$

is one of the most famous integrable equations, and it is a member of an integrable hierarchy (see [18, 21, 37, 56, 64] for more details).

The multiline soliton solutions are a special class of solutions realized starting from the soliton data $(\mathcal{K}, [A])$, where \mathcal{K} is a set of real ordered phases $\kappa_1 < \dots < \kappa_n$, $[A]$ denotes a point in the finite dimensional real Grassmannian $Gr(k, n)$ represented by a $k \times n$ real matrix $A = (A_j^i)$ ($i \in [k], j \in [n]$), of maximal rank k . Following [55], see also [29], to such data we associate k linearly independent solutions $f^{(i)}(\vec{t}) = \sum_{j=1}^n A_j^i e^{\theta_j}$, $i \in [k]$, to the heat hierarchy $\partial_{t_l} f = \partial_x^l f$, $l = 2, 3, \dots$. Then

$$(3.2) \quad u(\vec{t}) = 2\partial_x^2 \log(\tau(\vec{t}))$$

is a multiline soliton solution to (3.1) with

$$\tau(\vec{t}) = Wr_{t_1}(f^{(1)}, \dots, f^{(k)}) = \sum_I \Delta_I(A) \prod_{\substack{i_1 < i_2 \\ i_1, i_2 \in I}} (\kappa_{i_2} - \kappa_{i_1}) e^{\sum_{i \in I} \theta_i},$$

where the sum is over all k -element ordered subsets I in $[n]$, i.e. $I = \{1 \leq i_1 < i_2 < \dots < i_k \leq n\}$ and $\Delta_I(A)$ are the maximal minors of the matrix A with respect to the columns I , i.e. the Plücker coordinates for the corresponding point in the finite dimensional Grassmannian $Gr(k, n)$. Since linear recombinations of the rows of A preserve the KP multisoliton solution $u(\vec{t})$ in (3.2), the soliton data is the corresponding point $[A] \in Gr(k, n)$.

$u(\vec{t}) = 2\partial_x^2 \log(\tau(\vec{t}))$ is a real regular multi-line soliton solution to the KP equation (3.1) bounded for all real x, y, t if and only if $\Delta_I(A) \geq 0$, for all I , that is if and only if $[A] \in Gr^{\text{TNN}}(k, n)$ [41]. We remark that the weaker statement that the solution of the KP hierarchy is bounded for all real times if and only if all Plücker coordinates are non-negative was earlier proven in [54].

Any given soliton solution is associated to an infinite set of soliton data $(\mathcal{K}, [A])$. However there exists a unique **minimal** pair (k, n) such that the soliton solution can be realized with n phases $\kappa_1 < \dots < \kappa_n$, $[A] \in Gr^{\text{TNN}}(k, n)$ but not with $n - 1$ phases and $[A'] \in Gr^{\text{TNN}}(k', n')$ and either $(k', n') = (k, n - 1)$ or $(k', n') = (k - 1, n - 1)$. In the following, to avoid excessive technicalities we consider only regular and irreducible soliton data.

Definition 3.0.1. Regular and irreducible soliton data [16] *We call $(\mathcal{K}, [A])$ regular soliton data if $\mathcal{K} = \{\kappa_1 < \dots < \kappa_n\}$ and $[A] \in Gr^{\text{TNN}}(k, n)$, that is if the KP soliton solution as in (3.2) is real regular and bounded for all $(x, y, t) \in \mathbb{R}^3$.*

Moreover we call the regular soliton data $(\mathcal{K}, [A])$ irreducible if $[A]$ is a point in the irreducible part of the real Grassmannian, i.e. if the reduced row echelon matrix A has the following properties:

- (1) *Each column of A contains at least a non-zero element;*
- (2) *Each row of A contains at least one nonzero element in addition to the pivot.*

If either (1) or (2) doesn't occur, we call the soliton data $(\mathcal{K}, [A])$ reducible.

The class of solutions associated to irreducible regular soliton data has remarkable asymptotic properties both in the (x, y) plane at fixed time t and in the tropical limit ($t \rightarrow \pm\infty$), which have been related to the combinatorial classification of the irreducible part $Gr^{\text{TNN}}(k, n)$ for generic choice of the phases \mathcal{K} in a series of papers (see [14, 16, 19, 40, 41] and references therein).

According to Sato theory [64], the wave function associated to regular soliton data $(\mathcal{K}, [A])$, can be obtained from the dressing (inverse gauge) transformation of the vacuum (zero-potential) eigenfunction $\phi^{(0)}(\zeta, \bar{t}) = \exp(\theta(\zeta, \bar{t}))$, which solves $\partial_x \phi^{(0)}(\zeta, \bar{t}) = \zeta \phi^{(0)}(\zeta, \bar{t})$, $\partial_{t_l} \phi^{(0)}(\zeta, \bar{t}) = \zeta^l \phi^{(0)}(\zeta, \bar{t})$, $l \geq 2$, via the dressing (*i.e.* gauge) operator $W = 1 - \mathfrak{w}_1(\bar{t})\partial_x^{-1} - \dots - \mathfrak{w}_k(\bar{t})\partial_x^{-k}$, where $\mathfrak{w}_1(\bar{t}), \dots, \mathfrak{w}_k(\bar{t})$ are the solutions to the following linear system of equations $\partial_x^k f^{(i)} = \mathfrak{w}_1 \partial_x^{k-1} f^{(i)} + \dots + \mathfrak{w}_k f^{(i)}$, $i \in [k]$. Then,

$$L = W \partial_x W^{-1} = \partial_x + \frac{u(\bar{t})}{2} \partial_x^{-1} + \dots, \quad u(\bar{t}) = 2 \partial_x \mathfrak{w}_1(\bar{t}), \quad \psi^{(0)}(\zeta; \bar{t}) = W \phi^{(0)}(\zeta; \bar{t}),$$

respectively are the KP-Lax operator, the KP-potential (KP solution) and the KP-eigenfunction, *i.e.*

$$(3.3) \quad L \psi^{(0)}(\zeta; \bar{t}) = \zeta \psi^{(0)}(\zeta; \bar{t}), \quad \partial_{t_l} \psi^{(0)}(\zeta; \bar{t}) = B_l \psi^{(0)}(\zeta; \bar{t}), \quad l \geq 2,$$

where $B_l = (W \partial_x^l W^{-1})_+ = (L^l)_+$ (here and in the following the symbol $(\cdot)_+$ denotes the differential part of the operator).

The KP-eigenfunction associated to this class of solutions may be equivalently expressed as

$$(3.4) \quad \mathfrak{D}^{(k)} \phi^{(0)}(\zeta; \bar{t}) = W \partial_x^k \phi^{(0)}(\zeta; \bar{t}) = (\zeta^k - \mathfrak{w}_1(\bar{t})\zeta^{k-1} - \dots - \mathfrak{w}_k(\bar{t})) \phi^{(0)}(\zeta; \bar{t}) = \zeta^k \psi^{(0)}(\zeta; \bar{t}),$$

with

$$(3.5) \quad \mathfrak{D}^{(k)} = W \partial_x^k = \partial_x^k - \mathfrak{w}_1(\bar{t}) \partial_x^{k-1} - \dots - \mathfrak{w}_k(\bar{t}).$$

Definition 3.0.2. Sato divisor coordinates

Let the regular soliton data be $(\mathcal{K}, [A])$, $\mathcal{K} = \{\kappa_1 < \dots < \kappa_n\}$, $[A] \in Gr^{TNN}(k, n)$. We call Sato divisor coordinates at time \bar{t} , the set of roots $\zeta_j(\bar{t})$, $j \in [k]$, of the characteristic equation associated to the Dressing transformation

$$(3.6) \quad \zeta_j^k(\bar{t}) - \mathfrak{w}_1(\bar{t}) \zeta_j^{k-1}(\bar{t}) - \dots - \mathfrak{w}_{k-1}(\bar{t}) \zeta_j(\bar{t}) - \mathfrak{w}_k(\bar{t}) = 0.$$

In [54] it is proven the following proposition

Proposition 3.0.1. Reality and simplicity of the KP soliton divisor [54]. Let the regular soliton data be $(\mathcal{K}, [A])$, $\mathcal{K} = \{\kappa_1 < \dots < \kappa_n\}$, $[A] \in Gr^{TNN}(k, n)$. Then for all \bar{t} , $\zeta_j^k(\bar{t})$ are real and satisfy $\zeta_j(\bar{t}) \in [\kappa_1, \kappa_n]$, $j \in [k]$. Moreover for almost every \bar{t} the roots of (3.6) are simple.

The following definition is then fully justified.

Definition 3.0.3. Sato algebraic-geometric data Let $(\mathcal{K}, [A])$ be given regular soliton data with $[A]$ belonging to a $|D|$ dimensional positroid cell in $Gr^{TNN}(k, n)$. Let Γ_0 be a copy of \mathbb{CP}^1 with marked points P_0 , local coordinate ζ such that $\zeta^{-1}(P_0) = 0$ and $\zeta(\kappa_1) < \zeta(\kappa_2) < \dots < \zeta(\kappa_n)$. Let \bar{t}_0 be real and such that the real roots $\zeta_j(\bar{t}_0)$ in (3.6) are simple.

Then to the data $(\mathcal{K}, [A], \Gamma_0 \setminus \{P_0\}, \bar{t}_0)$ we associate the **Sato divisor** $\mathcal{D}_{S, \Gamma_0} = \mathcal{D}_{S, \Gamma_0}(\bar{t}_0)$

$$(3.7) \quad \mathcal{D}_{S, \Gamma_0} = \{\gamma_{S, j} \in \Gamma_0 : \zeta(\gamma_{S, j}) = \zeta_j(\bar{t}_0), \quad j \in [k]\},$$

and the normalized **Sato wave function**

$$(3.8) \quad \hat{\psi}(P, \bar{t}) = \frac{\mathfrak{D} \phi^{(0)}(P; \bar{t})}{\mathfrak{D} \phi^{(0)}(P; \bar{t}_0)} = \frac{\psi^{(0)}(P; \bar{t})}{\psi^{(0)}(P; \bar{t}_0)}, \quad \forall P \in \Gamma_0 \setminus \{P_0\},$$

with $\mathfrak{D} \phi^{(0)}(\zeta; \bar{t})$ as in (3.4). By definition $(\hat{\psi}_0(P, \bar{t})) + \mathcal{D}_{S, \Gamma_0} \geq 0$, for all \bar{t} .

In the following, we use the same symbol for the points in Γ_0 and their local coordinates to simplify notations. In particular, we use the symbol $\gamma_{S, j}$ both for the Sato divisor points and Sato divisor coordinates.

Remark 3.0.1. Incompleteness of Sato algebraic–geometric data *Let $1 \leq k < n$ and let \vec{t}_0 be fixed. Given the phases $\kappa_1 < \dots < \kappa_n$ and the spectral data $(\Gamma_0 \setminus \{P_0\}, \mathcal{D}_{S, \Gamma_0})$, where $\mathcal{D}_{S, \Gamma_0} = \mathcal{D}_{S, \Gamma_0}(\vec{t}_0)$ is a k point divisor satisfying Proposition 3.0.1, it is, in general, impossible to identify uniquely the point $[A] \in Gr^{TNN}(k, n)$ corresponding to such spectral data. Indeed, assume that $[A]$ belongs to an irreducible positroid cell of dimension $|D|$. Then the degree of $\mathcal{D}_{S, \Gamma_0}$ equals k , but $\max\{k, n - k\} \leq |D| \leq k(n - k)$.*

In our construction we propose a completion of the Sato algebraic–geometric data based on singular finite–gap theory on reducible algebraic curves [45, 3, 5] and we use the representation of totally non–negative Grassmannians via directed planar networks [61] to preserve the reality and regularity of the KP divisor in the solitonic limit.

Indeed, soliton KP solutions can be obtained from regular finite–gap solutions of (3.1) by proper degenerations of the spectral curve [44], [21]. The spectral data for KP finite–gap solutions are introduced and described in [43, 44]. The spectral data for this construction are: a finite genus g compact Riemann surface Γ with a marked point P_0 , a local parameter $1/\zeta$ near P_0 and a non-special divisor $\mathcal{D} = \gamma_1 + \dots + \gamma_g$ of degree g in Γ .

The Baker-Akhiezer function $\hat{\psi}(P, \vec{t})$, $P \in \Gamma$, is defined by the following analytic properties:

- (1) For any fixed \vec{t} the function $\hat{\psi}(P, \vec{t})$ is meromorphic in P on $\Gamma \setminus P_0$;
- (2) On $\Gamma \setminus P_0$ the function $\hat{\psi}(P, \vec{t})$ is regular outside the divisor points γ_j and has at most first order poles at the divisor points. Equivalently, if we consider the line bundle $\mathcal{L}(\mathcal{D})$ associated to \mathcal{D} , then for each fixed \vec{t} the function $\hat{\psi}(P, \vec{t})$ is a holomorphic section of $\mathcal{L}(\mathcal{D})$ outside P_0 .
- (3) $\hat{\psi}(P, \vec{t})$ has an essential singularity at the point P_0 with the following asymptotics:

$$\hat{\psi}(\zeta, \vec{t}) = e^{\zeta x + \zeta^2 y + \zeta^3 t + \dots} (1 - \chi_1(\vec{t})\zeta^{-1} - \dots - \chi_k(\vec{t})\zeta^{-k} - \dots).$$

For generic data these properties define a unique function, which is a common eigenfunction to all KP hierarchy auxiliary linear operators $-\partial_{t_j} + B_j$, where $B_j = (L^j)_+$, and the Lax operator $L = \partial_x + \frac{u(\vec{t})}{2}\partial_x^{-1} + u_2(\vec{t})\partial_x^{-2} + \dots$. Therefore all these operators commute and the potential $u(\vec{t})$ satisfies the KP hierarchy. In particular, the KP equation arises in the Zakharov-Shabat commutation representation [70] as the compatibility for the second and the third operator: $[-\partial_y + B_2, -\partial_t + B_3] = 0$, with $B_2 \equiv (L^2)_+ = \partial_x^2 + u$, $B_3 = (L^3)_+ = \partial_x^3 + \frac{3}{4}(u\partial_x + \partial_x u) + \tilde{u}$ and $\partial_x \tilde{u} = \frac{3}{4}\partial_y u$. The Its-Matveev formula represents the KP hierarchy solution $u(\vec{t})$ in terms of the Riemann theta-functions associated with Γ (see, for example, [20]).

In [22] there were established the necessary and sufficient conditions on spectral data to generate real regular KP hierarchy solutions for all real \vec{t} , under the assumption that Γ is smooth and has genus g :

- (1) Γ possesses an antiholomorphic involution $\sigma : \Gamma \rightarrow \Gamma$, $\sigma^2 = \text{id}$, which has the maximal possible number of fixed components (real ovals), $g + 1$, therefore (Γ, σ) is an M-curve [36, 58, 69].
- (2) P_0 lies in one of the ovals, and each other oval contains exactly one divisor point. The oval containing P_0 is called “infinite” and all other ovals are called “finite”.

The set of real ovals divides Γ into two connected components. Each of these components is homeomorphic to a sphere with $g + 1$ holes. The sufficient condition of the Theorem in [22] still holds true if the spectral curve Γ degenerates in such a way that the divisor remains in the finite ovals at a finite distance from the essential singularity [22]. Of course, this condition is not necessary for degenerate curves. Moreover, the algebraic–geometric data for a given soliton data

$(\mathcal{K}, [A])$ are not unique since we can construct infinitely many reducible curves generating the same soliton solutions.

In [3], for any soliton data in $Gr^{\text{TP}}(k, n)$ and any fixed value of the parameter $\xi \gg 1$, we have constructed a curve Γ_ξ , which is the rational degeneration of a smooth \mathbf{M} -curve of minimal genus $k(n-k)$ and a degree $k(n-k)$ divisor satisfying the reality conditions of Dubrovin and Natanzon's theorem. In [5] we have then extended this construction to any soliton data in $Gr^{\text{TN}}(k, n)$ by modeling the spectral curve Γ on Postnikov Le-graph so that components, marked points and ovals of the curve correspond to vertices, edges and ovals in the graph. In particular for any given positroid cell, such Γ is a rational degeneration of an \mathbf{M} -curve of minimal genus equal to its dimension.

In the following Sections, we generalize the construction in [5] to the trivalent plabic (= planar bicolored) networks in the disk in Postnikov equivalence class for $[A]$ and prove the invariance of the KP divisor. Following [5], we define the desired properties of Baker-Akhiezer functions on reducible curves associated with a given soliton data.

Definition 3.0.4. Real regular algebraic-geometric data associated with a given soliton solution. *Let the soliton data $(\mathcal{K}, [A])$ be fixed, where \mathcal{K} is a collection of real phases $\kappa_1 < \kappa_2 < \dots < \kappa_n$, $[A] \in Gr^{\text{TN}}(k, n)$. Let $|D|$ be the dimension of the irreducible positroid cell to which $[A]$ belongs. Let $(\Gamma_0, P_0, \mathcal{D}_{S, \Gamma_0})$ be the Sato algebraic-geometric data for $(\mathcal{K}, [A])$ as in Definition 3.0.3 for a given \tilde{t}_0 . Let Γ be a reducible connected curve with a marked point P_0 , a local parameter $1/\zeta$ near P_0 such that*

- (1) Γ_0 is the irreducible component of Γ containing P_0 ;
- (2) Γ may be obtained from a rational degeneration of a smooth \mathbf{M} -curve of genus g , with $g \geq |D|$ and the antiholomorphic involution preserves the maximum number of the ovals in the limit, so that Γ possesses $g+1$ real ovals.

Assume that \mathcal{D} is a degree g non-special divisor on $\Gamma \setminus P_0$, and that $\hat{\psi}$ is the normalized Baker-Akhiezer function associated to such data, i.e. for any \tilde{t} its pole divisor is contained in \mathcal{D} : $(\hat{\psi}(P, \tilde{t})) + \mathcal{D} \geq 0$ on $\Gamma \setminus P_0$, where (f) denotes the divisor of f .

We say that **the algebraic-geometric data $(\Gamma, P_0, \mathcal{D})$ are associated to the soliton data $(\mathcal{K}, [A])$** , if the restriction of \mathcal{D} to Γ_0 coincides with the Sato divisor $\mathcal{D}_{S, \Gamma_0}$ and the restriction of $\hat{\psi}$ to Γ_0 coincides with the Sato normalized dressed wave function for the soliton data $(\mathcal{K}, [A])$.

We say that **the divisor \mathcal{D} satisfies the reality and regularity conditions** if P_0 belongs to one of the fixed ovals and the boundary of each other oval contains exactly one divisor point.

4. ALGEBRAIC-GEOMETRIC APPROACH FOR IRREDUCIBLE KP SOLITON DATA IN $Gr^{\text{TN}}(k, n)$

In [5] we provided a construction associating a reducible \mathbf{M} -curve and real regular KP soliton divisor to the canonically oriented Le-network representing a given real regular irreducible soliton data $(\mathcal{K}, [A])$ with $[A] \in Gr^{\text{TN}}(k, n)$, and such that the restriction of the divisor to the component Γ_0 is the Sato divisor. In this Section we generalize this construction to any PBDTP network representing $[A]$. We also prove the invariance of this KP divisor with respect to geometrical transformations of the graph and the weight gauge. In the case of reducible graphs there is an extra gauge freedom in fixing the weights representing the same point in the Grassmannian, and the divisor changes non-trivially with respect to this extra gauge freedom. This is natural since in this case the dimension of the parametrization space is strictly bigger than the dimension of the positroid cell.

In the following we fix the regular irreducible soliton data $(\mathcal{K}, [A])$, and for a given PBDTP network representing $[A]$ we present a **direct** construction of the algebraic geometric data associated to points in irreducible positroid cells of $Gr^{\text{TN}}(k, n)$. Γ_0 is the rational curve associated

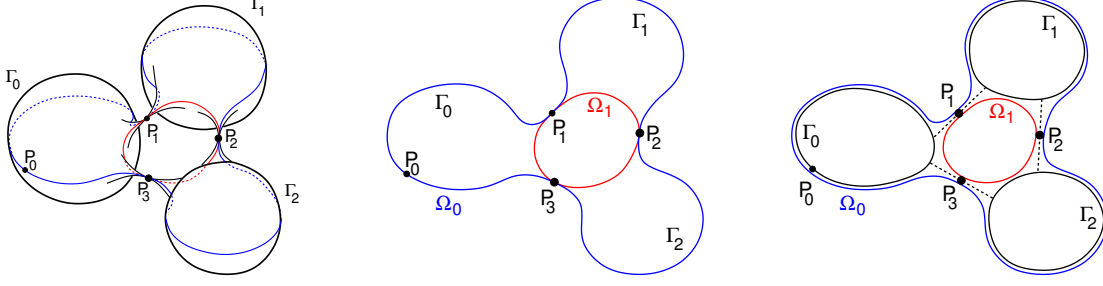


FIGURE 9. The model of reducible rational curve. On the left we have three Riemann spheres Γ_0 , Γ_1 and Γ_2 glued at the points P_1 , P_2 , P_3 . The real part of the curve is drawn in blue and red. In the middle we draw just the real part of the curve and evidence the two real ovals Ω_0 (drawn blue) and Ω_1 (drawn red). On the right we provide the representation of the real topological model of the curve used throughout the paper: The real parts of each rational component is a circle and the double points are represented by dashed segments.

to Sato dressing and is equipped with a finite number of marked points: the ordered real phases $\mathcal{K} = \{\kappa_1 < \dots < \kappa_n\}$, the essential singularity P_0 of the wave function and the Sato divisor $\mathcal{D}_{S, \Gamma_0}$ as in Definition 3.0.3. The normalized wave function $\hat{\psi}$ on $\Gamma_0 \setminus \{P_0\}$ is the normalized Sato wave function (3.8). In the present paper, we do the following:

Main construction Assume we are given a real regular bounded multiline KP soliton solution generated by the following soliton data:

- (1) A set of n real ordered phases $\mathcal{K} = \{\kappa_1 < \kappa_2 < \dots < \kappa_n\}$;
- (2) A point $[A] \in \mathcal{S}_{\mathcal{M}}^{TNN} \subset Gr^{TNN}(k, n)$, where $\mathcal{S}_{\mathcal{M}}^{TNN}$ is an irreducible positroid cell of dimension $|D|$.

Let \mathcal{N} be a PBDTP network in the disk in Postnikov equivalence class representing $[A]$ and let \mathcal{G} be the graph of \mathcal{N} . If the network is reduced, there are no extra conditions, otherwise we assume the data to be generic in the sense that the system of edge vectors on \mathcal{N} does not possess zero vectors. Then, we associate the following algebraic-geometric objects to each triple $(\mathcal{K}, [A]; \mathcal{N})$:

- (1) A reducible curve $\Gamma = \Gamma(\mathcal{G})$ which is a rational degeneration of a smooth M-curve of genus $g \geq |D|$, where $g + 1$ is the number of faces of \mathcal{G} . In our approach, the curve Γ_0 is one of the irreducible components of Γ . The marked point P_0 belongs to the intersection of Γ_0 with an oval (infinite oval);
- (2) A unique real and regular degree g non-special KP divisor $\mathcal{D}_{KP, \Gamma}(\mathcal{K}, [A])$ such that any finite oval contains exactly one divisor point and $\mathcal{D}_{KP, \Gamma}(\mathcal{K}, [A]) \cap \Gamma_0$ coincides with the Sato divisor;
- (3) A unique KP wave-function $\hat{\psi}$ as in Definition 3.0.4 such that
 - (a) Its restriction to $\Gamma_0 \setminus \{P_0\}$ coincides with the normalized Sato wave function (3.8);
 - (b) Its pole divisor has degree $\mathfrak{d} \leq g$ and is contained in $\mathcal{D}_{KP, \Gamma}(\mathcal{K}, [A])$.

In particular, if $\mathcal{G} = \mathcal{G}_T$ is the trivalent bicolored Le-graph [61], then $\Gamma(\mathcal{G}_T)$ is a rational degeneration of on M-curve of minimal genus $|D|$, it has exactly $|D| + 1$ ovals, and $\mathfrak{d} = g = |D|$ [5].

4.1. The reducible rational curve $\Gamma = \Gamma(\mathcal{G})$. The construction of $\Gamma(\mathcal{G})$ is a straightforward modification of a special case in the classical construction of nodal curves by dual graphs [9].

Remark 4.1.1. Labeling of edges at vertices Let \mathcal{G} be a PBDTP graph as in Definition 2.1.3. We number the edges at an internal vertex V anticlockwise in increasing order with the following

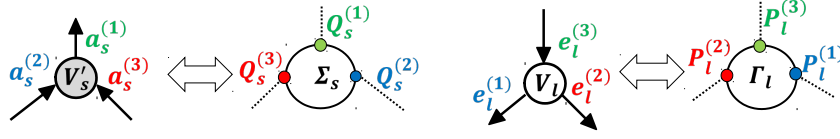


FIGURE 10. The rule for the marked points on the copies Σ_j and Γ_l corresponding to the edges of trivalent black and white vertices under the assumption that the boundary vertices lie on a horizontal line.

TABLE 1. The graph \mathcal{G} vs the reducible rational curve Γ

\mathcal{G}	Γ
Boundary of disk	Copy of \mathbb{CP}^1 denoted Γ_0
Boundary vertex b_l	Marked point κ_l on Γ_0
Black vertex V'_s	Copy of \mathbb{CP}^1 denoted Σ_s
White vertex V_l	Copy of \mathbb{CP}^1 denoted Γ_l
Internal Edge	Double point
Face	Oval
Infinite face	Infinite oval Ω_0

rule: the unique edge starting at a black vertex is numbered 1 and the unique edge ending at a white vertex is numbered 3 (see also Figure 10).

We construct the curve $\Gamma = \Gamma(\mathcal{G})$ gluing a finite number of copies of \mathbb{CP}^1 , each corresponding to an internal vertex in \mathcal{G} , and one copy of $\mathbb{CP}^1 = \Gamma_0$, corresponding to the boundary of the disk, at pairs of points corresponding to the edges of \mathcal{G} . On each component, we fix a local affine coordinate ζ (see Definition 4.2.1) so that the coordinates at each pair of glued points are real. The points with real ζ form the real part of the given component. We represent the real part of Γ as the union of the ovals (circles) corresponding to the faces of \mathcal{G} . For the case in which \mathcal{G} is the Le-network see [5].

We use the following representation for real rational curves (see Figure 9 and [3, 5]): we only draw the real part of the curve, i.e. we replace each $\Gamma_j = \mathbb{CP}^1$ by a circle. Then we schematically represent the real part of the curve by drawing these circles separately and connecting the glued points by dashed segments. The planarity of the graph implies that Γ is a reducible rational M-curve.

Construction 4.1.1. The curve $\Gamma(\mathcal{G})$. Let $\mathcal{K} = \{\kappa_1 < \dots < \kappa_n\}$ and let $\mathcal{S}_M^{TNN} \subset Gr^{TNN}(k, n)$ be a fixed irreducible positroid cell of dimension $|D|$. Let \mathcal{G} be a PBDTP graph representing \mathcal{S}_M^{TNN} with $g + 1$ faces, $g \geq |D|$. Then the curve $\Gamma = \Gamma(\mathcal{G})$ is associated to \mathcal{G} using the correspondence in Table 1, after reflecting the graph w.r.t. a line orthogonal to the one containing the boundary vertices (we reflect the graph to have the natural increasing order of the marked points κ_j on $\Gamma_0 \subset \Gamma(\mathcal{G})$). More precisely:

- (1) We denote Γ_0 the copy of \mathbb{CP}^1 corresponding to the boundary of the disk and mark on it the points $\kappa_1 < \dots < \kappa_n$ corresponding to the boundary vertices b_1, \dots, b_n on \mathcal{G} . We assume that $P_0 = \infty$;

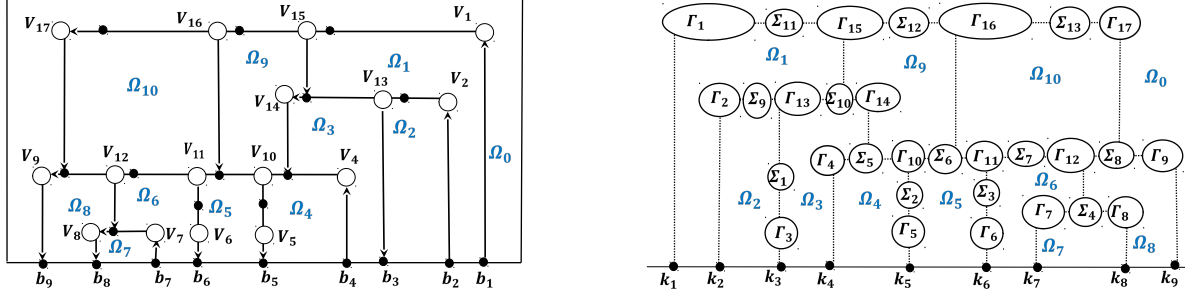


FIGURE 11. The correspondence between the graph \mathcal{G} and the curve $\Gamma(\mathcal{G})$ for an irreducible positroid cell in $Gr^{TNN}(4,9)$.

- (2) A copy of \mathbb{CP}^1 corresponds to any internal vertex of \mathcal{G} . We use the symbol Γ_l (respectively Σ_s) for the copy of \mathbb{CP}^1 corresponding to the white vertex V_l (respectively the black vertex V'_s);
- (3) On each copy of \mathbb{CP}^1 corresponding to an internal vertex V , we mark as many points as edges at V . In Remark 4.1.1 we number the edges at V anticlockwise in increasing order, so that, on the corresponding copy of \mathbb{CP}^1 , the marked points are numbered clockwise because of the mirror rule (see Figure 10);
- (4) Gluing rules between copies of \mathbb{CP}^1 are ruled by edges: we glue copies of \mathbb{CP}^1 in pairs at the marked points corresponding to the end points of the edge;
- (5) The faces of \mathcal{G} correspond to the ovals of Γ .

In Figure 11 we present an example of curve corresponding to a network representing an irreducible positroid cell in $Gr^{TNN}(4,9)$. Other examples are studied in Sections 9 and 10. We remark that the vertex gauge freedom of the graph defined in Section 2.3 has no effect on the curve Γ .

Remark 4.1.2. Universality of the reducible rational curve $\Gamma(\mathcal{G})$. If \mathcal{G} is a trivalent graph representing \mathcal{S} , the construction of $\Gamma = \Gamma(\mathcal{G})$ does **not** require the introduction of parameters. Therefore it provides a **universal** curve $\Gamma = \Gamma(\mathcal{S}; \mathcal{G})$ for the whole positroid cell \mathcal{S} . In Section 5, we show that the points of \mathcal{S} are parametrized (in the sense of birational equivalence) by the divisor positions at the finite ovals.

The number of copies of \mathbb{CP}^1 used to construct $\Gamma(\mathcal{G})$ is **excessive** in the sense that the number of ovals and the KP divisor is invariant if we eliminate all copies of \mathbb{CP}^1 corresponding to bivalent vertices (see Section 8 and [5]).

The curve $\Gamma(\mathcal{G})$ is a partial normalization [9] of a connected reducible nodal plane curve with $g+1$ ovals and is a rational degeneration of a genus g smooth M-curve.

Proposition 4.1.1. $\Gamma(\mathcal{G})$ is the rational degeneration of a smooth M-curve of genus g . Let $\mathcal{K} = \{\kappa_1 < \dots < \kappa_n\}$ and $\mathcal{S}_{\mathcal{M}}^{TNN}$ be an irreducible positroid cell in $Gr^{TNN}(k, n)$ corresponding to the matroid \mathcal{M} . Let $\Gamma = \Gamma(\mathcal{G})$ be as in Construction 4.1.1. Then

- (1) Γ possesses $g+1$ ovals which we label Ω_s , $s \in [0, g]$;
- (2) Γ is the rational degeneration of a regular M-curve of genus g .

Proof. The proof follows along similar lines as in [5], where we prove the analogous statement in the case of the Le-graph. Let t_W, t_B, d_W and d_B respectively be the number of trivalent white, trivalent black, bivalent white and bivalent black internal vertices of \mathcal{G} . Let n_I be the number of

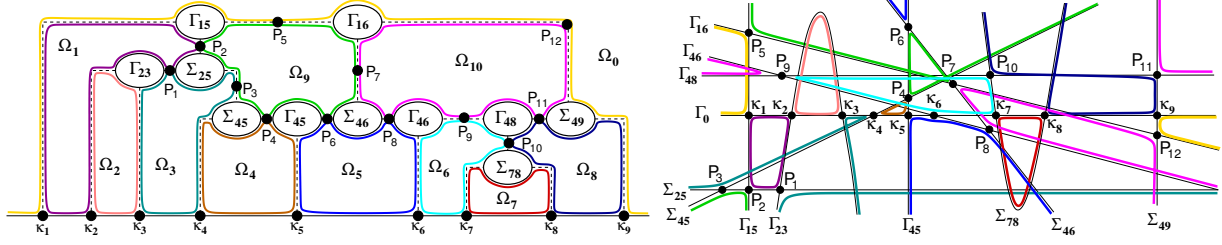


FIGURE 12. The topological model of the oval structure of Γ [left] is the partial normalization of the reducible plane nodal curve [right]. The nodal points, P_s , $s \in [12]$, and κ_j , $j \in [9]$, surviving the partial normalization are marked on the nodal curve [right] and are represented by dashed segments as usual on topological model [left].

internal edges (i.e. edges not connected to a boundary vertex) of \mathcal{G} . By Euler formula we have $g = n_I + n - (t_W + t_B + d_W + d_B)$. Moreover, there hold the following relations between the number of edges and that of vertices $3(t_W + t_B) + 2(d_W + d_B) = 2n_I + n$, $2t_B + t_W + d_W + d_B = n_I + k$. Therefore

$$(4.1) \quad t_W = g - k, \quad t_B = g - n + k, \quad d_W + d_B = n_I + 2n - 3g.$$

By definition, Γ is represented by $d = 1 + t_W + t_B + d_W + d_B = n_I + n - g + 1$ complex projective lines which intersect generically in $d(d-1)/2$ double points. The regular curve is obtained keeping the number of ovals fixed while perturbing the double points corresponding to the edges in \mathcal{G} creating regular gaps (see [5] for explicit formulas for the perturbations). The total number of desingularized double points, N_d equals the total number of edges in \mathcal{G} : $N_d = n_I + n$. Then the genus of the smooth curve is given by the following formula $N_d - d + 1 = g$. \square

The regular M-curve is the normalization of the nodal plane curve whose explicit construction follows along similar lines as in [5], see also [46]. In Figure 12 we show such continuous deformation for the example in Figure 11 after the elimination of all copies of \mathbb{CP}^1 corresponding to bivalent vertices in the network. In this case $d = 14$ (Γ is representable by the union of two quadrics and 10 lines). Under genericity assumptions, the reducible rational curve Γ has $\Delta = 89$ singular points before partial normalization. The perturbed regular curve is obtained by perturbing $N_d = 21$ ordinary intersection points (for each of them $\delta = 1$), corresponding to the double points in the topological representation in Figure 12[left]. $\Delta - N_d = 68$ points remain intersections after this deformation and are resolved during normalization. Finally, the normalized perturbed regular curve has then genus $g = \frac{(d-1)(d-2)}{2} - \Delta + N_d = 10$.

4.2. The KP divisor on $\Gamma(\mathcal{G})$ for the soliton data $(\mathcal{K}, [A])$. Throughout this Section we fix both the soliton stratum $(\mathcal{K}, \mathcal{S}_{\mathcal{M}}^{\text{TNN}})$, with $\mathcal{K} = \{\kappa_1 < \dots < \kappa_n\}$ and $\mathcal{S}_{\mathcal{M}}^{\text{TNN}} \subset Gr^{\text{TNN}}(k, n)$ an irreducible positroid cell of dimension $|D|$, and the PBDTP graph \mathcal{G} in the disk representing $\mathcal{S}_{\mathcal{M}}^{\text{TNN}}$ in Postnikov equivalence class. Let $g+1$ be the number of faces of \mathcal{G} with $g \geq |D|$, and let $\Gamma = \Gamma(\mathcal{G})$ be the curve corresponding to \mathcal{G} as in Construction 4.1.1. In this Section we state the main results of our paper:

- (1) **Construction of the KP divisor $\mathcal{D}_{\text{KP}, \Gamma}$ on a given curve Γ for soliton data $(\mathcal{K}, [A])$:** Given the data $(\mathcal{K}, \mathcal{S}_{\mathcal{M}}^{\text{TNN}}; \mathcal{G})$
 - (a) If \mathcal{G} is either reduced or reducible and there exists a network \mathcal{N} of graph \mathcal{G} representing $[A] \in \mathcal{S}_{\mathcal{M}}^{\text{TNN}}$ such that all edge vectors on \mathcal{N} are non-zero, then we prove that the curve $\Gamma = \Gamma(\mathcal{G})$ can be used as the spectral curve for the soliton data $(\mathcal{K}, [A])$

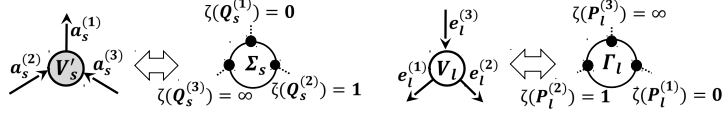


FIGURE 13. Local coordinates on the components Γ_l and Σ_s (reflection w.r.t. the vertical line): the marked point $P_l^{(m)} \in \Gamma_l$ corresponds to the edge $e_l^{(m)}$ at the white vertex V_l and the marked point $Q_s^{(m)} \in \Sigma_s$ corresponds to the edge $a_s^{(m)}$ at the black vertex V'_s .

by constructing a unique degree g effective real and regular KP divisor $\mathcal{D}_{\text{KP},\Gamma}$ and a unique real and regular KP wave function $\hat{\psi}(P, \bar{t})$ on Γ ;

- (b) If the network \mathcal{N} of reducible graph \mathcal{G} representing $[A] \in \mathcal{S}_{\mathcal{M}}^{\text{TNN}}$ possesses zero vectors, we distinguish two cases in Definition 11.2.1 and we briefly explain the modification to our construction in such case in Section 11.2. We plan to discuss thoroughly the problem of networks admitting zero vectors in a future publication.
- (2) **Invariance of $\mathcal{D}_{\text{KP},\Gamma}$** The construction of $\mathcal{D}_{\text{KP},\Gamma}$ is carried out using a directed network \mathcal{N} representing $[A]$ of graph \mathcal{G} and fixing a gauge ray direction. We prove that $\mathcal{D}_{\text{KP},\Gamma}$ is independent on the weight gauge, the vertex gauge, the gauge ray direction and the orientation of the network. In particular, if \mathcal{G} is a reduced graph move-equivalent to the Le-graph, we get a parametrization of $\mathcal{S}_{\mathcal{M}}^{\text{TNN}}$ via KP divisors on $\Gamma(\mathcal{G})$.
- (3) **Transformation laws between curves and divisors induced by Postnikov moves and reductions on networks:** Postnikov [61] introduces moves and reductions which transform networks preserving the boundary measurement, thus classifying networks representing a given point $[A] \in \mathcal{S}_{\mathcal{M}}^{\text{TNN}}$. In our construction, any such transformation induces a change of the spectral curve and of the KP divisor. In Section 8, we provide the explicit transformation of the divisor under the action of such moves and reductions.

Throughout the paper, we assign affine coordinates to each component of $\Gamma(\mathcal{G})$ using the orientation of the graph \mathcal{G} , and we use the same symbol ζ for any such affine coordinate to simplify notations.

Definition 4.2.1. Affine coordinates on $\Gamma(\mathcal{G})$ On each copy of \mathbb{CP}^1 the local coordinate ζ is uniquely identified by the following properties:

- (1) On Γ_0 , $\zeta^{-1}(P_0) = 0$ and $\zeta(\kappa_1) < \dots < \zeta(\kappa_n)$. To abridge notations, we identify the ζ -coordinate with the marked points $\kappa_j = \zeta(\kappa_j)$, $j \in [n]$;
- (2) On the component Γ_l corresponding to the internal white vertex V_l :

$$\zeta(P_l^{(1)}) = 0, \quad \zeta(P_l^{(2)}) = 1, \quad \zeta(P_l^{(3)}) = \infty,$$

whereas on the component Σ_s corresponding to the internal black vertex V'_s :

$$\zeta(Q_s^{(1)}) = 0, \quad \zeta(Q_s^{(2)}) = 1, \quad \zeta(Q_s^{(3)}) = \infty.$$

We illustrate Definition 4.2.1 in Figure 13 (see also Figure 10).

In view of Definition 3.0.4, the desired properties of the KP divisor and of the KP wave function on $\Gamma(\mathcal{G})$ for given soliton data $(\mathcal{K}, [A])$ are the following.

Definition 4.2.2. Real regular KP divisor compatible with $[A] \in \mathcal{S}_{\mathcal{M}}^{\text{TNN}}$. Let Ω_0 be the infinite oval containing the marked point $P_0 \in \Gamma_0$ and let Ω_s , $s \in [g]$ be the finite ovals of Γ . Let $\mathcal{D}_{\text{S},\Gamma_0} = \mathcal{D}_{\text{S},\Gamma_0}(\bar{t}_0)$ be the Sato divisor for the soliton data $(\mathcal{K}, [A])$. We call a degree g divisor $\mathcal{D}_{\text{KP},\Gamma} \in \Gamma \setminus \{P_0\}$ a real and regular KP divisor compatible with $(\mathcal{K}, [A])$ if:

- (1) $\mathcal{D}_{\text{KP},\Gamma} \cap \Gamma_0 = \mathcal{D}_{\text{S},\Gamma_0}$;
- (2) There is exactly one divisor point on each component of Γ corresponding to a trivalent white vertex;
- (3) In any finite oval Ω_s , $s \in [g]$, there is exactly one divisor point;
- (4) In the infinite oval Ω_0 , there is no divisor point.

Definition 4.2.3. A real regular KP wave function on Γ corresponding to $\mathcal{D}_{\text{KP},\Gamma}$: Let $\mathcal{D}_{\text{KP},\Gamma}$ be a degree g real regular divisor on Γ satisfying Definition 4.2.2. A function $\hat{\psi}(P, \vec{t})$, where $P \in \Gamma \setminus \{P_0\}$ and \vec{t} are the KP times, is called a real and regular KP wave function on Γ corresponding to $\mathcal{D}_{\text{KP},\Gamma}$ if:

- (1) $\hat{\psi}(P, \vec{t}_0) = 1$ at all points $P \in \Gamma \setminus \{P_0\}$;
- (2) The restriction of $\hat{\psi}$ to $\Gamma_0 \setminus \{P_0\}$ coincides with the normalized Sato wave function defined in (3.8): $\hat{\psi}(P, \vec{t}) = \frac{\psi^{(0)}(P; \vec{t})}{\psi^{(0)}(P; \vec{t}_0)}$;
- (3) For all $P \in \Gamma \setminus \Gamma_0$ the function $\hat{\psi}(P, \vec{t})$ satisfies all equations (3.3) of the dressed hierarchy;
- (4) If both \vec{t} and $\zeta(P)$ are real, then $\hat{\psi}(\zeta(P), \vec{t})$ is real. Here $\zeta(P)$ is the local affine coordinate on the corresponding component of Γ as in Definition 4.2.1;
- (5) $\hat{\psi}$ takes equal values at pairs of glued points $P, Q \in \Gamma$, for all \vec{t} : $\hat{\psi}(P, \vec{t}) = \hat{\psi}(Q, \vec{t})$;
- (6) For each fixed \vec{t} the function $\hat{\psi}(P, \vec{t})$ is meromorphic of degree $\leq g$ in P on $\Gamma \setminus \{P_0\}$: for any fixed \vec{t} we have $(\hat{\psi}(P, \vec{t})) + \mathcal{D}_{\text{KP},\Gamma} \geq 0$ on $\Gamma \setminus P_0$, where (f) denotes the divisor of f . Equivalently, for any fixed \vec{t} on $\Gamma \setminus \{P_0\}$ the function $\hat{\psi}(\zeta, \vec{t})$ is regular outside the points of $\mathcal{D}_{\text{KP},\Gamma}$ and at each of these points either it has a first order pole or is regular;
- (7) For each $P \in \Gamma \setminus \{P_0\}$ outside $\mathcal{D}_{\text{KP},\Gamma}$ the function $\hat{\psi}(P, \vec{t})$ is regular in \vec{t} for all times.

Theorem 4.2.1. *Existence and uniqueness of a real and regular KP divisor and KP wave function on Γ .* Let the phases \mathcal{K} , the irreducible positroid cell $\mathcal{S}_{\mathcal{M}}^{\text{TNN}} \subset \text{Gr}^{\text{TNN}}(k, n)$, the PBDTP graph \mathcal{G} representing $\mathcal{S}_{\mathcal{M}}^{\text{TNN}}$ be fixed. Let $\Gamma = \Gamma(\mathcal{G})$ with marked point $P_0 \in \Gamma_0$ be as in Construction 4.1.1.

If \mathcal{G} is reduced and equivalent to the Le-network via a finite sequence of moves of type (M1), (M3) and flip moves (M2), there are no extra conditions and, for any $[A] \in \mathcal{S}_{\mathcal{M}}^{\text{TNN}}$, let \mathcal{N} of graph \mathcal{G} be a network representing $[A]$. Otherwise if \mathcal{G} is reducible, let $[A] \in \mathcal{S}_{\mathcal{M}}^{\text{TNN}}$ such that there exists a network \mathcal{N} of graph \mathcal{G} representing $[A]$ not possessing zero edge vectors.

Then, there exists a reference time \vec{t}_0 such that, to the following data $(\mathcal{K}, [A]; \Gamma, P_0; \mathcal{N}; \vec{t}_0)$, we associate

- (1) A **unique** real regular degree g KP divisor $\mathcal{D}_{\text{KP},\Gamma}$ as in Definition 4.2.2;
- (2) A **unique** real regular KP wave function $\hat{\psi}(P, \vec{t})$ corresponding to this divisor satisfying Definition 4.2.3.

Moreover, $\mathcal{D}_{\text{KP},\Gamma}$ and $\hat{\psi}(P, \vec{t})$ are both invariant with respect to changes of the vertex, the weight and the ray direction gauges and of the orientation of the graph \mathcal{G} .

Sketch of the proof: The construction of the KP divisor $\mathcal{D}_{\text{KP},\Gamma}$ and of the Baker–Akhiezer function $\hat{\psi}(P, \vec{t})$ on $\Gamma(\mathcal{G})$ is carried in several steps:

- (1) **The edge wave function** In Section 5, we define a non normalized dressed edge wave function $\Psi_e(\vec{t})$ at the edges $e \in \mathcal{N}$ using the system of vectors introduced in Section 2. We then assign a degree $g - k$ dressed network divisor $\mathcal{D}_{\text{dr},\mathcal{N}}$ to \mathcal{N} using the linear relations at the trivalent white vertices. The dependence of both the edge wave function and of the network divisor on the gauge ray direction, the weight gauge, the vertex gauge and

the orientation of the network is ruled by the corresponding transformation properties of the edge vectors discussed in Section 2;

- (2) **The KP divisor on Γ** In Section 6.1, we define the KP divisor on Γ . We rule the value of the KP wave function at the double points using the system of edge vectors introduced in Section 2. Therefore each dressed network divisor number is the local coordinate of a KP divisor point $P_l^{(\text{dr})} \in \Gamma_l$ and the position of $P_l^{(\text{dr})}$ is independent on the orientation of the network, on the gauge ray direction, on the weight gauge and on the vertex gauge. This set of divisor points has degree $g - k$ equal to the number of trivalent white vertices in the PBDTP graph \mathcal{G} . The KP divisor $\mathcal{D}_{\text{KP},\Gamma}$ is defined as the sum of this divisor with the degree k Sato divisor $\mathcal{D}_{\text{S},\Gamma_0}$;
- (3) **Counting the divisor points in the ovals** In Section 6.2 we prove that there is one divisor point in each finite oval and no divisor point in the infinite oval;
- (4) **The KP wave function on Γ** The normalized KP wave function $\hat{\psi}(P, \vec{t})$ on Γ is constructed imposing that it coincides for all times at each marked point P with the value of the normalized dressed edge wave function $\hat{\Psi}_e(\vec{t})$ at the corresponding edge $e = e(P) \in \mathcal{N}$. The normalized wave function is then meromorphically extended so that, for any fixed \vec{t} , we have $(\hat{\psi}(P, \vec{t})) + \mathcal{D}_{\text{KP},\Gamma} \geq 0$ on $\Gamma \setminus P_0$. By construction it coincides with the Sato wave function on Γ_0 .

As a consequence of Theorem 4.2.1 and of the absence of zero vectors on reduced networks (see [7] and Remark 2.3.3) we get the first statement in the following Corollary. The second part follows from the explicit characterization of the effect of moves and reductions on the wave function and the divisor carried in Section 8.

Corollary 4.2.2. *Under the hypotheses of Theorem 4.2.1:*

- (1) **Parametrization of $\mathcal{S}_{\mathcal{M}}^{\text{TNN}}$ via KP divisors:** *If the PBDTP graph \mathcal{G} representing $\mathcal{S}_{\mathcal{M}}^{\text{TNN}}$ is reduced and equivalent to the Le-graph via a finite sequence of moves (M1), (M3) and flip moves (M2), then for any fixed \vec{t}_0 , there is a local one-to-one correspondence between KP divisors on $\Gamma(\mathcal{G})$ and points $[A] \in \mathcal{S}_{\mathcal{M}}^{\text{TNN}}$.*
- (2) **Discrete transformation between curves and divisors induced by moves and reductions:** *Let \mathcal{G} and \mathcal{G}' be two PBDTP graphs equivalent by a finite sequence of moves and reductions for which Theorem 4.2.1 holds true for the same \vec{t}_0 , then there is an explicit transformation of the KP divisor on $\Gamma(\mathcal{G})$ to the KP divisor on $\Gamma(\mathcal{G}')$.*

Remark 4.2.1. Global parametrization of positroid cells via divisors We claim that given a curve Γ associated to a reduced PBDTP graph \mathcal{G} representing a positroid cell $\mathcal{S}_{\mathcal{M}}^{\text{TNN}}$, real and regular KP divisors $\mathcal{D}_{\text{KP},\Gamma}$ such that $\#(\mathcal{D}_{\text{KP},\Gamma} \cap \Gamma_0) = k$ provide a global minimal parametrization of $\mathcal{S}_{\mathcal{M}}^{\text{TNN}}$ after applying some blow-ups in all cases where some of the divisor points occur at double points. We plan to discuss thoroughly this issue in a future publication and we just discuss the question for soliton data associated to $\text{Gr}^{\text{TP}}(1, 3)$ in Section 11.1.

In Section 11.2, we briefly explain how to modify the construction to the case in which some of the edge vectors are zero.

In principle the construction of $\mathcal{D}_{\text{KP},\Gamma}$ may be carried out also on reducible positroid cells (see [5] for the case of Le-networks).

5. CONSTRUCTION OF THE KP DIVISOR ON $\Gamma(\mathcal{G})$

Throughout this Section, we fix the phases $\mathcal{K} = \{\kappa_1 < \dots < \kappa_n\}$ and the PBDTP graph in the disk \mathcal{G} representing the irreducible positroid cell $\mathcal{S}_{\mathcal{M}}^{\text{TNN}} \subset \text{Gr}^{\text{TNN}}(k, n)$ as in Definition 2.1.3. $\Gamma = \Gamma(\mathcal{G})$ is the curve as in Construction 4.1.1. We denote by $g + 1$ the number of faces (ovals) of

$\mathcal{G}(\Gamma)$. \mathcal{O} is the orientation of \mathcal{G} and \mathfrak{l} a fixed gauge direction. Finally $I = \{1 \leq i_1 < \dots < i_k \leq n\}$ is the base in \mathcal{M} associated to \mathcal{O} , whereas $\bar{I} = [n] \setminus I$.

For any $[A] \in \mathcal{S}_{\mathcal{M}}^{\text{TNN}}$, $(\mathcal{N}, \mathcal{O})$ is a directed network of graph \mathcal{G} representing such point. Using the weight gauge freedom and Lemma 2.3.1, in the following we assume that edges at boundary vertices carry unit weights. E_e is the system of edge vectors constructed in Section 2 on $(\mathcal{N}, \mathcal{O}, \mathfrak{l})$ with boundary conditions E_j at the boundary vertices and we assume from now on that all edge vectors are not zero. We recall that, if an edge vector is zero in one orientation then it is zero in any other orientation of \mathcal{N} and that zero vectors can't appear in PBDTP networks possessing an acyclic orientation (see [7] and Remark 2.3.3).

In this Section we define the dressed edge wave function on $(\mathcal{N}, \mathcal{O}, \mathfrak{l})$ and introduce an effective dressed network divisor.

5.1. The dressed edge wave function. For the rest of the paper we denote $\mathfrak{E}_\theta(\vec{t}) = (e^{\theta_1(\vec{t})}, \dots, e^{\theta_n(\vec{t})})$, $\theta_j(\vec{t}) = \sum_{l \geq 1} \kappa_j^l t_l$, where $\vec{t} = (t_1 = x, t_2 = y, t_3 = t, t_4, \dots)$ are the KP times, and $\langle \cdot, \cdot \rangle$ denotes the usual scalar product. Moreover we assume that only a finite number of entries of \vec{t} are non zero. To simplify the construction we suppose that the edges at the boundary vertices are parallel to each other and each one ends at an internal bivalent vertex.

Definition 5.1.1. *The dressed edge wave function (dressed e.w.) on $(\mathcal{N}, \mathcal{O}, \mathfrak{l})$. Let $(\mathcal{N}, \mathcal{O}, \mathfrak{l})$ be the oriented network associated to the soliton data $(\mathcal{K}, [A])$ and let us denote E_e , $z_{U,e}$ respectively its system of vectors and of half-edge vectors. Finally let A be the RREF matrix of $[A]$ w.r.t. the base I associated to the orientation \mathcal{O} , so that $f^{(r)}(\vec{t}) = \sum_{j=1}^n A_j^r e^{\theta_j(\vec{t})}$, $r \in [k]$, are the heat hierarchy solutions generating the Darboux transformation $\mathfrak{D}^{(k)}$ for the soliton data $(\mathcal{K}, [A])$.*

We define the dressed edge wave function (dressed e.w.) for the edge e in $(\mathcal{N}, \mathcal{O}, \mathfrak{l})$ as

$$(5.1) \quad \Psi_{e, \mathcal{O}, \mathfrak{l}}(\vec{t}) \equiv \langle E_e, \mathfrak{D}^{(k)} \mathfrak{E}_\theta(\vec{t}) \rangle,$$

In particular, e is the edge at the boundary vertex b_j ,

$$(5.2) \quad \Psi_{e, \mathcal{O}, \mathfrak{l}}(\vec{t}) = \begin{cases} (-1)^{\text{int}(e)} \mathfrak{D}^{(k)} e^{\theta_j(\vec{t})}, & \text{if } b_j \text{ is a sink;} \\ -\mathfrak{D}^{(k)} e^{\theta_j(\vec{t})}, & \text{if } b_j \text{ is a source,} \end{cases}$$

where $\text{int}(e)$ is the number of gauge rays intersecting e .

We also define the dressed half-edge wave function (dressed h.e.w.) for the half-edge (e, U) as

$$(5.3) \quad \Psi_{U, e; \mathcal{O}, \mathfrak{l}}(\vec{t}) \equiv \langle z_{U, e}, \mathfrak{D}^{(k)} \mathfrak{E}_\theta(\vec{t}) \rangle.$$

We remark that the different behavior at sources in (5.2) is due to the fact that $E_e = A[r] - E_j$, if j is the r -th source in the network (see (2.7) in Theorem 2.2.1).

Lemma 5.1.1. *Let the dressed e.w. $\Psi_{e, \mathcal{O}, \mathfrak{l}}(\vec{t})$. Then $\Psi_{e, \mathcal{O}, \mathfrak{l}}(\vec{t}) \neq 0$, for all $e \in \mathcal{N}$.*

Remark 5.1.1. *The reference time \vec{t}_0 . Let the dressed e.w. be as above. In the following we fix a reference time $\vec{t}_0 = (x_0, 0, \dots)$ such that for any $e \in \mathcal{E}$, the dressed e.w. $\Psi_{e, \mathcal{O}, \mathfrak{l}}(\vec{t}_0) \neq 0$.*

The full rank linear system for the edge vectors (see Section 2.4) induces a full rank linear system satisfied by the edge and half-edge wave functions:

- (1) At any trivalent white vertex U incident with incoming edge e_3 and outgoing edges e_1, e_2 ,

$$(5.4) \quad \begin{aligned} \Psi_{e_3, \mathcal{O}, \mathfrak{l}}(\vec{t}) &= (-1)^{\text{int}(e_3)} w_3 \left((-1)^{\text{wind}(e_3, e_1)} \Psi_{e_1, \mathcal{O}, \mathfrak{l}}(\vec{t}) + (-1)^{\text{wind}(e_3, e_2)} \Psi_{e_2, \mathcal{O}, \mathfrak{l}}(\vec{t}) \right), \\ \sum_{k=1}^3 \Psi_{U, e_k; \mathcal{O}, \mathfrak{l}}(\vec{t}) &= 0; \end{aligned}$$

- (2) At any trivalent black vertex U incident with incoming edges e_2, e_3 and outgoing edge e_1 ,

$$(5.5) \quad \begin{aligned} \Psi_{e_m, \mathcal{O}, \mathfrak{l}}(\vec{t}) &= (-1)^{\text{int}(e_m) + \text{wind}(e_m, e_1)} w_m \Psi_{e_1, \mathcal{O}, \mathfrak{l}}(\vec{t}), \quad m = 2, 3, \\ \Psi_{U, e_1; \mathcal{O}, \mathfrak{l}}(\vec{t}) &= \Psi_{U, e_2; \mathcal{O}, \mathfrak{l}}(\vec{t}) = \Psi_{U, e_3; \mathcal{O}, \mathfrak{l}}(\vec{t}). \end{aligned}$$

Finally, in the following Proposition the transformation rules for the half-edge wave functions are a consequence of the transformation rules for the (half)-edge vectors (Theorem 2.3.3 and Lemma 2.4.4). The last item is a key observation which will be used both to prove the invariance of the position of the divisor point in the oval with respect to the geometric transformations of the directed graph dual to the reducible M-curve and to count the number of divisors points in each oval.

Proposition 5.1.2. The dependence of the dressed e.w. on the geometric transformations Let $\epsilon_{U,V}^{(1)}$ and $\epsilon_{U,V}^{(2)}$ respectively be the edge signatures on $\mathcal{N}^{(1)} \equiv (\mathcal{N}, \mathcal{O}, \mathfrak{l})$ and on $\mathcal{N}^{(2)} \equiv (\hat{\mathcal{N}}, \hat{\mathcal{O}}, \hat{\mathfrak{l}})$, PBDTP networks representing the same point $[A] \in \mathcal{S}_{\mathcal{M}}^{TNN} \subset Gr^{TNN}(k, n)$. Denote $\Psi_{U,e}^{(i)}(\vec{t})$, $i = 1, 2$, the respective half-edge wave functions at the half-edge (U, e) . Then:

- (1) If $\mathcal{N}^{(2)}$ is obtained from $\mathcal{N}^{(1)}$ by either changing the gauge ray direction on the same directed graph or acting with a vertex gauge transformation on the graph of $\mathcal{N}^{(1)}$ keeping fixed the orientation,

$$(5.6) \quad \Psi_{U,e}^{(2)}(\vec{t}) = (-1)^{\eta(U)} \Psi_{U,e}^{(1)}(\vec{t}),$$

where $\eta(U)$ is the gauge equivalence transformation of the two signatures;

- (2) If $\mathcal{N}^{(2)}$ is obtained from $\mathcal{N}^{(1)}$ by changing the orientation of the given graph, then, for any edge e there exists a real constant $\alpha_e \neq 0$ such that

$$(5.7) \quad \Psi_{U,e}^{(2)}(\vec{t}) = \alpha_e \Psi_{U,e}^{(1)}(\vec{t});$$

- (3) Let V be an internal vertex and e, f be edges at V . If $\mathcal{N}^{(2)}$ is obtained from $\mathcal{N}^{(1)}$ by either changing the orientation of the given graph, or the gauge ray direction on the same directed graph or acting with a vertex gauge transformation or a weight gauge transformation, then, for any \vec{t}

$$(5.8) \quad \text{sign} \left(\Psi_{U,e}^{(2)}(\vec{t}) \Psi_{U,f}^{(2)}(\vec{t}) \right) = \text{sign} \left(\Psi_{U,e}^{(1)}(\vec{t}) \Psi_{U,f}^{(1)}(\vec{t}) \right).$$

The last statement may be easily checked case by case using the definition of the half-edge wave function and items (1) and (2) in the same Proposition.

5.2. The dressed network divisor. Next we associate the dressed network divisor to $(\mathcal{N}, \mathcal{O}, \mathfrak{l})$ as follows.

Definition 5.2.1. *The dressed network divisor $\mathcal{D}_{\text{dr},\mathcal{N}}$. At each trivalent white vertex V of $(\mathcal{N}, \mathcal{O}, \mathfrak{l})$, let $\Psi_{e_m, \mathcal{O}, \mathfrak{l}}(\vec{t})$ be the dressed e.w. on the edge e_m , $m \in [3]$, with the convention that the edges are numbered anticlockwise and e_3 is the incoming edge at V . Then, to V we assign the dressed network divisor number*

$$(5.9) \quad \gamma_{\text{dr}, V} = \frac{(-1)^{\text{wind}(e_3, e_1)} \Psi_{e_1, \mathcal{O}, \mathfrak{l}}(\vec{t}_0)}{(-1)^{\text{wind}(e_3, e_1)} \Psi_{e_1, \mathcal{O}, \mathfrak{l}}(\vec{t}_0) + (-1)^{\text{wind}(e_3, e_2)} \Psi_{e_2, \mathcal{O}, \mathfrak{l}}(\vec{t}_0)} = \frac{\Psi_{V, e_1; \mathcal{O}, \mathfrak{l}}(\vec{t}_0)}{\Psi_{V, e_1; \mathcal{O}, \mathfrak{l}}(\vec{t}_0) + \Psi_{V, e_2; \mathcal{O}, \mathfrak{l}}(\vec{t}_0)}.$$

We call $\mathcal{D}_{\text{dr}, \mathcal{N}} = \{(\gamma_{\text{dr}, V_l}, V_l), l \in [g - k]\}$ the dressed network divisor on \mathcal{N} , where V_l , $l \in [g - k]$, are the trivalent white vertices of the network.

If \mathcal{N} is the acyclically oriented Le-network representing $[A]$, then the dressed network divisor constructed in [5] coincides with the above definition for the choice of the gauge ray \mathfrak{l} as in Figure 1.

By definition, the dressed network divisor number at each trivalent white vertex is real and represents the local coordinate of a point on the corresponding copy of \mathbb{CP}^1 in Γ . In general, on $(\mathcal{N}, \mathcal{O}, \mathfrak{l})$, the value of the dressed network divisor number at a given trivalent white vertex V depends on the choice of \vec{t}_0 . If this is not the case we call the corresponding **network divisor number trivial**. If \mathcal{N} is the Le-network, there are no trivial network divisor numbers. In the general case, trivial network divisor numbers occur at all vertices where the linear system in (2.15) involves linearly dependent vectors.

Lemma 5.2.1. Trivial network divisor numbers Let E_{e_m} , $m \in [3]$, be the edge vectors at a trivalent white vertex V of $(\mathcal{N}, \mathcal{O}, \mathfrak{l})$ and $\gamma_{\text{dr}, V}$ be the dressed network divisor number at V . If there exists a non zero constant c_V such that either $E_{e_2} = c_V E_{e_1}$ or $E_{e_3} = c_V E_{e_1}$ or $E_{e_3} = c_V E_{e_2}$, then the dressed network divisor number $\gamma_{\text{dr}, V}$ is trivial.

Proof. Indeed in the first case for all \vec{t} , $\Psi_{e_2, \mathcal{O}, \mathfrak{l}}(\vec{t}) = c_V \Psi_{e_1, \mathcal{O}, \mathfrak{l}}(\vec{t})$, so that

$$\gamma_{\text{dr}, V} = (1 + c_V (-1)^{\text{wind}(e_3, e_2) - \text{wind}(e_3, e_1)})^{-1}. \text{ The other cases may be treated similarly. } \quad \square$$

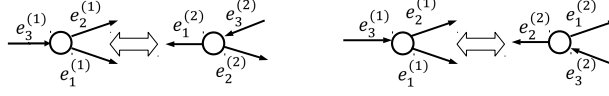
All gauge transformations (change of ray direction, of the vertex gauge and of weight gauge) leave invariant the divisor number on V . Those associated to changes of orientation correspond to a well defined change of the local coordinate on the corresponding copy of \mathbb{CP}^1 , and the dressed network divisor numbers change in agreement with such coordinate transformation (Proposition 5.2.3). We shall use such transformation properties of the divisor numbers to prove the invariance of the KP divisor on Γ in Theorem 6.1.2.

Proposition 5.2.2. Independence of the network divisor on the gauge ray direction, the weight gauge and the vertex gauge. Let $\mathcal{N}^{(1)}, \mathcal{N}^{(2)}$ be two oriented networks representing the same point in the Grassmannian and obtained from each other by changing either the gauge ray direction or the weight gauge or the vertex gauge. Let $\gamma_{\text{dr}, V}^{(i)}$ respectively be the divisor numbers at the vertex V in $\mathcal{N}^{(i)}$, $i = 1, 2$. Then

$$\gamma_{\text{dr}, V}^{(2)} = \gamma_{\text{dr}, V}^{(1)}.$$

The proof follows by computing the divisor numbers at V using (5.9) and inserting (2.18) into the half-edge wave functions (5.3).

Proposition 5.2.3. The dependence of the dressed network divisor on the orientation. Let \mathcal{O}_1 and \mathcal{O}_2 be two perfect orientations for network \mathcal{N} . Then for any trivalent white

FIGURE 14. The change of orientation at a vertex V .

vertex V , such that all edges at V have the same versus in both orientations, $(e_1^{(2)}, e_2^{(2)}, e_3^{(2)}) = (e_1^{(1)}, e_2^{(1)}, e_3^{(1)})$, the dressed network divisor number is the same in both orientations

$$(5.10) \quad \gamma_{\text{dr}, V, \mathcal{O}_2} = \gamma_{\text{dr}, V, \mathcal{O}_1}.$$

If at the vertex V we change orientation of edges from $(e_1^{(1)}, e_2^{(1)}, e_3^{(1)})$ to $(e_2^{(2)}, e_3^{(2)}, e_1^{(2)}) = (e_1^{(1)}, -e_2^{(1)}, -e_3^{(1)})$ (Figure 14[left]), then the relation between the dressed network divisor numbers at V in the two orientations is

$$(5.11) \quad \gamma_{\text{dr}, V, \mathcal{O}_2} = \frac{1}{1 - \gamma_{\text{dr}, V, \mathcal{O}_1}}.$$

If at the vertex V we change orientation of edges from $(e_1^{(1)}, e_2^{(1)}, e_3^{(1)})$ to $(e_3^{(2)}, e_1^{(2)}, e_2^{(2)}) = (-e_1^{(1)}, e_2^{(1)}, -e_3^{(1)})$ (Figure 14[right]), then the relation between the dressed network divisor numbers at V in the two orientations is

$$(5.12) \quad \gamma_{\text{dr}, V, \mathcal{O}_2} = \frac{\gamma_{\text{dr}, V, \mathcal{O}_1}}{\gamma_{\text{dr}, V, \mathcal{O}_1} - 1}.$$

Proof The proof follows by direct computation of the dressed network divisor numbers using (5.7) and the linear system (5.4) at V for both orientations. For instance, (5.11) follows observing that $\Psi_{e_m^{(2)}, \mathcal{O}_2, \mathfrak{l}}(\vec{t}) = \alpha_{m-1} \Psi_{e_{m-1}^{(1)}, \mathcal{O}_1, \mathfrak{l}}(\vec{t}) \pmod{3}$, and that the linear system w.r.t. both orientations imposes the constraint

$$\frac{\alpha_1}{\alpha_3} (-1)^{\text{wind}_{\mathcal{O}_2}(e_3^{(2)}, e_2^{(2)}) - \text{wind}_{\mathcal{O}_2}(e_3^{(2)}, e_1^{(2)})} = -w_3 (-1)^{\text{int}_{\mathcal{O}_1}(e_3^{(1)}) + \text{wind}_{\mathcal{O}_1}(e_3^{(1)}, e_1^{(1)})},$$

where w_3 is the weight of $e_3^{(1)}$ in the initial orientation, so that

$$\gamma_{\text{dr}, V, \mathcal{O}_2} = \left(1 + \frac{(-1)^{\text{wind}_{\mathcal{O}_2}(e_3^{(2)}, e_2^{(2)})} \Psi_{e_2^{(2)}, \mathcal{O}_2, \mathfrak{l}}}{(-1)^{\text{wind}_{\mathcal{O}_2}(e_3^{(2)}, e_1^{(2)})} \Psi_{e_1^{(2)}, \mathcal{O}_2, \mathfrak{l}}} \right)^{-1} = \left(1 + \frac{(-1)^{\text{wind}_{\mathcal{O}_2}(e_3^{(2)}, e_2^{(2)})} \alpha_1 \Psi_{e_1^{(1)}, \mathcal{O}_1, \mathfrak{l}}}{(-1)^{\text{wind}_{\mathcal{O}_2}(e_3^{(2)}, e_1^{(2)})} \alpha_3 \Psi_{e_3^{(1)}, \mathcal{O}_1, \mathfrak{l}}} \right)^{-1} = (1 - \gamma_{\text{dr}, V, \mathcal{O}_1})^{-1}. \quad \square$$

Remark 5.2.1. In the next Section we prove the invariance of the KP divisor on Γ with respect to changes of orientation of the graph using Proposition 5.2.3. Indeed, on Γ_l , the copy of \mathbb{CP}^1 corresponding to V , the transformation rule of the network divisor number coincides with the change of coordinates of the divisor point induced by the change of orientation of the network.

We end this Section normalizing the dressed edge wave function.

Definition 5.2.2. *The KP edge wave function $\hat{\Psi}$.* Let $(\mathcal{N}, \mathcal{O}, \mathfrak{l})$ be the gauge-oriented network representing the soliton data $(\mathcal{K}, [A])$. Let \vec{t}_0 be as in the Remark 5.1.1. Then the **KP edge wave function (KP e.w)** on the edge e in \mathcal{N} is

$$(5.13) \quad \hat{\Psi}_e(\vec{t}) = \begin{cases} \frac{\Psi_{e, \mathcal{O}, \mathfrak{l}}(\vec{t})}{\Psi_{e, \mathcal{O}, \mathfrak{l}}(\vec{t}_0)}, & \text{for all } e \in \mathcal{E}, \\ \frac{\mathfrak{D}^{(k)} e^{i\theta_j(\vec{t})}}{\mathfrak{D}^{(k)} e^{i\theta_j(\vec{t}_0)}}, & \text{if } e = e_j^{(D)}, \quad j \in [n], \end{cases} \quad \forall \vec{t}.$$

Remark 5.2.2. The KP edge wave function on \mathcal{N} . The name KP wave function for $\hat{\Psi}_e(\vec{t})$ on \mathcal{N} is fully justified. Indeed $\hat{\Psi}_e(\vec{t})$ just depends on the soliton data $(\mathcal{K}, [A])$ and on the chosen network representing $[A]$ since $\hat{\Psi}_e(\vec{t})$ takes the same value on a given edge e for any choice of orientation, gauge ray direction, weight gauge and vertex gauge. Moreover, by construction it satisfies the Sato boundary conditions at the edges at the boundary, and takes real values for real \vec{t} . This function is a common eigenfunction to all KP hierarchy auxiliary linear operators $-\partial_{t_j} + B_j$, where $B_j = (L^j)_+$, and the Lax operator $L = \partial_x + \frac{u(\vec{t})}{2}\partial_x^{-1} + u_2(\vec{t})\partial_x^{-2} + \dots$, the coefficients of these operators are the same for all edges. $\hat{\Psi}_e(\vec{t})$ takes equal values at all edges e at the same bivalent or black trivalent vertex, whereas, at any trivalent white vertex, it takes either the same value at all three edges for all times or distinct values at some $\vec{t} \neq \vec{t}_0$.

6. CONSTRUCTION OF THE KP WAVE FUNCTION $\hat{\psi}$ AND CHARACTERIZATION OF THE KP DIVISOR $\mathcal{D}_{\text{KP},\Gamma}$ ON Γ .

In this Section we define the KP wave function $\hat{\psi}(P, \vec{t})$ on the curve $\Gamma = \Gamma(\mathcal{G})$ and the KP divisor $\mathcal{D}_{\text{KP},\Gamma}$ as the union of the Sato divisor on Γ_0 and the divisor points on the components of Γ corresponding to the white vertices whose local coordinates are the network divisor points defined in the previous Section. Then the following properties of $\mathcal{D}_{\text{KP},\Gamma}$ easily follow from its definition:

- (1) $\mathcal{D}_{\text{KP},\Gamma}$ is contained in the union of the ovals of Γ ;
- (2) The position of the divisor point associated to a given trivalent white vertex only depends on the relative signs of the KP half-edge wave function;
- (3) The KP divisor does not depend on the geometrical indices chosen to construct the network divisor numbers;
- (4) There is exactly one divisor point in each finite oval and no divisor point in the infinite oval containing P_0 .

6.1. The KP wave function and its pole divisor. We start the Section defining both the KP wave function $\hat{\psi}$ and the KP divisor $\mathcal{D}_{\text{KP},\Gamma}$. We use the (half)-edge wave function to assign the value of the KP wave function at the double points of Γ and then extend it meromorphically on each component of Γ .

Construction 6.1.1. The KP wave function $\hat{\psi}$ on Γ . Let the soliton data $(\mathcal{K}, [A])$ be given, with $\mathcal{K} = \{\kappa_1 < \dots < \kappa_n\}$ and $[A] \in \mathcal{S}_{\mathcal{M}}^{\text{TNN}} \subset \text{Gr}^{\text{TNN}}(k, n)$. Let $I \in \mathcal{M}$ be fixed. Let \mathcal{G} be a PBDTP graph representing $\mathcal{S}_{\mathcal{M}}^{\text{TNN}}$ as in Definition 2.1.3 with $(g+1)$ faces and let the curve $\Gamma = \Gamma(\mathcal{G})$ be as in Construction 4.1.1. Let $(\mathcal{N}, \mathcal{O}(I), \mathfrak{l})$ be a network of graph \mathcal{G} representing $[A]$ with no zero edge vectors. Let $\mathcal{D}_{\text{dr},\mathcal{N}}$ and $\hat{\Psi}_e(\vec{t})$ respectively be the dressed network divisor of Definition 5.2.1 and the KP edge wave function of Definition 5.2.2. Finally on each component of Γ let the coordinate ζ be as in Definition 4.2.1 (see also Figure 13).

We define the KP wave function $\hat{\psi}(P, \vec{t})$ on $\Gamma \setminus \{P_0\}$ as follows:

- (1) The restriction of $\hat{\psi}$ to Γ_0 is the normalized dressed Sato wave function defined in (3.8)

$$\hat{\psi}(\zeta, \vec{t}) = \frac{\mathfrak{D}^{(k)}\phi_0(\zeta, \vec{t})}{\mathfrak{D}^{(k)}\phi_0(\zeta, \vec{t}_0)};$$

- (2) If Σ_l is the component of Γ corresponding to the black vertex V_l' , then, for any $P \in \Sigma_l$ and for all \vec{t} , $\hat{\psi}(P, \vec{t})$ is assigned the value of the KP e.w. $\hat{\Psi}_e(\vec{t})$, where e is one of the edges at V_l' : $\hat{\psi}(\zeta(P), \vec{t}) = \hat{\Psi}_e(\vec{t})$;

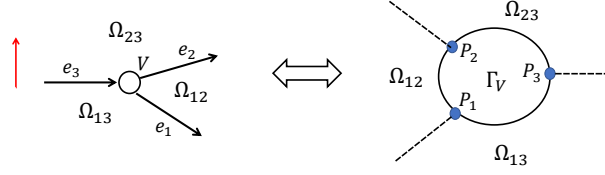


FIGURE 15. The correspondence between faces at V (left) and ovals bounded by Γ_V (right) under the assumption that the curve is constructed reflecting the graph w.r.t. a vertical ray (all boundary vertices in the original network lay on a horizontal line).

- (3) Similarly if Γ_l is the component of Γ corresponding to a white vertex V_l with KP e.w. coinciding on all edges at V_l for all \vec{t} , then, $\hat{\psi}(P, \vec{t})$ is assigned the value $\hat{\Psi}_e(\vec{t})$ for any $P \in \Gamma_l$, where e is one of the edges at V_l : $\hat{\psi}(\zeta(P), \vec{t}) = \hat{\Psi}_e(\vec{t})$;
- (4) If Γ_l is the component of Γ corresponding to a trivalent white vertex V_l with KP e.w. taking distinct values on the edges at V_l for some $\vec{t} \neq \vec{t}_0$, then we define $\hat{\psi}$ at the marked points as $\hat{\psi}(\zeta(P_l^{(m)}), \vec{t}) = \hat{\Psi}_{e_m}(\vec{t})$, $m \in [3]$, for all \vec{t} , where e_m are the edges at V_l , and we uniquely extend $\hat{\psi}$ to a degree one meromorphic function on Γ_l imposing that it has a simple pole at $P_{\text{dr}}^{(l)}$ with real coordinate $\zeta(P_{\text{dr}}^{(l)}) = \gamma_{\text{dr}, V_l}$, with γ_{dr, V_l} as in (5.9):

$$(6.1) \quad \hat{\psi}(\zeta(P), \vec{t}) = \frac{\hat{\Psi}_{e_3}(\vec{t})\zeta - \gamma_{\text{dr}, V_l}\hat{\Psi}_{e_1}(\vec{t})}{\zeta - \gamma_{\text{dr}, V_l}} = \frac{\Psi_{V_l, e_1}(\vec{t})(\zeta - 1) + \Psi_{V_l, e_2}(\vec{t})\zeta}{[\Psi_{V_l, e_1}(\vec{t}_0) + \Psi_{V_l, e_2}(\vec{t}_0)](\zeta - \gamma_{\text{dr}, V_l})},$$

where Ψ_{V_l, e_s} are the half-edge d.w.f. at the outgoing half-edges (V_l, e_s) , $s = 1, 2$, labeled as in Figure 10.

By construction, the KP wave function has k real simple poles on Γ_0 . Therefore the following definition of KP divisor is fully justified.

Definition 6.1.1. *The KP divisor on Γ . The KP divisor $\mathcal{D}_{\text{KP}, \Gamma}$ is the sum of the following g simple poles,*

- (1) the k poles on Γ_0 coinciding with the Sato divisor at $\vec{t} = \vec{t}_0$;
- (2) the $g - k$ poles $P_{\text{dr}}^{(l)} \in \Gamma_l$ uniquely identified by the condition that, in the local coordinate induced by the orientation \mathcal{O} , $\zeta(P_{\text{dr}}^{(l)}) = \gamma_{\text{dr}, V_l}$, where V_l , $l \in [g - k]$, are the trivalent white vertices.

Next we explain how to detect the position of the divisor point associated to a white vertex. Let e_m , P_m , $m \in [3]$ respectively denote the edge at V and the corresponding marked point on Γ_V . Let Ω_{ij} , $i, j \in [3]$ be both the face of \mathcal{N} bounded by the edges e_i, e_j and the corresponding oval in $\Gamma(\mathcal{G})$ bounded by the double points P_i, P_j (see also Figure 15). Let $\Psi_{V, m} \equiv \Psi_{V, e_m; \mathcal{N}, \mathcal{O}, \vec{t}(\vec{t}_0)}$ be the dressed h.e.w. at the half-edge (V, e_m) , $m \in [3]$, at a given trivalent white vertex V as in Definition 5.1.1. Then the network divisor number γ_V is the local coordinate of the divisor point P_V on the component Γ_V corresponding to V :

$$(6.2) \quad \zeta(P_V) \equiv \gamma_V = \frac{\Psi_{V, a}}{\Psi_{V, a} + \Psi_{V, b}} = -\frac{\Psi_{V, b}}{\Psi_{V, c}} = 1 + \frac{\Psi_{V, b}}{\Psi_{V, c}}.$$

Then the following Lemma explains to which oval the divisor point belongs to.

Lemma 6.1.1. *Position of the divisor point on Γ_V In the above notations, the divisor point P_V belongs to the unique oval Ω_{ij} , $i, j \in [m]$, such that the half-edge wave function at V satisfies*

$$(6.3) \quad \Psi_{V, i} \Psi_{V, j} > 0.$$

The proof easily follows using $\Psi_{V,1} + \Psi_{V,2} + \Psi_{V,3} = 0$ and the assumption that $\Psi_{V,s} \neq 0$, for $s \in [3]$. Then (6.3) holds comparing (6.2) and Figure 15 since, in the local coordinate ζ associated to the graph orientation at V , $\zeta(P_1) = 0$, $\zeta(P_2) = 1$ and $\zeta(P_3) = \infty$. For instance $\zeta(P_V) \equiv \gamma_V \in]0, 1[$ if and only if $\Psi_{V,1}\Psi_{V,2} > 0$ and similarly in the other two cases.

Theorem 6.1.2. Properties of the KP divisor on Γ

- (1) $\mathcal{D}_{\text{KP},\Gamma}$ is independent on the gauge ray direction, on the weight gauge, on the vertex gauge and on the orientation of the network used to construct it;
- (2) $\mathcal{D}_{\text{KP},\Gamma}$ is contained in the union of the ovals of Γ .

Proof. The only untrivial statement is the independence of the divisor on the orientation of the network. For any fixed orientation \mathcal{O} , on the copy Γ_l corresponding to the trivalent white vertex V_l , there are four real ordered marked points: $P_m^{(l)}$, $m \in [3]$, represented by the ordered edges at V_l , and the dressed divisor point $P_{\text{dr}}^{(l)}$ with local coordinate $\zeta(P_{\text{dr}}^{(l)}) = \gamma_{\text{dr},V_l}$. From the definition of the KP wave function on Γ , Proposition 5.2.3 and the definition of $\mathcal{D}_{\text{KP},\Gamma}$, it follows that any change of orientation in \mathcal{N} acts on the four marked points in Γ_l as a change of coordinate which leaves invariant the position of the pole divisor in the oval. Indeed, let $e_m^{(s)}$, $m \in [3]$, $s = 1, 2$, be the edges at the trivalent white vertex V_l , where $e_3^{(s)}$ is the unique edge pointing inwards at V_l in orientation \mathcal{O}_s (see also Figure 14). Let ζ_s , $s = 1, 2$, be the local coordinates on Γ_l respectively for orientations \mathcal{O}_1 and \mathcal{O}_2 of \mathcal{N} and let $P_m^{(s)}$ be the marked point on Γ_l corresponding to $e_m^{(s)}$ as in Definition 4.2.1 (see also Figure 13). Then

- (1) If all edges at V_l have the same versus in both orientations, then $P_m^{(2)} = P_m^{(1)}$, $m \in [3]$, $\zeta_1 = \zeta_2$ and (5.10) implies that the divisor point on Γ_l is the same and has the same coordinate $\zeta_2(P_{\text{dr}}^{(l)}) = \zeta_1(P_{\text{dr}}^{(l)})$;
- (2) If at V_l we change orientation of edges from $(e_1^{(1)}, e_2^{(1)}, e_3^{(1)})$ to $(e_2^{(2)}, e_3^{(2)}, e_1^{(2)})$ (Figure 14[left]), then $P_m^{(2)} = P_{m-1}^{(1)} \pmod{3}$ and $\zeta_2 = (1 - \zeta_1)^{-1}$ on Γ_l . Therefore (5.11) implies that the divisor point on Γ_l is the same and its local coordinate changes as $\zeta_2(P_{\text{dr}}^{(l)}) = (1 - \zeta_1(P_{\text{dr}}^{(l)}))^{-1}$;
- (3) If at V_l we change orientation of edges from $(e_1^{(1)}, e_2^{(1)}, e_3^{(1)})$ to $(e_3^{(2)}, e_1^{(2)}, e_2^{(2)})$ (Figure 14[right]), then $P_m^{(2)} = P_{m+1}^{(1)} \pmod{3}$ and $\zeta_2 = \zeta_1/(\zeta_1 - 1)$ on Γ_l . Therefore (5.12) implies that the divisor point on Γ_l is the same and its local coordinate changes as $\zeta_2(P_{\text{dr}}^{(l)}) = \zeta_1(P_{\text{dr}}^{(l)})/(\zeta_1(P_{\text{dr}}^{(l)}) - 1)^{-1}$.

□

By construction, each double point in Γ corresponds to an edge; therefore the KP wave function takes the same value at all double points for all times and, at the double points κ_j corresponding to edges at boundary vertices b_j , $j \in [n]$, it coincides for all times with the normalized Sato wave function. $\hat{\psi}$ is meromorphic of degree $\mathfrak{d}_{\text{KP}} \leq g$, and its poles are all simple and belong to $\mathcal{D}_{\text{KP},\Gamma}$, which is contained in the union of all the real ovals of Γ . Therefore $\hat{\psi}$ satisfies the properties in Definition 4.2.3, that is it is the KP wave function for the soliton data $(\mathcal{K}, [A])$ and the divisor $\mathcal{D}_{\text{KP},\Gamma}$ on Γ .

Theorem 6.1.3. $\hat{\psi}$ is the unique KP wave function on Γ for $(\mathcal{K}, [A])$ and the divisor $\mathcal{D}_{\text{KP},\Gamma}$. Let $\hat{\psi}$, $\mathcal{D}_{\text{dr},\mathcal{N}'}$, $\mathcal{D}_{\text{KP},\Gamma}$ on Γ be as in Construction 6.1.1 and Definitions 5.2.1 and 6.1.1. Then $\hat{\psi}$ satisfies the following properties of Definition 4.2.3 on $\Gamma \setminus \{P_0\}$:

- (1) At $\vec{t} = \vec{t}_0$ $\hat{\psi}(P, \vec{t}_0) = 1$ at all points $P \in \Gamma \setminus \{P_0\}$;

- (2) $\hat{\psi}(\zeta(P), \vec{t})$ is real for real values of the local coordinate ζ and for all real \vec{t} on each component of Γ ;
- (3) $\hat{\psi}$ takes the same value at pairs of glued points $P, Q \in \Gamma$, for all \vec{t} : $\hat{\psi}(P, \vec{t}) = \hat{\psi}(Q, \vec{t})$;
- (4) $\hat{\psi}(\zeta, \vec{t})$ is either constant or meromorphic of degree one w.r.t. to the spectral parameter on each copy of \mathbb{CP}^1 corresponding on any trivalent white vertex common to \mathcal{N} and \mathcal{N}' . $\hat{\psi}(\zeta, \vec{t})$ is constant w.r.t. to the spectral parameter on each other copy of \mathbb{CP}^1 ;
- (5) $\mathcal{D}_{\text{KP}, \Gamma} + (\hat{\psi}(P, \vec{t})) \geq 0$ for all \vec{t} .

The proof of the assertions is straightforward and is omitted. We remark that, in the special case of the Le-network the divisor $\mathcal{D}_{\text{KP}, \Gamma}$ coincides with the one constructed in [5]. In the next Section we complete the proof of Theorem 4.2.1 by showing that the KP divisor $\mathcal{D}_{\text{KP}, \Gamma}$ satisfies the regularity and reality conditions (Items (3) and (4) of Definition 4.2.2).

6.2. Combinatorial characterization of the regularity of $\mathcal{D}_{\text{KP}, \Gamma}$. In this Section we complete the proof of Theorem 4.2.1: using Theorem 2.5.1 we prove that there is exactly one divisor point in each finite oval. The first proof of this statement was obtained in [6] using a different set of indexes. The use of the edge signatures considerably simplifies the previous proof. In the following Ω denotes both the face in the network and the corresponding oval of the curve Γ .

Let ν_Ω be the number of divisor points in Ω associated to the white vertices bounding Ω . By definition ν_Ω is equal to the number of pairs of half-edges at white vertices bounding Ω where the half-edge wave function has the same sign. When the face Ω intersects the boundary of the disk, the total number of divisor points in Ω is the sum of ν_Ω and of the number the Sato divisor points in $\Omega \cap \Gamma_0$.

By construction, along $\partial\Omega$ the half-edge wave function keeps the same sign at each pair of edges at a given black vertex and at each pair of edges at a trivalent white vertex associated to a divisor point in $\partial\Omega$, whereas it changes of sign at all other pair of edges at white vertices in $\partial\Omega$. Let c_Ω denote the total number of pair of half edges bounding Ω where the half-edge wave function changes sign.

Let us start with the case in which Ω is an internal oval (face). We use the notations introduced in Section 2.5. Let $\epsilon_{U,V}$ be the geometric signature of the network $(\mathcal{N}, \mathcal{O}, \mathbf{l})$ and ϵ_Ω be the total contribution of the geometric signature at the edges $e = (U, V)$ bounding Ω :

$$(6.4) \quad \epsilon_\Omega = \sum_{e \in \partial\Omega} \epsilon_e.$$

$n_{w, \Omega}$ denotes the total number of white vertices in $\partial\Omega$.

In this case ν_Ω , the number of divisor points in Ω , equals $n_{w, \Omega} - c_\Omega$. By definition c_Ω has the same parity as ϵ_Ω , the sum of the geometric signature over all edges bounding Ω . Then using (2.23) in Theorem 2.5.1, we immediately conclude that in each internal oval there is an odd number of divisor points since c_Ω and $n_{w, \Omega}$ have opposite parities:

$$(6.5) \quad c_\Omega \equiv \epsilon_\Omega = n_{w, \Omega} - 1 \pmod{2}.$$

We have thus proven the following Lemma:

Lemma 6.2.1. *The number of divisor points at internal ovals* With the above notations, at each internal oval Ω the number of KP divisor points is odd: $\nu_\Omega \equiv 1 \pmod{2}$.

Next we count the number of divisor points when the face Ω intersects the boundary of the disk. As in Section 2.5, b_Ω and s_Ω respectively are half the number of boundary vertices bounding Ω and the number of boundary sources belonging to Ω .

As a first step we compute the total number of changes of sign along $\partial\Omega$. Let ρ_Ω be the number of pairs of consecutive boundary vertices in $\partial\Omega \cap \Gamma_0$ where the edge wave function changes sign.

By construction, at each boundary source b_j the value of the half-edge wave function is opposite to the value of the Sato wave function $\Psi_{e(b_j)}(\vec{t}_0)$ (see (5.2)). Therefore to count the correct number of changes of signs in $\partial\Omega$ we must keep track of s_Ω , the number of boundary sources in the corresponding face Ω in the network.

Lemma 6.2.2. *Counting changes of sign of the half edge-wave function at the ovals intersecting the boundary* Let Ω be an oval intersecting the boundary of the disk. Then

$$(6.6) \quad c_\Omega + \rho_\Omega + \epsilon_\Omega + s_\Omega = 0 \pmod{2}.$$

At each finite oval Ω intersecting Γ_0 the number of Sato divisor points in $\Omega \cap \Gamma_0$ is equal to ρ_Ω , the number of pairs of consecutive boundary vertices in $\partial\Omega$ where the edge wave function changes sign. Indeed each portion of Γ_0 bounding Ω_s is marked by two consecutive boundary vertices b_j, b_{j+1} . Let $e(b_j)$ be the edge at b_j . Then $\Psi_{e(b_j)}(\vec{t}_0)\Psi_{e(b_{j+1})}(\vec{t}_0) < 0$ (> 0) implies that there is an odd (even) number of Sato divisor points in $\Gamma_0 \cap \Omega$ belonging to the interval $]\kappa_j, \kappa_{j+1}[$. The total number of divisor points is then the sum of ρ_Ω and of ν_Ω , that is the sum of Sato and non Sato divisor points in $\partial\Omega$. Then using $\nu_\Omega = n_{w,\Omega} - c_\Omega$, (2.24) and (6.6), we easily conclude that there is an odd number of divisor points also in each finite oval intersecting Γ_0 ,

$$(6.7) \quad \nu_\Omega + \rho_\Omega = n_{w,\Omega} + \epsilon_\Omega + s_\Omega = 1 \pmod{2}.$$

We have thus proven the following Lemma:

Lemma 6.2.3. *The number of divisor points at finite ovals intersecting Γ_0* With the above notations, at each finite oval Ω having non-empty intersection with Γ_0 the number of KP divisor points is odd: $\nu_\Omega + \rho_\Omega = 1 \pmod{2}$.

Finally, in the infinite oval Ω_0 , we also have $\Psi_{e(b_1)}(\vec{t}_0)\Psi_{e(b_n)}(\vec{t}_0) < 0$ (> 0) respectively when k is odd (even). Therefore, the number of Sato divisor points in Ω_0 has the same parity as $\rho_{\Omega_0} + k$. Then, proceeding as before, we conclude that the number of divisor points in the infinite oval is even

$$(6.8) \quad \nu_{\Omega_0} + \rho_{\Omega_0} + k = n_{w,\Omega_0} + \epsilon_{\Omega_0} + s_{\Omega_0} + k = 0 \pmod{2}.$$

Since the total number of divisor points is g and the ovals are $g + 1$, we have thus proven the following Theorem.

Theorem 6.2.4. *Number of divisor points in the ovals* There is exactly one divisor point in each finite oval Ω_s , $s \in [g]$, and no divisor point in the infinite oval Ω_0 . In particular, a finite oval contains a Sato divisor point if and only if $\rho_\Omega = 1, \pmod{2}$.

7. AMALGAMATION OF POSITROID CELLS AND DIVISOR STRUCTURE

In [24] Fock and Goncharov introduced amalgamation of cluster varieties, which has turned out to be relevant both for constructing integrable systems on Poisson cluster varieties [35] and for computation of scattering amplitudes on on-shell diagrams in $N = 4$ SYM theory [10]. Amalgamation of positroid varieties admits a very simple representation in terms of simple operations on the corresponding plabic graphs. In our setting the vertices are those of the graph and the frozen ones are those at the boundary. Since the planarity property is essential, amalgamation is represented by compositions of the following elementary operations:

- (1) Disjoint union of a pair of planar graphs (see Figure 16) corresponding to the direct sum of the corresponding Grassmannians via a map $Gr^{\text{TNN}}(k_1, n_1) \times Gr^{\text{TNN}}(k_2, n_2) \rightarrow Gr^{\text{TNN}}(k_1 + k_2, n_1 + n_2)$;

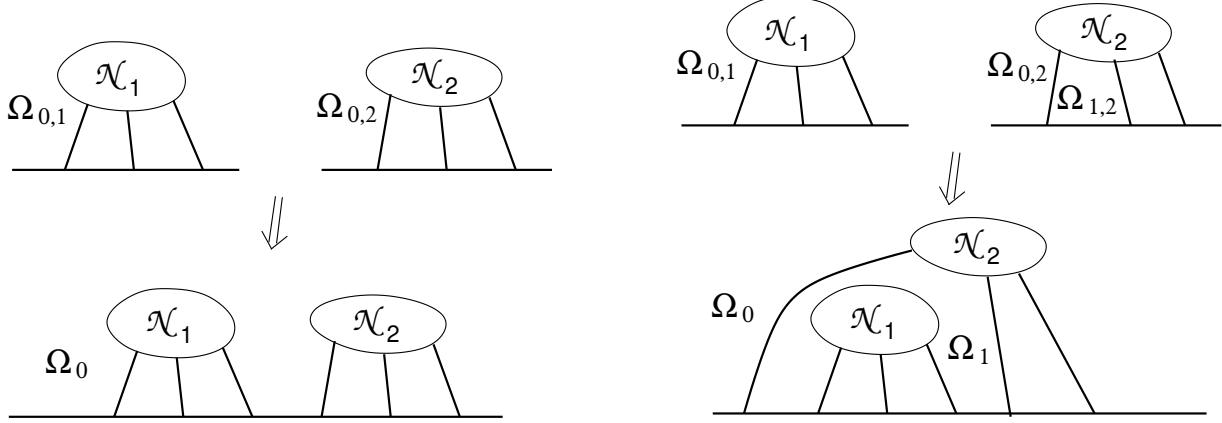


FIGURE 16. The two possible ways to construct disjoint union of two given networks in the disk preserving planarity.

- (2) Defrosting of a pair of consecutive boundary vertices (see Figure 17) corresponding to a projection map $Gr^{TNN}(k, n) \rightarrow Gr^{TNN}(k-1, n-2)$.

We recall that the soliton data consist of a point $[A] \in Gr^{TNN}(k, n)$ and a set ordered real phases $\mathcal{K} = \{\kappa_1 < \kappa_2 < \dots < \kappa_n\}$. Moreover, in our construction one face at the boundary of the disk plays a distinguished role since we place the essential singularity of the KP wave function in the corresponding oval in the curve. Let the initial soliton data be $[A_i] \in Gr^{TNN}(k_i, n_i)$, $\mathcal{K}_i = \{\kappa_1^{(i)} < \kappa_2^{(i)} < \dots < \kappa_{n_i}^{(i)}\}$, $i = 1, 2$. Then we have exactly two ways to perform the disjoint union preserving the total non-negativity property:

- (1) All boundary vertices of one network precede all boundary vertices of the second one (see Figure 16 [left]). This situation occurs when $\kappa_{n_2}^{(2)} < \kappa_1^{(1)}$. In this case the resulting infinite oval Ω_0 is the union of the infinite ovals $\Omega_{0,1}$, $\Omega_{0,2}$ of the initial networks and all finite ovals are not modified;
- (2) All boundary vertices of one network are located between two consecutive boundary vertices of the other one (see Figure 16 [right]). This situation occurs when $\kappa_j^{(2)} < \kappa_1^{(1)} < \dots < \kappa_{n_1}^{(1)} < \kappa_{j+1}^{(2)}$. Let us denote $\Omega_{1,2}$, Ω_1 respectively the finite oval containing this pair of boundary vertices in the initial and final networks. In this case the infinite oval Ω_0 coincides with $\Omega_{0,2}$, the infinite oval of the “external” network (\mathcal{N}_2 in Figure 16 [right]), whereas Ω_1 is built out of $\Omega_{1,2}$ and of $\Omega_{0,1}$, the infinite oval of the “internal” network (\mathcal{N}_1 in Figure 16 [right]). All other ovals are not modified.

Let us remark that from the point of view of soliton solutions this procedure is non-trivial and generates some KP-II families of solutions discussed in the literature such as O-solitons and P-solitons [16].

Since we work only with planar directed graphs and we assume that any internal edge belongs to at least one path starting and ending at the boundary of the disk, in our setting defrosture corresponds to the elimination of two consecutive boundary vertices, one of which is a source and the other one is a sink, and to gluing the resulting directed half-edges (see Figure 17). Defrosture transforms the face Ω_2 into the face $\hat{\Omega}_2$, and the faces Ω_1 , Ω_3 are merged into the face $\hat{\Omega}_1$.

It is easy to check that any planar graph in the disk considered in our text can be obtained starting from several copies of Le-graphs associated with the small positive Grassmannians $Gr^{TP}(1, 3)$, $Gr^{TP}(2, 3)$ and $Gr^{TP}(1, 2)$ in such a way that at any step planarity is preserved and any edge

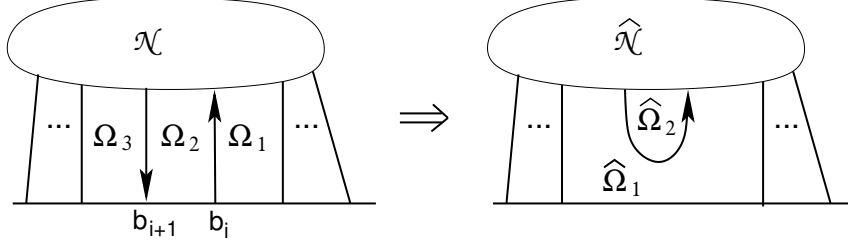


FIGURE 17. The projection procedure for the graph preserving planarity.

of the resulting graph belongs at least to one directed path starting and ending at the boundary of the disk.

Let us now explain the effect of amalgamation on the total edge signature and on the divisor structure. At this aim we use Lemmas 6.2.1 and 2.5.2 to compute the edge signatures of the faces of the amalgamated networks in terms of that of the initial networks. As in the previous section let \mathcal{N} be a PBDTP network representing a point in $Gr^{TNN}(k, n)$, and for any given face Ω , let the indices ϵ_Ω , $n_{w,\Omega}$ and s_Ω respectively denote the edge signature, the number of white vertices and the number of sources of $\partial\Omega$. Then the proof of the next Lemmas follows from Theorem 2.5.1

$$(7.1) \quad \epsilon_\Omega + n_{w,\Omega} + s_\Omega = \begin{cases} 1 & \text{mod } 2, & \text{if } \Omega \text{ is a finite oval;} \\ k & \text{mod } 2, & \text{if } \Omega \text{ is the infinite oval.} \end{cases}$$

Lemma 7.0.1. Edge signature of the direct sum Let \mathcal{N}_i be PBDTP networks representing points in $Gr^{TNN}(k_i, n_i)$, $i = 1, 2$ and \mathcal{N} be their disjoint union representing a point in $Gr^{TNN}(k_1 + k_2, n_1 + n_2)$ with notations as in Figure 16. Then, the edge signature behaves as follows:

(1) If all boundary vertices of \mathcal{N}_2 precede all boundary vertices of \mathcal{N}_1 (Figure 16 [left]),

$$(7.2) \quad \epsilon_{\Omega_0} = \epsilon_{\Omega_{0,1}} + \epsilon_{\Omega_{0,2}} \quad \text{mod } 2,$$

and is unchanged in all other faces;

(2) If all boundary vertices of \mathcal{N}_1 are located between two consecutive boundary vertices of \mathcal{N}_2 (Figure 16 [right]),

$$(7.3) \quad \epsilon_{\Omega_0} = \epsilon_{\Omega_{0,2}} + k_1 \quad \text{mod } 2, \quad \epsilon_{\Omega_1} = \epsilon_{\Omega_{0,1}} + \epsilon_{\Omega_{1,2}} + k_1, \quad \text{mod } 2,$$

and is unchanged in all other faces.

We now describe the action of defrosting on the edge signatures. We remark that if both ovals Ω_1, Ω_3 are finite, then $\hat{\Omega}_1$ is also a finite oval, otherwise it is the infinite oval. Similarly, $\hat{\Omega}_2$ is the infinite oval if and only if Ω_2 is the infinite oval.

Lemma 7.0.2. Effect of defrosting on edge signatures Let \mathcal{N} be PBDTP network representing a point in $Gr^{TNN}(k, n)$, and $\hat{\mathcal{N}}$ be the defrosted network representing a point in $Gr^{TNN}(k-1, n-2)$ with notations as in Figure 17. Then, the edge signature behaves as follows:

$$(7.4) \quad \epsilon_{\hat{\Omega}_1} = \epsilon_{\Omega_1} + \epsilon_{\Omega_3} \quad \text{mod } 2,$$

$$(7.5) \quad \epsilon_{\hat{\Omega}_2} = \begin{cases} \epsilon_{\Omega_2} + 1 & \text{mod } 2 & \text{if } \Omega_2 \text{ is a finite oval;} \\ \epsilon_{\Omega_2} & \text{mod } 2, & \text{if } \Omega_2 \text{ is the infinite oval,} \end{cases}$$

and is unchanged in all other faces.

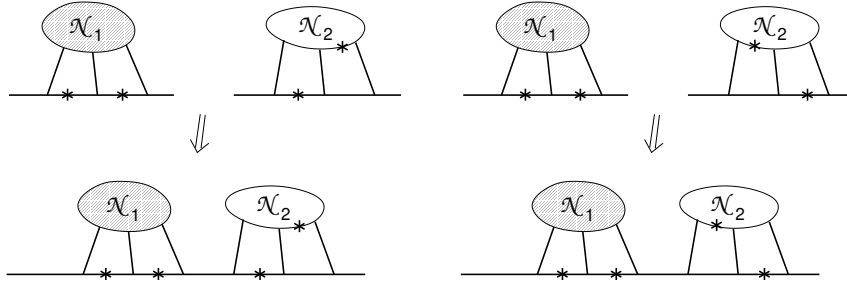


FIGURE 18. Real regular divisor configurations for disjoint union of positroid cells if we place one graph next to another one.

Next we discuss the effect of amalgamation on real regular divisor configurations. The direct sum is trivial in terms of matrices, but non-trivial superposition in terms of the corresponding soiton solutions. The possible real regular divisor configurations depend on the type of the disjoint union. If we place one graph next to the other one, the allowed real regular divisor configurations coincide with the union of all possible configurations on both initial networks. If one graph is placed inside another one, we have more admissible divisor configurations provided that the infinite face $\Omega_{0,1}$ contains at least one trivalent white vertex.

Lemma 7.0.3. Real regular divisor configurations for direct sum of networks Let \mathcal{N}_i be PBDTP networks representing points in $Gr^{TNN}(k_i, n_i)$, $i = 1, 2$ and \mathcal{N} be their disjoint union representing a point in $Gr^{TNN}(k_1 + k_2, n_1 + n_2)$. Then the degree of the divisor (Sato divisor) associated to \mathcal{N} is the sum of the degrees of the divisors (Sato divisors) associated to \mathcal{N}_1 and \mathcal{N}_2 . Moreover,

- (1) If all boundary vertices of \mathcal{N}_2 precede all boundary vertices of \mathcal{N}_1 (Figure 18), then all admissible divisors \mathcal{D} on \mathcal{N} are sums $\mathcal{D} = \mathcal{D}_1 + \mathcal{D}_2$, where \mathcal{D}_i , are admissible divisors on \mathcal{N}_i , $i = 1, 2$;
- (2) If all boundary vertices of \mathcal{N}_1 are located between two consecutive boundary vertices of \mathcal{N}_2 (Figure 19) and the infinite oval of \mathcal{N}_1 contains no trivalent white vertices, then the admissible divisors are exclusively sums $\mathcal{D} = \mathcal{D}_1 + \mathcal{D}_2$, where \mathcal{D}_i , are admissible divisors on \mathcal{N}_i , $i = 1, 2$ such that either there is no Sato divisor point in the oval $\Omega_{1,2}$, or the Sato divisor point in the oval $\Omega_{1,2}$ lies outside the interval $[\kappa_1^{(1)}, \kappa_{n_1}^{(1)}]$;
- (3) If all boundary vertices of \mathcal{N}_1 are located between two consecutive boundary vertices of \mathcal{N}_2 (Figure 19) and the infinite oval of \mathcal{N}_1 contains at least one trivalent white vertex, then either \mathcal{D} is as in Item 2, or is a configuration obtained starting from an admissible configuration \mathcal{D}_2 on \mathcal{N}_2 , by eliminating the Sato divisor point from the oval $\Omega_{1,2}$, adding a divisor on a trivalent white vertex in $\Omega_{0,1}$, placing $k_1 + 1$ Sato divisor points in \mathcal{N}_1 and completing the configuration respecting the regularity divisor rules for \mathcal{N}_1 .

In Figures 18, 19 we illustrate the direct sum of $Gr^{TP}(1, 3)$ and $Gr^{TP}(2, 3)$. The new configuration on Figure 19 is the middle one.

Finally we discuss the effect of defrosting consecutive boundary vertices on the divisor structure.

Lemma 7.0.4. Effect of defrosting on the regular divisors Let \mathcal{N} be PBDTP network representing a point in $Gr^{TNN}(k, n)$, and $\hat{\mathcal{N}}$ be the defrosted network representing a point in $Gr^{TNN}(k - 1, n - 2)$. Then the degrees of both the KP divisor and the Sato divisor associated to $\hat{\mathcal{N}}$ are one less than degrees of the corresponding initial divisors.

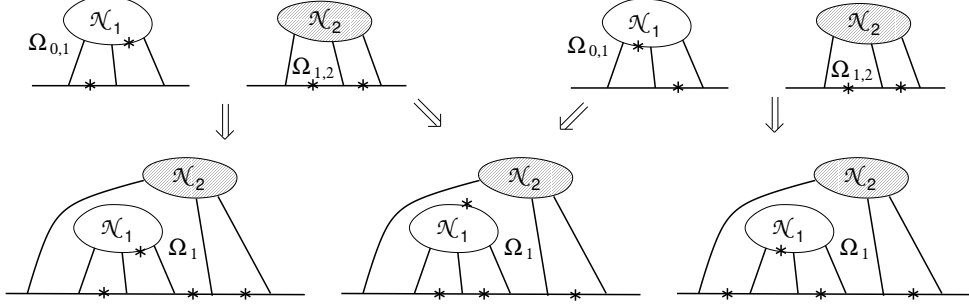


FIGURE 19. Real regular divisor configurations for disjoint union of positroid cells if we place one graph inside the other one.

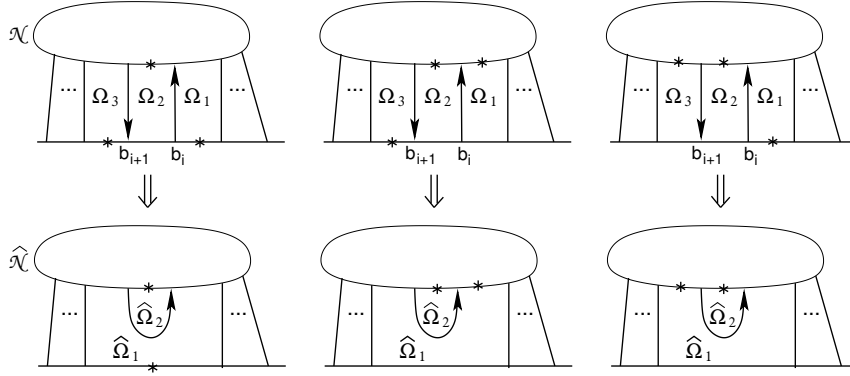


FIGURE 20. Real regular divisor configurations for projections of positroid cells involving 3 finite ovals.

Moreover, the admissible real regular divisor structures of $\hat{\mathcal{N}}$ correspond to the divisor structures of \mathcal{N} such that:

- (1) The oval Ω_2 does not contain a Sato divisor point;
 - (2) The union of ovals $\Omega_1 \cup \Omega_3$ contains at least one Sato divisor point,
- and are obtained by elimination of one Sato divisor point from $\Omega_1 \cup \Omega_3$.

We schematically illustrate the above Lemma in Figures 20–22.

8. EFFECT OF MOVES AND REDUCTIONS ON CURVES AND DIVISORS

In [61] the local transformations of planar bicolored networks in the disk which leave invariant the boundary measurement map are classified. There are three moves:

- (M1) The square move (see Figure 23);
- (M2) The unicolored edge contraction/uncontraction (see Figure 24);
- (M3) The middle vertex insertion/removal (see Figure 26);

and three reductions:

- (R1) The parallel edge reduction (see Figure 27);
- (R2) The dipole reduction (see Figure 28[left]);
- (R3) The leaf reduction (see Figure 28[right]);

such that two networks in the disk connected by a sequence of such moves and reductions represent the same point in $Gr^{\text{TN}}(k, n)$. In our construction each such transformation induces

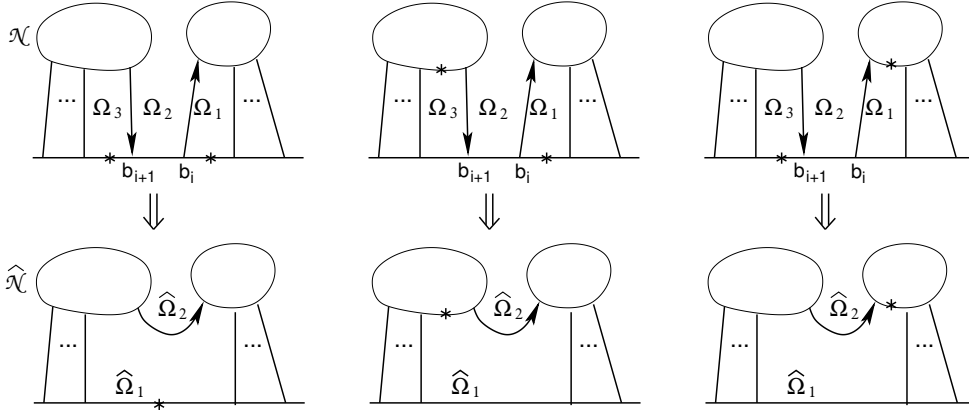


FIGURE 21. Real regular divisor configurations for projections of positroid cells when Ω_2 is the infinite oval.

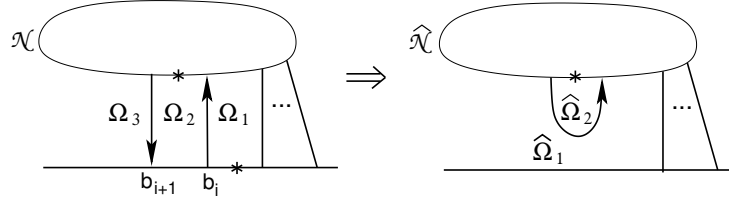


FIGURE 22. Real regular divisor configurations for dprojections of positroid cells when either Ω_1 or Ω_3 is the infinite oval.

a well defined change in both the curve, the system of edge vectors and the dressed divisor which we describe below.

In the following, we restrict ourselves to PBDTP networks and, without loss of generality, we fix both the orientation and the gauge ray direction. Indeed changes of orientation or of gauge direction produce effects on both the system of vectors, the edge wave function and the dressed divisor which are completely under control in view of the results of the previous Sections.

We label vertices, edges, faces in the network corresponding to components, double points, ovals in the curve with the same indices. $(\mathcal{N}, \mathcal{O}, \mathfrak{l})$ is the initial oriented network and $(\tilde{\mathcal{N}}, \tilde{\mathcal{O}}, \mathfrak{l})$ the oriented network after the move or reduction (R1)–(R3), where we assume that the orientation $\tilde{\mathcal{O}}$ coincides with \mathcal{O} at all edges except at those involved in the move or reduction where we use Postnikov rules to assign the orientation. We denote with the same symbol and a tilde any quantity referring to the transformed network or the transformed curve. For instance, g and \tilde{g} respectively denote the genus in the initial and transformed curves. To simplify notations, we use the same symbol γ_l , respectively $\tilde{\gamma}_l$ for the divisor number and the divisor point before and after the transformation.

(M1) The square move: If a network has a square formed by four trivalent vertices whose colors alternate as one goes around the square, then one can switch the colors of these four vertices and transform the weights of adjacent faces as shown in Figure 23[left]. The relation between the edge weights with the orientation in Figure 23 is [61]

$$(8.1) \quad \tilde{\alpha}_1 = \frac{\alpha_3 \alpha_4}{\tilde{\alpha}_2}, \quad \tilde{\alpha}_2 = \alpha_2 + \alpha_1 \alpha_3 \alpha_4, \quad \tilde{\alpha}_3 = \frac{\alpha_2 \alpha_3}{\tilde{\alpha}_2}, \quad \tilde{\alpha}_4 = \frac{\alpha_1 \alpha_3}{\tilde{\alpha}_2}.$$

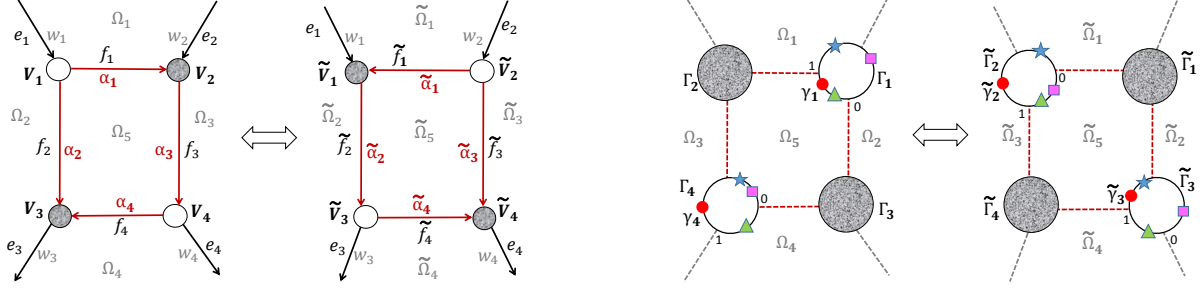


FIGURE 23. The effect of the square move [left] on the possible configurations of dressed divisor points [right].

TABLE 2. The effect of the square move on the dressed divisor

Position of poles in Γ	Position of poles in $\tilde{\Gamma}$	Symbol for divisor point	Range of parameter
$\gamma_1 \in \Omega_5, \gamma_4 \in \Omega_4$	$\tilde{\gamma}_2 \in \tilde{\Omega}_5, \tilde{\gamma}_3 \in \tilde{\Omega}_4$	\triangle	$\psi_0 > 0$
$\gamma_1 \in \Omega_5, \gamma_4 \in \Omega_3$	$\tilde{\gamma}_2 \in \tilde{\Omega}_3, \tilde{\gamma}_3 \in \tilde{\Omega}_5$	\circ	$-\alpha_4 < \psi_0 < 0$
$\gamma_1 \in \Omega_1, \gamma_4 \in \Omega_5$	$\tilde{\gamma}_2 \in \tilde{\Omega}_1, \tilde{\gamma}_3 \in \tilde{\Omega}_5$	\star	$-(\tilde{\alpha}_4)^{-1} < \psi_0 < -\alpha_4$
$\gamma_1 \in \Omega_2, \gamma_4 \in \Omega_5$	$\tilde{\gamma}_2 \in \tilde{\Omega}_5, \tilde{\gamma}_3 \in \tilde{\Omega}_2$	\square	$\psi_0 < -(\tilde{\alpha}_4)^{-1}$

The system of equations on the edges outside the square is the same before and after the move and also the boundary conditions remain unchanged. The uniqueness of the solution implies that all vectors outside the square including E_1, E_2, E_3, E_4 remain the same [7].

The relation between the dressed divisor points before and after the square move in the local coordinates induced by the orientation in Figure 23 follow by direct inspection of the formulas and the relative positions are easy to check using $\alpha_2 < \tilde{\alpha}_2, \alpha_4 < (\tilde{\alpha}_4)^{-1}$.

Lemma 8.0.1. *The effect of the square move on the position of the divisor* Let the local coordinates on $\Gamma_i, \tilde{\Gamma}_i, i = 1, 2$, be as in Figure 23 and let $\psi_0 = (-1)^{\epsilon_{V_4, V_3}} \frac{\Psi_{V_4, e_4}(\vec{t}_0)}{\Psi_{V_3, e_3}(\vec{t}_0)}$, where $\Psi_{V_j, e_j}(\vec{t}_0)$ is the value of the dressed half-edge wave function at the half edges $(V_j, e_j), j = 3, 4$. Then

$$\gamma_1 = \frac{\alpha_2 \tilde{\alpha}_2^{-1}}{1 + \tilde{\alpha}_4 \psi_0}, \quad \gamma_4 = \frac{\alpha_4}{\alpha_4 + \psi_0}, \quad \tilde{\gamma}_2 = \frac{\alpha_4(1 + \tilde{\alpha}_4 \psi_0)}{\alpha_4 + \psi_0}, \quad \tilde{\gamma}_3 = \frac{1}{1 + \tilde{\alpha}_4 \psi_0},$$

and the position of the divisor points in the ovals depends on ψ_0 as shown in Table 2. In particular, there is exactly one dressed divisor point in $(\Gamma_1 \cup \Gamma_2) \cap \Omega_5, (\tilde{\Gamma}_1 \cup \tilde{\Gamma}_2) \cap \tilde{\Omega}_5$.

The proof follows using the definition of divisor number and the following identities

$$\text{wind}(e_2, f_3) + \epsilon_{V_2, V_3} + \epsilon_{V_3, V_4} \equiv \epsilon_{\tilde{V}_2, \tilde{V}_1} + \epsilon_{\tilde{V}_1, \tilde{V}_3} + \text{wind}(f_2, e_3) \pmod{2},$$

$$\epsilon_{V_1, V_2} + \epsilon_{V_2, V_4} + \text{wind}(f_3, e_4) \equiv \text{wind}(e_1, f_2) + \epsilon_{\tilde{V}_1, \tilde{V}_3} + \epsilon_{\tilde{V}_3, \tilde{V}_4} \pmod{2}.$$

The square move leaves the number of ovals invariant, eliminates the divisor points γ_1, γ_2 and creates the divisor points $\tilde{\gamma}_1, \tilde{\gamma}_2$. We summarize such properties in the following Lemma.

Lemma 8.0.2. *The effect of the square move (M1) on the curve and the divisor* Let $\tilde{\mathcal{N}}$ be obtained from \mathcal{N} via move (M1). Let $\mathcal{D} = \mathcal{D}(\mathcal{N}), \tilde{\mathcal{D}} = \mathcal{D}(\tilde{\mathcal{N}})$ respectively be the dressed network divisor before and after the square move. Then

- (1) $\tilde{g} = g$, and the number of ovals is invariant;

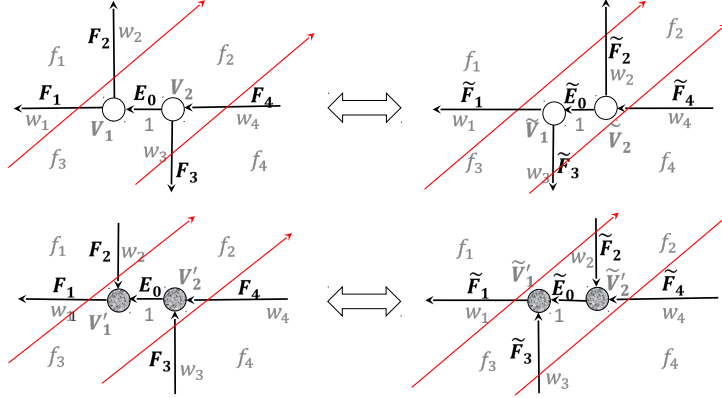


FIGURE 24. The insertion/removal of an uncolored internal vertex is equivalent to a flip move of the uncolored vertices.

- (2) The number of dressed divisor points is invariant in every oval: $\tilde{\nu}_l = \nu_l$, $l \in [0, g]$;
- (3) $\tilde{\mathcal{D}} = (\mathcal{D} \setminus \{\gamma_1, \gamma_2\}) \cup \{\tilde{\gamma}_1, \tilde{\gamma}_2\}$, where γ_l (respectively $\tilde{\gamma}_l$), $l = 1, 2$, is the divisor point on Γ_l (respectively $\tilde{\Gamma}_l$), the component of \mathbb{CP}^1 associated to the white vertex V_l (respectively \tilde{V}_l) involved in the square move transforming \mathcal{N} into $\tilde{\mathcal{N}}$;
- (4) Either $\gamma_l, \tilde{\gamma}_l$, $l = 1, 2$, are all untrivial divisor points or all trivial divisor points.

(M2) The uncolored edge contraction/uncontraction The uncolored edge contraction/uncontraction consists in the elimination/addition of an internal vertex of equal color and of an unit edge, and it leaves invariant the face weights and the boundary measurement map. Such move consists in a flip of uncolored vertices in the case of trivalent graphs (see Figure 24). A generic contraction/uncontraction of uncolored internal edges can be expressed as a combination of elementary flip moves each involving a pair of consecutive uncolored vertices. A flip move at black vertices leaves the divisor invariant. The flip move at white vertices preserves the total index in each oval. In the following lemma we label Ω_l , $l \in [4]$, the ovals involved in the flip move as in Figure 25.

Lemma 8.0.3. *The effect of the flip move (M2) at a pair of white vertices on the divisor* Let $\tilde{\mathcal{N}}$ be obtained from \mathcal{N} via a flip move (M2) at a pair of trivalent white vertices. Let $\mathcal{D} = \mathcal{D}(\mathcal{N})$, $\tilde{\mathcal{D}} = \mathcal{D}(\tilde{\mathcal{N}})$, respectively be the dressed network divisor before and after such move. Then

- (1) $\tilde{g} = g$ and the number of ovals is invariant;
- (2) The number of divisor points is invariant in every oval except possibly at the ovals involved in the move. In the ovals Ω_l , $l \in [4]$ the parity of the number of divisor points before and after the move is invariant: $\tilde{\nu}_l - \nu_l = 0 \pmod{2}$, $l \in [4]$;
- (3) $\tilde{\mathcal{D}} = (\mathcal{D} \setminus \{\gamma_1, \gamma_2\}) \cup \{\tilde{\gamma}_1, \tilde{\gamma}_2\}$, where we use the same notations as in Figure 25.

The proof is omitted. In Figure 25 we show the position of the divisor points before and after the flip move [top-left], in function of the relative signs of the value of the dressed wave function at the double points of Γ . Faces f_l correspond to ovals Ω_l , the orientation of the edges in the graph at each vertex induces the local coordinates at each copy of \mathbb{CP}^1 in Γ .

Corollary 8.0.4. *The effect of the flip move on the divisor* Let the local coordinates on $\Gamma_i, \tilde{\Gamma}_i$, $i = 1, 2$, be as in Figure 25 and let $\Psi_1 = \Psi_1(\vec{t}_0)$,

$$\Psi_j = \Psi_{V_1, e_j}(\vec{t}_0), \quad j = 1, 2, \quad \Psi'_3 = (-1)^{1+\epsilon_{V_2, V_1}} \Psi_{V_2, e_3}(\vec{t}_0),$$

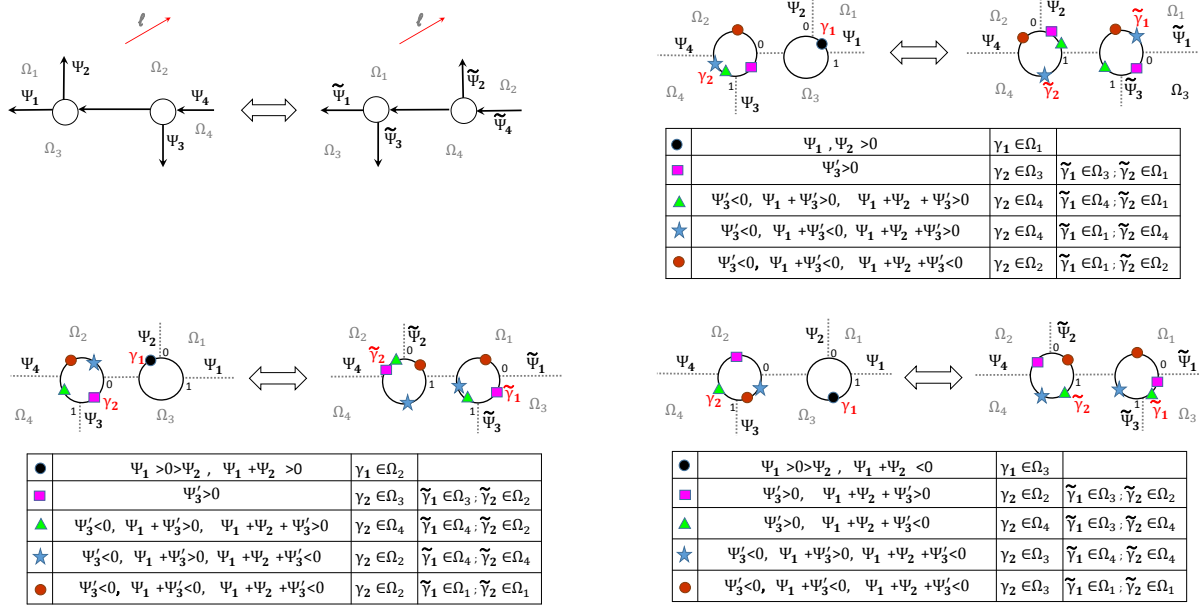


FIGURE 25. The effect of the flip move [top-left] on the possible configurations of dressed divisor points [top-right],[bottom-left],[bottom-right].

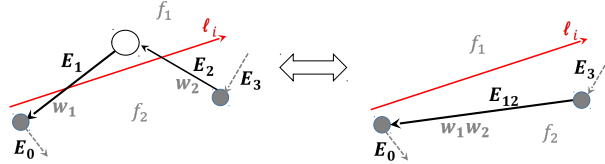


FIGURE 26. The middle edge insertion/removal.

where $\Psi_{V_i, e_j}(\vec{t}_0)$ is the value of the half-edge dressed wave function at (V_i, e_j) in the initial configuration and ϵ_{V_2, V_1} is the edge signature at $e_0 = (V_2, V_1)$. Then

$$\gamma_1 = \frac{\Psi_2}{\Psi_1 + \Psi_2}, \quad \gamma_2 = \frac{\Psi_1 + \Psi_2}{\Psi_1 + \Psi_2 + \Psi'_3}, \quad \tilde{\gamma}_1 = \frac{\Psi_1}{\Psi_1 + \Psi'_3}, \quad \tilde{\gamma}_2 = \frac{\Psi_2}{\Psi_1 + \Psi_2 + \Psi'_3},$$

and the position of the divisor points in the ovals is shown in Figure 25.

The proof is straightforward using the definition of divisor coordinates and the relations between the winding numbers before and after the flip move. We remark that not all combinations of signs are realizable at the finite ovals for real regular divisors. For instance in Figure 25[bottom, left] the star-shaped combination corresponds to the following choice of sign of the half-edge wave function $\Psi_2(\vec{t}_0), \Psi'_3(\vec{t}_0) < 0 < \Psi_1(\vec{t}_0), \Psi_1(\vec{t}_0) + \Psi_2(\vec{t}_0) < 0 < \Psi_1(\vec{t}_0) + \Psi'_3(\vec{t}_0)$, and to divisor configurations $\gamma_1, \gamma_2 \in \Omega_2$ and $\tilde{\gamma}_1, \tilde{\gamma}_2 \in \Omega_4$, which are not allowed for real regular divisors, since every finite oval may contain only one divisor point.

Finally, if $F_3 = c_{13}F_1$ for some $c_{13} \neq 0$, whereas F_2, F_1 are linearly independent, then also $\Psi'_3(\vec{t}) = \pm c_{13}\Psi_1(\vec{t})$, for all \vec{t} . In such case $\gamma_l, l = 1, 2$, and $\tilde{\gamma}_2$ are untrivial divisor points, whereas $\tilde{\gamma}_1$ is a trivial divisor point, i.e. the normalized wave function is constant on the corresponding copy of \mathbb{CP}^1 .

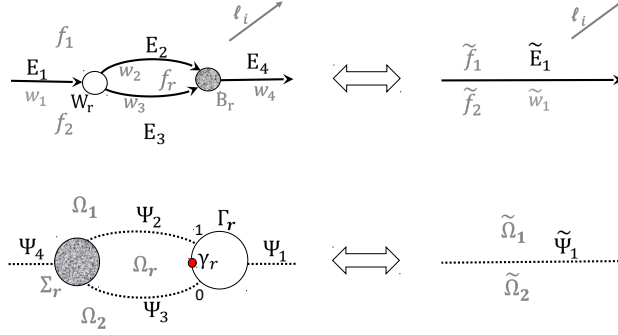


FIGURE 27. The parallel edge reduction [top] eliminates an oval, diminishes by one the genus and eliminates a divisor point γ_r [bottom].

(M3) The middle edge insertion/removal The middle edge insertion/removal concerns bivalent vertices (see Figure 26) without changing the face configuration. i.e. the triangle formed by the edges e_1, e_2, e_{12} does not contain other edges of the network. Then the relation between the vectors is simply $E_{12} = (-1)^{\text{wind}(e_3, e_2) - \text{wind}(e_3, e_{12})} E_2$ [7]. This move does not affect neither the number of ovals nor the divisor configuration.

(R1) The parallel edge reduction The parallel edge reduction consists of the removal of two trivalent vertices of different color connected by a pair of parallel edges (Figure 27[top]) and eliminates an oval and a trivial divisor point:

Lemma 8.0.5. The effect of (R1) on the divisor Let $\tilde{\mathcal{N}}$ be obtained from \mathcal{N} via the parallel edge reduction (R1), and denote $\tilde{\Gamma}$ and Γ the curve after and before such reduction. Then

- (1) The genus \tilde{g} of $\tilde{\Gamma}$ is one less than that in Γ : $\tilde{g} = g - 1$;
- (2) The oval Ω_r corresponding to the face f_r and the components Γ_r, Σ_r corresponding to the white and black vertices W_r, B_r , are removed by effect of the parallel edge reduction;
- (3) The trivial divisor point $\gamma_r \in \Gamma_r \cap \Omega_r$ is removed;
- (4) All other divisor points are not effected by the reduction.

In Figure 27[bottom] we show the effect of the parallel edge reduction on the curve. The divisor point in $\Gamma_{\text{red}}^{(1)}$ is trivial

$$\gamma_r = \frac{\Psi_3(\vec{t}_0)}{\Psi_2(\vec{t}_0) + \Psi_3(\vec{t}_0)} = \frac{w_3}{w_2 + w_3},$$

since $\Psi_2(\vec{t}) = (-1)^{\text{int}(e_2)} w_2 \Psi_4(\vec{t})$, $\Psi_3(\vec{t}) = (-1)^{\text{int}(e_2)} w_3 \Psi_4(\vec{t})$, $\Psi_1(\vec{t}) = (-1)^{\text{int}(e_1)} w_1 (\Psi_2(\vec{t}) + \Psi_3(\vec{t}))$, for all \vec{t} . On both $\Gamma_{\text{red}}^{(1)}$ and $\Sigma_{\text{red}}^{(1)}$ the normalized wave function is independent of the spectral parameter and takes the value $\frac{\Psi_1(\vec{t})}{\Psi_1(\vec{t}_0)} \equiv \frac{\Psi_4(\vec{t})}{\Psi_4(\vec{t}_0)}$. After the reduction, on the edge \tilde{e}_1 , the edge wave function $\tilde{\Psi}_1(\vec{t})$ takes the value $\tilde{\Psi}_1(\vec{t}) = \Psi_1(\vec{t})$, so that, for any \vec{t} , the normalized wave function keeps the same value after the reduction at the double point corresponding to such edge in $\tilde{\Gamma}$.

(R2) the dipole reduction and (R3) The leaf reduction: The dipole reduction consists of the elimination of an isolated component consisting of two vertices joined by an edge e (see Figure 28[left]). The transformation leaves invariant the weight of the face containing such component. Since the edge vector at e is $E_e = 0$, this transformation acts trivially on the vector

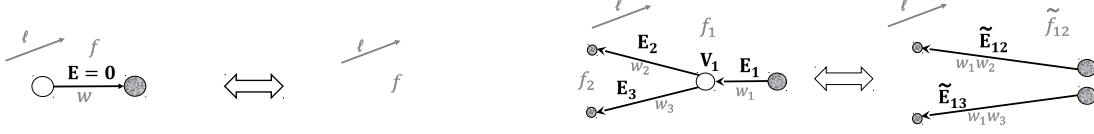
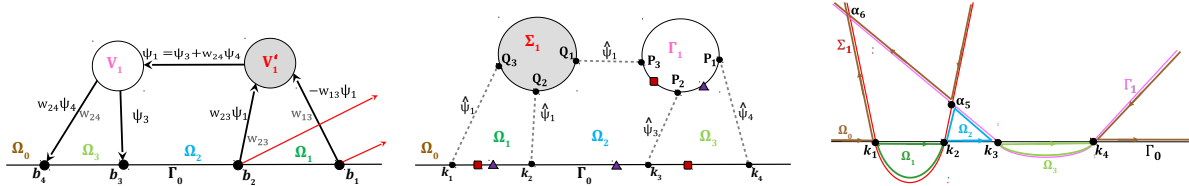


FIGURE 28. Left: the dipole reduction. Right: the leaf reduction.

FIGURE 29. The reduced Le-network \mathcal{N}_{red} [left], the topological model of the corresponding spectral curve $\Gamma_{T,\text{red}}$ [center] and its plane curve representation [right] for soliton data in $\mathcal{S}_{34}^{\text{TNN}} \subset \text{Gr}^{\text{TNN}}(2, 4)$. $\Psi_1(\bar{t}) = \Psi_3(\bar{t}) + w_{24}\Psi_4(\bar{t})$. The configurations of the KP divisor (triangles/squares) depend only on the sign of $\Psi_3(\bar{t}_0)$. On the curve double points are represented as dotted segments and $\hat{\psi}_l \equiv \hat{\psi}_l(\bar{t})$ is as in (9.5).

system. The dipole reduction (R2) corresponds to the removal of an edge carrying a zero vector and leaves invariant the number of ovals and the position of the divisor points.

The leaf reduction occurs when a network contains a vertex u incident to a single edge e_1 ending at a trivalent vertex (see Figure 28[right]): in this case one removes u and e_1 , disconnects e_2 and e_3 , assigns the color of u at all newly created vertices of the edges e_{12} and e_{13} . We assume that e_1 is short enough, it does not intersect the gauge rays and that the newly created vertices are close enough to V_1 so that the windings are not affected. Then $E_1 = \tilde{E}_{12} + \tilde{E}_{13}$ and $\tilde{E}_{12} = w_1 E_2$, $\tilde{E}_{13} = w_1 E_3$. In the leaf reduction (R3) the only non-trivial case corresponds to the situation where the faces f_1, f_2 are distinct in the initial configuration. In this case we eliminate one oval and one divisor point.

Lemma 8.0.6. The effect of (R3) on the divisor Let $\tilde{\mathcal{N}}$ is obtained from \mathcal{N} via reduction (R3) and the faces f_1, f_2 be distinct. Let $\mathcal{D} = \mathcal{D}(\mathcal{N})$ and $\tilde{\mathcal{D}} = \mathcal{D}(\tilde{\mathcal{N}})$, respectively be the dressed network divisor before and after the reduction. Then

- (1) $\tilde{g} = g - 1$ and the number of ovals diminishes by one;
- (2) $\tilde{\mathcal{D}} = \mathcal{D} \setminus \{\gamma_1\}$, where γ_1 is the divisor point on the component associated to the white vertex V_1 involved in the reduction.

9. PLANE CURVES AND DIVISORS FOR SOLITON DATA IN $\mathcal{S}_{34}^{\text{TNN}} \subset \text{Gr}^{\text{TNN}}(2, 4)$

$\mathcal{S}_{34}^{\text{TNN}}$ is the 3-dimensional positroid cell in $\text{Gr}^{\text{TNN}}(2, 4)$ corresponding to the matroid

$$\mathcal{M} = \{ 12, 13, 14, 23, 24 \},$$

and its elements $[A]$ are equivalence classes of real 2×4 matrices with all maximal minors positive, except $\Delta_{34} = 0$. The three positive weights w_{13}, w_{23}, w_{24} of the Le-tableau (see Figure 29[top,left]) parametrize $\mathcal{S}_{34}^{\text{TNN}}$ and correspond to the matrix in the reduced row echelon form (RREF),

$$(9.1) \quad A = \begin{pmatrix} 1 & 0 & -w_{13} & -w_{13}w_{24} \\ 0 & 1 & w_{23} & w_{23}w_{24} \end{pmatrix}.$$

The generators of the Darboux transformation $\mathfrak{D} = \partial_x^2 - \mathfrak{w}_1(\bar{t})\partial_x - \mathfrak{w}_2(\bar{t})$ are $f^{(1)}(\bar{t}) = e^{\theta_1(\bar{t})} - w_{13}e^{\theta_3(\bar{t})} - w_{13}w_{24}e^{\theta_4(\bar{t})}$, $f^{(2)}(\bar{t}) = e^{\theta_2(\bar{t})} + w_{23}e^{\theta_3(\bar{t})} + w_{23}w_{24}e^{\theta_4(\bar{t})}$.

In the following sections we construct a reducible rational curve $\Gamma_{T,\text{red}}$ and the divisor for soliton data $(\mathcal{K}, [A])$ with $\mathcal{K} = \{\kappa_1 < \kappa_2 < \kappa_3 < \kappa_4\}$ and $[A] \in \mathcal{S}_{34}^{\text{TNN}}$. We represent $\Gamma_{T,\text{red}}$ as a plane curve given by the intersection of a line and two quadrics (see (9.2) and (9.3)) and we verify that it is a rational degeneration of the genus 3 M-curve Γ_ε ($0 < \varepsilon \ll 1$) in (9.4). We then apply a parallel edge unredution and a flip move to the reduced network and compute the transformed KP divisor on the transformed curves.

9.1. Spectral curves for the reduced Le-network and their desingularizations. We briefly illustrate the construction of a rational spectral curve $\Gamma_{T,\text{red}}$ for soliton data in $\mathcal{S}_{34}^{\text{TNN}}$. We choose the reduced Le-graph $\mathcal{N}_{T,\text{red}}$ as dual to the reducible rational curve and use Postnikov rules to assign the weights to construct the corresponding Le-network representing $[A] \in \mathcal{S}_{34}^{\text{TNN}}$ (Figure 29[left]). In Figure 29[center], we show the topological model of the curve $\Gamma_{T,\text{red}}$.

The reducible rational curve $\Gamma_{T,\text{red}}$ is obtained gluing three copies of \mathbb{CP}^1 , $\Gamma_{T,\text{red}} = \Gamma_0 \sqcup \Gamma_1 \sqcup \Sigma_1$, and it may be represented as a plane curve given by the intersection of a line (Γ_0) and two quadrics (Γ_1, Σ_1). We plot both the topological model and the plane curve for this example in Figure 29[right]. To simplify its representation, we impose that Γ_0 is one of the coordinate axis in the (λ, μ) -plane, say $\mu = 0$, that $P_0 \in \Gamma_0$ is the infinite point, that the quadrics Σ_1 and Γ_1 are parabolas with two real finite intersection points $\alpha_5 = (\lambda_5, \mu_5)$, $\alpha_6 = (\lambda_6, \mu_6)$:

$$(9.2) \quad \Gamma_0 : \mu = 0, \quad \Gamma_1 : \mu - (\lambda - \kappa_3)(\lambda - \kappa_4) = 0, \quad \Sigma_1 : \mu - c_1(\lambda - \kappa_1)(\lambda - \kappa_2) = 0.$$

In the following we also take $c_1 > 1$ and choose $\lambda(P_3) = \lambda(Q_1) = \lambda_5$. Then, by construction, $\lambda_5 \in]\kappa_2, \kappa_3[$ and $\lambda_6 < \kappa_1$. As usual we denote Ω_0 the infinite oval, that is $P_0 \in \Omega_0$, and Ω_j , $j \in [3]$, the finite ovals. Since the singularity at infinity is completely resolved, the quadrics Σ_1 and Γ_1 do not intersect at infinity. The intersection point α_6 does not correspond to any of the marked points of the topological model of Γ . Such singularity is resolved in the partial normalization and therefore there are no extra conditions to be satisfied by the dressed wave functions at α_6 .

The relation between the coordinate λ in the plane curve representation and the coordinate ζ introduced in Definition 4.2.1 may be easily worked out at each component of $\Gamma_{T,\text{red}}$. On Γ_1 , we have 3 real ordered marked points P_m , $m \in [3]$, with ζ -coordinates: $\zeta(P_1) = 0 < \zeta(P_2) = 1 < \zeta(P_3) = \infty$. Comparing with (9.2) we then easily conclude that

$$\lambda = \frac{\lambda_5(\kappa_4 - \kappa_3)\zeta + (\kappa_3 - \lambda_5)\kappa_4}{(\kappa_4 - \kappa_3)\zeta + \kappa_3 - \lambda_5}.$$

Similarly, on Σ_1 , we have 3 real ordered marked points Q_m , $m \in [3]$, with ζ -coordinates: $\zeta(Q_1) = 0 < \zeta(Q_2) = 1 < \zeta(Q_3) = \infty$. Comparing with (9.2) we then easily conclude that

$$\lambda = \frac{\kappa_1(\lambda_5 - \kappa_2)\zeta + (\kappa_2 - \kappa_1)\lambda_5}{(\lambda_5 - \kappa_2)\zeta + \kappa_2 - \kappa_1}.$$

$\Gamma_{T,\text{red}}$ is represented by the reducible plane curve $\Pi_0(\lambda, \mu) = 0$, with

$$(9.3) \quad \Pi_0(\lambda, \mu) = \mu \cdot (\mu - (\lambda - \kappa_3)(\lambda - \kappa_4)) \cdot (\mu - c_1(\lambda - \kappa_1)(\lambda - \kappa_2)),$$

and is a rational degeneration of the genus 3 M-curve Γ_ε ($0 < \varepsilon \ll 1$):

$$(9.4) \quad \Gamma_\varepsilon : \quad \Pi(\lambda, \mu; \varepsilon) = \Pi_0(\lambda, \mu) - \varepsilon^2 (\lambda - \lambda_6)^2 = 0.$$

Remark 9.1.1. *The plane curve representation for a given cell is not unique. For example, a rational spectral curve $\Gamma_{T,\text{red}}$ for soliton data in $\mathcal{S}_{34}^{\text{TNN}}$ can be also represented as the union of one quadric and two lines.*

9.2. The KP divisor on $\Gamma_{T,\text{red}}$. We now construct the wave function and the KP divisor on $\Gamma_{T,\text{red}}$. For this example, the KP wave function may take only three possible values at the marked points:

$$(9.5) \quad \hat{\psi}_l(\vec{t}) = \frac{\mathfrak{D}e^{\theta_l(\vec{t})}}{\mathfrak{D}e^{\theta_l(\vec{t}_0)}}, \quad l = 1, 3, 4,$$

where $\theta_l(\vec{t}) = \kappa_l x + \kappa_l^2 y + \kappa_l^3 t$. In Figure 29 [right] we show which double point carries which of the above values of $\hat{\psi}$. At each marked point the value $\hat{\psi}_l(\vec{t})$ is independent on the choice of local coordinates on the components, i.e. of the orientation in the network.

The local coordinate of each divisor point may be computed using (6.2). On $\Gamma = \Gamma_{T,\text{red}}$, the KP divisor $\mathcal{D}_{\text{KP},\Gamma}$ consists of the degree $k = 2$ Sato divisor $(\gamma_{S,1}, \gamma_{S,2}) = (\gamma_{S,1}(\vec{t}_0), \gamma_{S,2}(\vec{t}_0))$ defined in (3.7) and of 1 simple pole $\gamma_1 = \gamma_1(\vec{t}_0)$ belonging to the intersection of Γ_1 with the union of the finite ovals. In the local coordinates induced by the orientation of the network (see Definition 4.2.1), we have

$$(9.6) \quad \zeta(\gamma_{S,1}) + \zeta(\gamma_{S,2}) = \mathfrak{w}_1(\vec{t}_0), \quad \zeta(\gamma_{S,1})\zeta(\gamma_{S,2}) = -\mathfrak{w}_2(\vec{t}_0), \quad \zeta(\gamma_1) = \frac{w_{24}\mathfrak{D}e^{\theta_4(\vec{t}_0)}}{\mathfrak{D}e^{\theta_3(\vec{t}_0)} + w_{24}\mathfrak{D}e^{\theta_4(\vec{t}_0)}}.$$

It is easy to verify that $\mathfrak{D}e^{\theta_1(\vec{t})}, \mathfrak{D}e^{\theta_4(\vec{t})} > 0$ and $\mathfrak{D}e^{\theta_2(\vec{t})} = -\frac{w_{23}}{w_{13}}\mathfrak{D}e^{\theta_1(\vec{t})}$. Therefore, for generic soliton data $[A] \in \mathcal{S}_{34}^{\text{TNN}}$, the KP-II pole divisor configuration is one of the two shown in Figure 29 [center]:

- (1) If $\mathfrak{D}e^{\theta_3(\vec{t}_0)} > 0$, then $\gamma_{S,1} \in \Omega_1$, $\gamma_{S,2} \in \Omega_2$ and $\gamma_1 \in \Omega_3$. One such configuration is illustrated by triangles in the Figure;
- (2) If $\mathfrak{D}e^{\theta_3(\vec{t}_0)} < 0$, then $\gamma_{S,1} \in \Omega_1$, $\gamma_{S,2} \in \Omega_3$ and $\gamma_1 \in \Omega_2$. One such configuration is illustrated by squares in the Figure.

As expected, there is exactly one KP divisor point in each finite oval of Γ , where we use the counting rule established in [3] for non-generic soliton data satisfying $\mathfrak{D}e^{\theta_3(\vec{t}_0)} = 0$.

9.3. The effect of Postnikov moves and reductions on the KP divisor. Next we show the effect of moves and reductions on the divisor position.

We first apply a parallel edge unredution to $\mathcal{N}_{T,\text{red}}$ (Figure 29) and obtain the network \mathcal{N}_{par} in Figure 30[top,left]. We remark that we have a gauge freedom in assigning the weights to the edges involved in this transformation provided that $p, q > 0$. The values on the unnormalized dressed wave function are shown in the Figure. The corresponding curve, Γ_{par} , is presented in Figure 30[top,right]. By construction the KP divisor $\mathcal{D}_{\text{KP},\Gamma}$ consists of the degree $k = 2$ Sato divisor $(\gamma_{S,1}, \gamma_{S,2}) = (\gamma_{S,1}(\vec{t}_0), \gamma_{S,2}(\vec{t}_0))$ computed in (9.6) and of the simple poles $\gamma_i = \gamma_i(\vec{t}_0)$ belonging to the intersection of Γ_i , $i = 1, 2$, with the union of the finite ovals. In the local coordinates induced by the orientation of the network (Definition 4.2.1), we have

$$(9.7) \quad \zeta(\gamma_1) = \frac{w_{24}\mathfrak{D}e^{\theta_4(\vec{t}_0)}}{\mathfrak{D}e^{\theta_3(\vec{t}_0)} + w_{24}\mathfrak{D}e^{\theta_4(\vec{t}_0)}}, \quad \zeta(\gamma_2) = -pq.$$

For generic soliton data $[A] \in \mathcal{S}_{34}^{\text{TNN}}$, the KP-II pole divisor configurations are shown in Figure 30 [top,right]:

- (1) $\gamma_2 \in \Omega_4$ independently of the sign of $\mathfrak{D}e^{\theta_3(\vec{t}_0)} > 0$;
- (2) If $\mathfrak{D}e^{\theta_3(\vec{t}_0)} > 0$, then $\gamma_{S,1} \in \Omega_1$, $\gamma_{S,2} \in \Omega_2$ and $\gamma_1 \in \Omega_3$. One such configuration is illustrated by triangles in the Figure;
- (3) If $\mathfrak{D}e^{\theta_3(\vec{t}_0)} < 0$, then $\gamma_{S,1} \in \Omega_1$, $\gamma_{S,2} \in \Omega_3$ and $\gamma_1 \in \Omega_2$. One such configuration is illustrated by squares in the Figure.

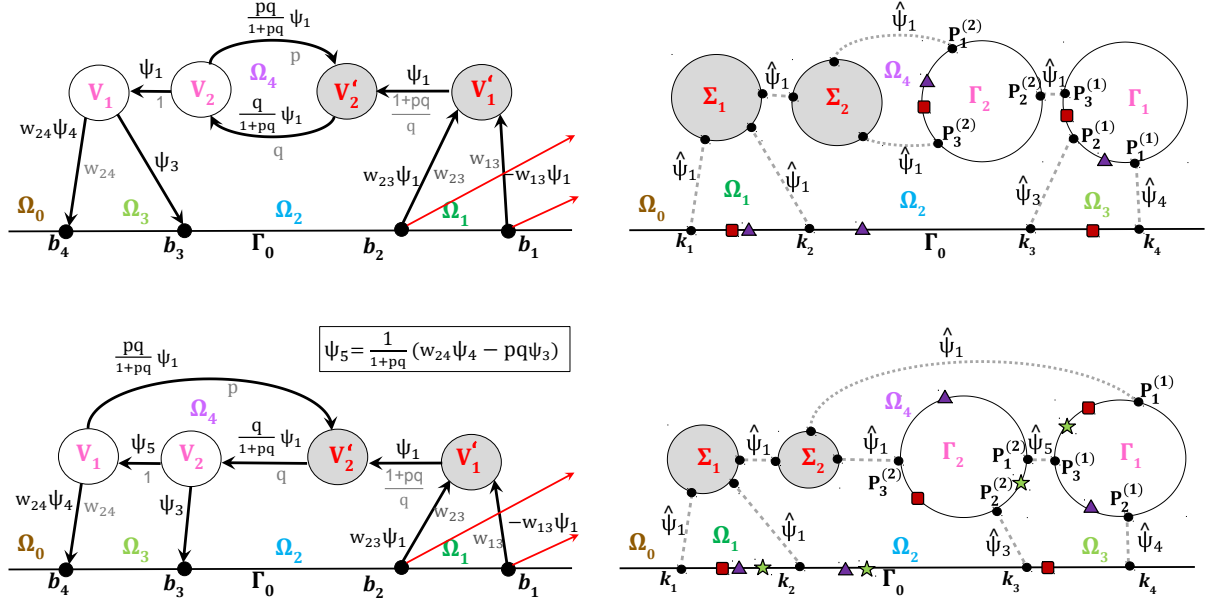


FIGURE 30. Left: \mathcal{N}_{par} [top] is obtained from the reduced Le-network $\mathcal{N}_{T,\text{red}}$ of Figure 29 applying the parallel edge unredution, whereas $\mathcal{N}_{\text{flip}}$ [bottom] is obtained from \mathcal{N}_{par} applying a flip move. Right: The partial normalization of the corresponding curves Γ_{par} [top], Γ_{flip} [bottom] and the possible divisor configurations.

Again, for any given $[A] \in \mathcal{S}_{34}^{\text{TNN}}$, there is exactly one KP divisor point in each finite oval.

Next we apply a flip move to \mathcal{N}_{par} and obtain the network $\mathcal{N}_{\text{flip}}$ in Figure 30[bottom,left] and show the values on the un-normalized dressed wave function in the Figure. The corresponding curve, Γ_{flip} , is presented in Figure 30[bottom,right]. By construction the KP divisor $\mathcal{D}_{\text{KP},\Gamma}$ consists of the degree $k = 2$ Sato divisor $(\gamma_{S,1}, \gamma_{S,2}) = (\gamma_{S,1}(\vec{t}_0), \gamma_{S,2}(\vec{t}_0))$ computed in (9.6) and of the simple poles $\tilde{\gamma}_i = \tilde{\gamma}_i(\vec{t}_0)$ belonging to the intersection of Γ_i , $i = 1, 2$, with the union of the finite ovals. In the local coordinates induced by the orientation of the network, we have

$$(9.8) \quad \zeta(\gamma_1) = \frac{pq \left(\mathfrak{D}e^{\theta_3(\vec{t}_0)} + w_{24} \mathfrak{D}e^{\theta_4(\vec{t}_0)} \right)}{pq \mathfrak{D}e^{\theta_3(\vec{t}_0)} - w_{24} \mathfrak{D}e^{\theta_4(\vec{t}_0)}}, \quad \zeta(\gamma_2) = -\frac{pq \mathfrak{D}e^{\theta_3(\vec{t}_0)} - w_{24} \mathfrak{D}e^{\theta_4(\vec{t}_0)}}{\mathfrak{D}e^{\theta_3(\vec{t}_0)} + w_{24} \mathfrak{D}e^{\theta_4(\vec{t}_0)}}.$$

For generic soliton data $[A] \in \mathcal{S}_{34}^{\text{TNN}}$, the KP-II pole divisor configuration is one of the three shown in Figure 29 [right]:

- (1) If $\mathfrak{D}e^{\theta_3(\vec{t}_0)} > 0$ and $pq \mathfrak{D}e^{\theta_3(\vec{t}_0)} > w_{24} \mathfrak{D}e^{\theta_4(\vec{t}_0)}$, then $\gamma_{S,1} \in \Omega_1$, $\gamma_{S,2} \in \Omega_2$, and $\tilde{\gamma}_1 \in \Omega_3$ and $\tilde{\gamma}_2 \in \Omega_4$. One such configuration is illustrated by triangles in the Figure;
- (2) If $\mathfrak{D}e^{\theta_3(\vec{t}_0)} > 0$ and $pq \mathfrak{D}e^{\theta_3(\vec{t}_0)} < w_{24} \mathfrak{D}e^{\theta_4(\vec{t}_0)}$, then $\gamma_{S,1} \in \Omega_1$, $\gamma_{S,2} \in \Omega_2$, and $\tilde{\gamma}_1 \in \Omega_4$ and $\tilde{\gamma}_2 \in \Omega_3$. One such configuration is illustrated by stars in the Figure;
- (3) If $\mathfrak{D}e^{\theta_3(\vec{t}_0)} < 0$, then $\gamma_{S,1} \in \Omega_1$, $\gamma_{S,2} \in \Omega_3$, $\tilde{\gamma}_1 \in \Omega_4$ and $\tilde{\gamma}_2 \in \Omega_2$. One such configuration is illustrated by squares in the Figure.

Again there is exactly one KP divisor point in each finite oval.

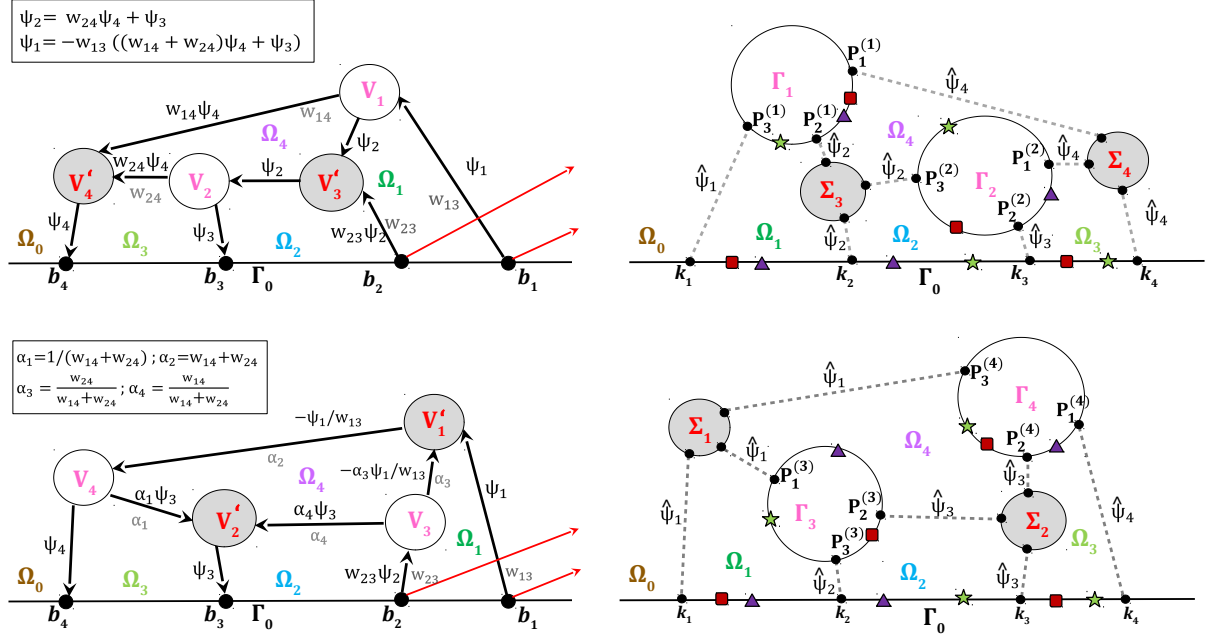


FIGURE 31. Left: \mathcal{N}_{sq-mv} [bottom] is obtained from the reduced Le-network $\mathcal{N}_{T, \text{top}}$ [top] applying a square move. Right: The partial normalization of the corresponding curves Γ_{top} [top], Γ_{sq-mv} [bottom] and the possible divisor configurations.

10. EFFECT OF THE SQUARE MOVE ON THE KP DIVISOR FOR SOLITON DATA IN $Gr^{\text{TP}}(2, 4)$

The simplest network to which the square move is applicable is the reduced Le-network $\mathcal{N}_{T, \text{top}}$ associated to soliton data in $Gr^{\text{TP}}(2, 4)$ and corresponds to the change of colour of all internal vertices. The latter transformation may be also interpreted as a self-dual transformation in $Gr^{\text{TP}}(2, 4)$.

The reduced networks and the topological models of the curves before and after the square move for soliton data in $Gr^{\text{TP}}(2, 4)$ are shown in Figure 31. In [2]-[5] we have already computed a plane curve representation and its desingularization, and discussed the divisor configurations on $\mathcal{N}_{T, \text{top}}$. The duality transformation implies that the same plane curve representation is associated both to Γ_{top} and Γ_{sq-mv} , by conveniently relabeling \mathbb{CP}^1 components from Σ_i, Γ_j to Γ_i, Σ_j (compare the topological models of curves in Figure 31).

Here we just compute the KP divisor after the square move and refer to [4] for more details on this example. The values on the dressed edge wave functions are shown in Figure 31.

By definition, the Sato divisor is not affected by the square move since the Darboux transformation is the same. Therefore the degree $k = 2$ Sato divisor $(\gamma_{S,1}, \gamma_{S,2}) = (\gamma_{S,1}(\bar{t}_0), \gamma_{S,2}(\bar{t}_0))$ is obtained solving $\zeta(\gamma_{S,1}) + \zeta(\gamma_{S,2}) = \mathbf{w}_1(\bar{t}_0)$, $\zeta(\gamma_{S,1})\zeta(\gamma_{S,2}) = -\mathbf{w}_2(\bar{t}_0)$, where the Darboux transformation $\mathcal{D} = \partial_x^2 - \mathbf{w}_1(\bar{t})\partial_x - \mathbf{w}_2(\bar{t})$ is generated by the heat hierarchy solutions $f^{(1)}(\bar{t}) = e^{\theta_1(\bar{t})} - w_{13}e^{\theta_3(\bar{t})} - w_{13}(w_{14} + w_{24})e^{\theta_4(\bar{t})}$, $f^{(2)}(\bar{t}) = e^{\theta_2(\bar{t})} + w_{23}e^{\theta_3(\bar{t})} + w_{23}w_{24}e^{\theta_4(\bar{t})}$.

On Γ_{top} , $\mathcal{D}_{KP, \Gamma} = (\gamma_{S,1}, \gamma_{S,2}, \gamma_1, \gamma_2)$ where the simple poles $\gamma_i = \gamma_i(\bar{t}_0)$ belong to the intersection of Γ_i , $i = 1, 2$, with the union of the finite ovals. In the local coordinates induced by the orientation

of $\mathcal{N}_{T,\text{top}}$, we have

$$(10.1) \quad \zeta(\gamma_1) = \frac{w_{14}\mathfrak{D}e^{\theta_4(\vec{t}_0)}}{\mathfrak{D}e^{\theta_3(\vec{t}_0)} + (w_{14} + w_{24})\mathfrak{D}e^{\theta_4(\vec{t}_0)}}, \quad \zeta(\gamma_2) = \frac{w_{24}\mathfrak{D}e^{\theta_4(\vec{t}_0)}}{\mathfrak{D}e^{\theta_3(\vec{t}_0)} + w_{24}\mathfrak{D}e^{\theta_4(\vec{t}_0)}}.$$

It is straightforward to verify that $\mathfrak{D}e^{\theta_1(\vec{t})}, \mathfrak{D}e^{\theta_4(\vec{t})} > 0$ for all \vec{t} . As observed in [2, 4], there are three possible generic configurations of the KP-II pole divisor depending on the signs of $\mathfrak{D}e^{\theta_2(\vec{t}_0)}$ and $\mathfrak{D}e^{\theta_3(\vec{t}_0)}$ (see also Figure 31 [top,right]):

- (1) If $\mathfrak{D}e^{\theta_2(\vec{t}_0)} < 0 < \mathfrak{D}e^{\theta_3(\vec{t}_0)}$, then $\gamma_{S,1} \in \Omega_1$, $\gamma_{S,2} \in \Omega_2$, $\gamma_1 \in \Omega_4$ and $\gamma_2 \in \Omega_3$. One such configuration is illustrated by triangles in the Figure;
- (2) If $\mathfrak{D}e^{\theta_2(\vec{t}_0)}, \mathfrak{D}e^{\theta_3(\vec{t}_0)} < 0$, then $\gamma_{S,1} \in \Omega_1$, $\gamma_{S,2} \in \Omega_3$, $\gamma_1 \in \Omega_4$ and $\gamma_2 \in \Omega_2$. One such configuration is illustrated by squares in the Figure;
- (3) If $\mathfrak{D}e^{\theta_3(\vec{t}_0)} < 0 < \mathfrak{D}e^{\theta_2(\vec{t}_0)}$, then $\gamma_{S,1} \in \Omega_2$, $\gamma_{S,2} \in \Omega_3$, $\gamma_1 \in \Omega_1$ and $\gamma_2 \in \Omega_4$. One such configuration is illustrated by stars in the Figure.

On $\Gamma_{\text{sq-mv}}$, $\mathcal{D}_{\text{KP},\Gamma} = (\gamma_{S,1}, \gamma_{S,2}, \gamma_3, \gamma_4)$ where the simple poles $\gamma_i = \gamma_i(\vec{t}_0)$ belong to the intersection of Γ_i , $i = 3, 4$, with the union of the finite ovals. In the local coordinates induced by the orientation of $\mathcal{N}_{\text{sq-mv}}$, we have

$$(10.2) \quad \zeta(\gamma_3) = \frac{w_{24}(\mathfrak{D}e^{\theta_3(\vec{t}_0)} + (w_{14} + w_{24})\mathfrak{D}e^{\theta_4(\vec{t}_0)})}{(w_{14} + w_{24})(\mathfrak{D}e^{\theta_3(\vec{t}_0)} + w_{24}\mathfrak{D}e^{\theta_4(\vec{t}_0)})}, \quad \zeta(\gamma_4) = \frac{(w_{14} + w_{24})\mathfrak{D}e^{\theta_4(\vec{t}_0)}}{\mathfrak{D}e^{\theta_3(\vec{t}_0)} + (w_{14} + w_{24})\mathfrak{D}e^{\theta_4(\vec{t}_0)}}.$$

The three possible generic configurations of the KP-II pole divisor after the square move are then (see also Figure 31 [bottom,right]):

- (1) If $\mathfrak{D}e^{\theta_2(\vec{t}_0)} < 0 < \mathfrak{D}e^{\theta_3(\vec{t}_0)}$, then $\gamma_{S,1} \in \Omega_1$, $\gamma_{S,2} \in \Omega_2$, $\gamma_3 \in \Omega_4$ and $\gamma_4 \in \Omega_3$. One such configuration is illustrated by triangles in the Figure;
- (2) If $\mathfrak{D}e^{\theta_2(\vec{t}_0)}, \mathfrak{D}e^{\theta_3(\vec{t}_0)} < 0$, then $\gamma_{S,1} \in \Omega_1$, $\gamma_{S,2} \in \Omega_3$, $\gamma_3 \in \Omega_2$ and $\gamma_4 \in \Omega_4$. One such configuration is illustrated by squares in the Figure;
- (3) If $\mathfrak{D}e^{\theta_3(\vec{t}_0)} < 0 < \mathfrak{D}e^{\theta_2(\vec{t}_0)}$, then $\gamma_{S,1} \in \Omega_2$, $\gamma_{S,2} \in \Omega_3$, $\gamma_3 \in \Omega_1$ and $\gamma_4 \in \Omega_4$. One such configuration is illustrated by stars in the Figure.

The transformation rule of the divisor points is in agreement with the effect of the square move discussed in Section 8. As expected, for any given $[A] \in Gr^{\text{TP}}(2, 4)$, there is exactly one KP divisor point in each finite oval. Non generic divisor configurations (squares) correspond either to $\mathfrak{D}e^{\theta_2(\vec{t}_0)} = 0$ or to $\mathfrak{D}e^{\theta_3(\vec{t}_0)} = 0$ since $\mathfrak{D}e^{\theta_2(\vec{t})} + w_{23}\mathfrak{D}e^{\theta_3(\vec{t})} < 0$, for all \vec{t} . We plan to discuss the exact definition of global parametrization in the case of non generic divisor configurations using resolution of singularities in a future publication, see also next Section 11.1 for the case $Gr^{\text{TP}}(1, 3)$.

11. GENERALIZATIONS AND OPEN PROBLEMS

The parametrization of a given positroid cell $\mathcal{S}_{\mathcal{M}}^{\text{TNN}}$ via KP-II divisors constructed in this paper, see also [5], is local in the following sense: for each point in $\mathcal{S}_{\mathcal{M}}^{\text{TNN}}$ and a collection of phases \mathcal{K} , we choose a fixed time \vec{t}_0 such that near this point the parametrization is locally regular. But globally we cannot exclude the situation in which at least two divisor points simultaneously approach the same node of the curve. In this case it is necessary to apply an appropriate blow-up procedure to resolve the singularity. We plan to study this problem in a future paper. Here in Section 11.1 we solve this problem in the simplest non-trivial case $Gr^{\text{TP}}(1, 3)$.

Another set of problems is associated to the possible appearance of null edge vectors on reducible networks. In such case the edge wave function would be identically zero for all times at

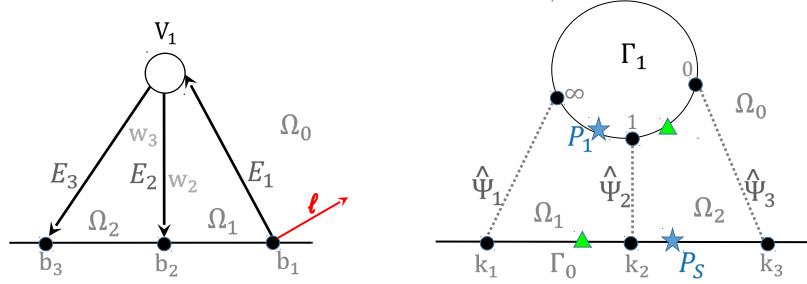


FIGURE 32. We consider the issue of the global parametrization of positroid cells via divisors in the simplest example $Gr^{TP}(1, 3)$.

some components, therefore there is no natural way to define the divisor. The first open problem is whether these null vectors can be avoided by a proper choice of the edge weights using the extra gauge freedom for reducible networks. If this is not possible, then construction presented in this paper require some modification, which we briefly outline in Section 11.2.

11.1. Global parametrization of positroid cells via KP divisors: the case $Gr^{TP}(1, 3)$.

As a case study for the global parametrization of positroid cells via divisors we take the totally positive Grassmannian $Gr^{TP}(1, 3)$. With usual affine coordinates, we have the cell parametrization $[1, w_2, w_3]$, the heat hierarchy solution $f(\vec{t}) = e^{\theta_1(\vec{t})} + w_2 e^{\theta_2(\vec{t})} + w_3 e^{\theta_3(\vec{t})}$ and the Darboux transformation $\mathfrak{D} = \partial_x - \frac{\partial_x f(\vec{t})}{f(\vec{t})}$. Then on the oriented network (Figure 32[left]) the vectors are $E_1 = E_2 + E_3$, $E_2 = (0, w_2, 0)$, $E_3 = (0, 0, w_3)$, and the edge wave function takes the values $\Psi_1(\vec{t}) = \Psi_2(\vec{t}) + \Psi_3(\vec{t})$, $\Psi_2(\vec{t}) = w_2(\kappa_2 - \gamma_S) e^{\theta_2(\vec{t})}$, $\Psi_3(\vec{t}) = w_3(\kappa_3 - \gamma_S) e^{\theta_3(\vec{t})}$, where γ_S is the coordinate of the Sato divisor point P_S . If we fix the reference time $\vec{t}_0 = \vec{0} = (0, 0, 0, \dots)$, then $\zeta(P_S) = \gamma_S = \frac{\kappa_1 + w_2 \kappa_2 + w_3 \kappa_3}{1 + w_2 + w_3}$. On the curve $\Gamma = \Gamma_0 \sqcup \Gamma_1$, at the double points the normalized KP wave function is $\hat{\Psi}_j(\vec{t}) = \frac{\Psi_j(\vec{t})}{\Psi_j(\vec{0})}$ and the divisor point $P_1 \in \Gamma_1$ has local coordinate $\zeta(P_1) = \gamma_1 = \frac{w_3(\kappa_3 - \gamma_S)}{w_3(\kappa_3 - \gamma_S) + w_2(\kappa_2 - \gamma_S)}$.

It is easy to check that the positivity of the weights is equivalent to $\gamma_S \in]\kappa_1, \kappa_3[$, $\gamma_1 > 0$ and the fact that there is exactly one divisor point in each one of the finite ovals, Ω_1 and Ω_2 , that is

- (1) Either $\kappa_1 < \gamma_S < \kappa_2$ and $\gamma_1 < 1$, i.e. $P_S \in \Omega_1$ and $P_1 \in \Omega_2$. In Figure 32 [right] we illustrate this case representing divisor points by triangles;
- (2) Or $\kappa_2 < \gamma_S < \kappa_3$ and $\gamma_1 > 1$, i.e. $P_S \in \Omega_2$ and $P_1 \in \Omega_1$. In Figure 32 [right] we illustrate this case representing divisor points by stars.

The transformation from (w_2, w_3) to (γ_S, γ_1) loses injectivity and full rank Jacobian along the line $w_3 = \frac{\kappa_2 - \kappa_1}{\kappa_3 - \kappa_2}$ so that, for any $w_2 > 0$,

$$\gamma_S(w_2, \frac{\kappa_2 - \kappa_1}{\kappa_3 - \kappa_2}) = \kappa_2, \quad \gamma_1(w_2, \frac{\kappa_2 - \kappa_1}{\kappa_3 - \kappa_2}) = 1.$$

If we invert the relation between divisor numbers and weights, we get

$$w_2(\gamma_S, \gamma_1) = \frac{(\gamma_1 - 1)(\gamma_S - \kappa_1)}{\gamma_S - \kappa_2}, \quad w_3(\gamma_S, \gamma_1) = \frac{\gamma_1(\gamma_S - \kappa_1)}{\kappa_3 - \gamma_S}.$$

Therefore in the non-generic case when $\gamma_S \rightarrow \kappa_2$ and $\gamma_1 \rightarrow 1$, we need to apply the blow-up procedure at the point $(\gamma_S, \gamma_1) = (\kappa_2, 1)$, by setting $\gamma_S = \kappa_2 + \epsilon$, $\gamma_1 = 1 + z\epsilon$ and take the limit

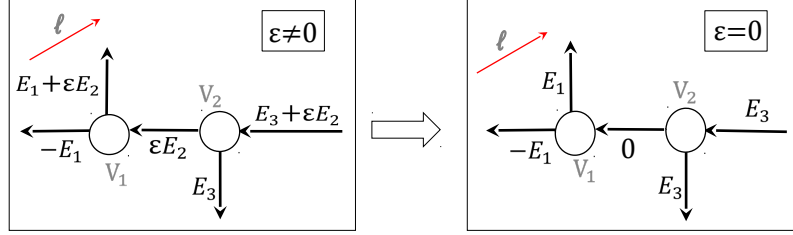


FIGURE 33. If E_1 and E_3 are proportional the edge carrying the zero vector when $\epsilon = 0$ is of type 1, otherwise of type 2.

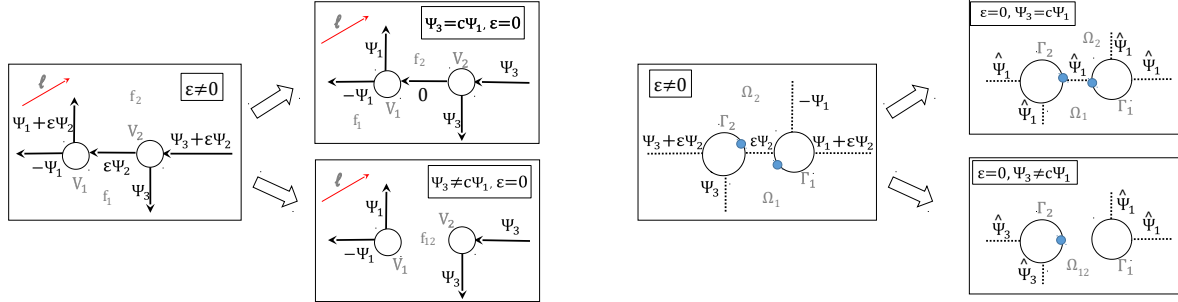


FIGURE 34. We present the construction of the divisor in case of edges carrying zero vectors in the simplest case: we show both the edge wave function Ψ on the oriented network [left] and the normalized wave function and divisor on the curve [right] and in the case of edges carrying zero vectors of type 1 [top] and type 2 [bottom].

$\epsilon \rightarrow 0$, so that

$$w_2(\kappa_2, 1) = z(\kappa_2 - \kappa_1), \quad w_3(\kappa_2, 1) = \frac{\kappa_2 - \kappa_1}{\kappa_3 - \kappa_2}.$$

11.2. Construction of the divisor in the case of zero edge vectors. We now discuss the modification of the technical construction in case of zero edge vectors on a simple example. In Definition 11.2.1 (see also Figure 33) edges carrying zero vectors are classified of type 1 and 2 depending on the properties of the non-zero edge vectors on the edges adjacent to them. Without loss of generality, in the following we assume that all vertices belonging to a given maximal connected subgraph carrying zero vectors are trivalent.

Definition 11.2.1. Zero edge vectors of type 1 and type 2 Let the PBDTP network $(\mathcal{N}, \mathcal{O}, \mathbb{I})$ of graph \mathcal{G} represent a point in the irreducible positroid cell $\mathcal{S}_{\mathcal{M}}^{\text{TNN}}$. Let $\mathcal{G}_0 \subset \mathcal{G}$ be a connected maximal subgraph carrying zero edge vectors, i.e. such that every edge belonging to \mathcal{G}_0 carries a zero vector and all edges belonging to its complement and having a vertex in common with \mathcal{G}_0 carry non zero vectors.

We say that the edges in \mathcal{G}_0 are of type 1 if there exists a vector E such that $E_f = c_f E$ for any edge $f \in \mathcal{G} \setminus \mathcal{G}_0$ having a vertex in common with \mathcal{G}_0 , for some $c_f \neq 0$. Otherwise we say that the edges in \mathcal{G}_0 are of type 2.

If the network carries only zero vectors of type 1 the construction of the divisor and the KP wave function can be carried out as above. On the contrary, in case of zero vectors of type 2

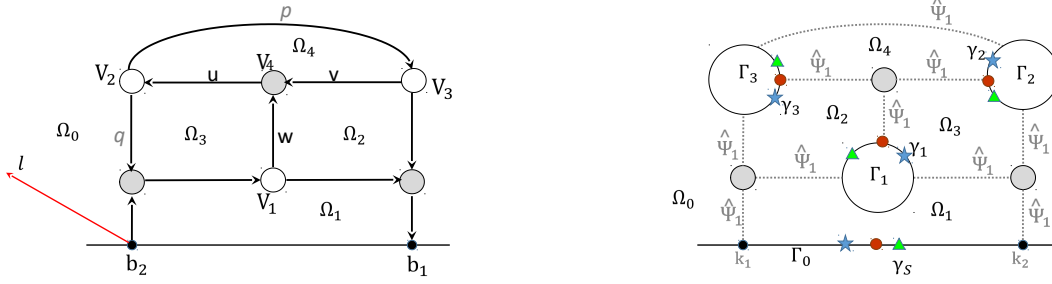


FIGURE 35. Left: the network possesses zero edge vectors E_u, E_v and E_w when $p = q$ [left]. Right: the KP divisor on the curve in the case $q < p$ (stars), $q = p$ (balls) and $q > p$ (triangles), where γ_S is the Sato divisor point.

we need to modify the network and the curve to carry out the construction of a divisor and meromorphic wave function for the given soliton data. We plan to discuss thoroughly this issue in a future publication and below we sketch the construction in both cases.

KP wave function and divisor for soliton data associated to a network with zero vectors of type 1: If the zero edge vectors are just of type 1, then the normalized wave function takes the same value at all edges adjacent to \mathcal{G}_0 . Then we simply extend analytically the normalized KP wave function to the components of Γ associated to \mathcal{G}_0 , by attributing such value of the normalized KP wave function also at the edges carrying zero vectors. Since the resulting wave function is regular and constant with respect to the spectral parameter on all components associated to \mathcal{G}_0 , the position of the divisor point on components corresponding to trivalent white vertices carrying zero vectors is completely irrelevant: we just attribute a divisor point to each component corresponding to a trivalent white vertex carrying zero vectors using the counting rule established in [3]. The resulting divisor is real and contained in the union of all the ovals. Finally, in this case it is always possible to attribute exactly one divisor point in each finite oval and no divisor point in the infinite oval in all cases of connected maximal subgraphs carrying zero edge vectors of type one.

In the simplest case \mathcal{G}_0 consists of one edge and two trivalent white vertices (see Figure 34, case $\epsilon = 0$ and $\Psi_3 = c\Psi_1$, $c \neq 0$). In such case, the edge (V_2, V_1) necessarily bounds two distinct faces, f_1 and f_2 , the network divisor numbers at the vertices V_1 and V_2 coincide with the coordinates of the corresponding points on the components Γ_1 and Γ_2 and the divisor points on Γ are trivial by definition. Then we may use the counting rule to attribute exactly one divisor point to each one of the corresponding ovals Ω_1 and Ω_2 .

A more complicated example is the network in Figure 35 [left] which represents the point $[a, 1] \in Gr^{\text{TP}}(1, 2)$, with $a = (2p + 1)/(1 + p + q)$ and possesses zero vectors $u = v = w = (0, 0)$ if $a = 1$ ($p = q$). The Sato divisor point $\gamma_S = \frac{a\kappa_1 + \kappa_2}{a+1}$ belongs to the intersection of the oval Ω_1 and the Sato component Γ_0 . The remaining divisor numbers are $\gamma_1 = \frac{1}{a}$, $\gamma_2 = 1 + \frac{aq}{a-1}$ and $\gamma_3 = \frac{a-1}{a-2}$, where, thanks to the extra gauge freedom for reducible networks, the divisor for fixed $[a, 1]$ depends on the choice of the parameter q . In Figure 35[right], we show the possible divisor configurations using the convention that no divisor point is attributed to black vertices in case of zero vectors: if $a = 1$, the divisor is represented by balls in Figure 35 [right]), whereas

- (1) $\gamma_1 \in \Gamma_1 \cap \Omega_3$, $\gamma_2 \in \Gamma_2 \cap \Omega_4$ and $\gamma_3 \in \Gamma_3 \cap \Omega_2$, if $0 < a < 1$ ($0 < p < q$). We represent one such configuration with stars in Figure 35 [right];
- (2) $\gamma_1 \in \Gamma_1 \cap \Omega_2$, $\gamma_2 \in \Gamma_2 \cap \Omega_3$ and $\gamma_3 \in \Gamma_3 \cap \Omega_4$ if $a > 1$ ($0 < q < p$). We represent one such configuration with triangles in Figure 35 [right].

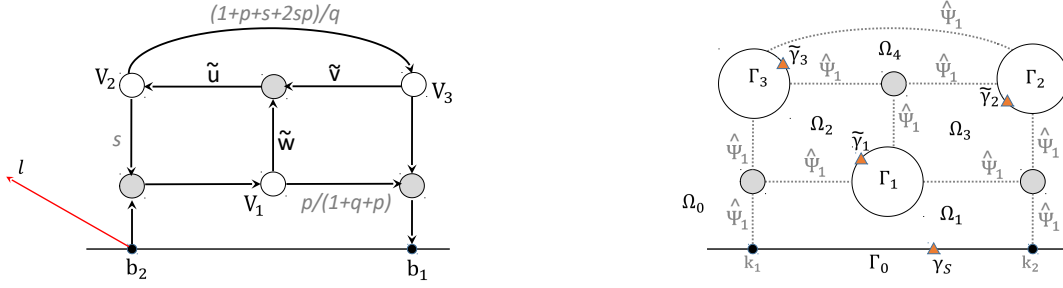


FIGURE 36. Left: the elimination of zero edge vectors for the example of Figure 35 using the gauge freedom for unreduced graphs. Right: the KP divisor on the curve for the gauged network.

Remark 11.2.1. Elimination of zero vectors using the gauge freedom for unreduced graphs The gauge freedom for unreduced graphs of Remark 2.3.2 acts untrivially on network divisor numbers and we conjecture that such gauge may be used to eliminate zero vectors. Indeed, for any fixed $s > 0$, the network in Figure 36[left] represents the same point $[a, 1] \in Gr^{TP}(1, 2)$, $a = (2p + 1)/(1 + p + q)$ as before, but it never possesses zero edge vectors (see also [7]). The divisor is $(\gamma_s, \tilde{\gamma}_1 = \frac{p}{1+2p}, \tilde{\gamma}_2 = 1 + s \frac{1+2p}{1+p}, \tilde{\gamma}_3 = \frac{(1+p)a}{(1+p)a-2p-1})$ and again it depends on the choice of the parameters p, q, s for given a .

Construction of the wave function and divisor for soliton data associated to a network carrying zero vectors of type 2: In this case, the graph (and the curve Γ) must be modified eliminating all edges of type 2 since the normalized wave function takes different values at the edges adjacent to \mathcal{G}_0 . Since the number of faces decreases, also some trivial divisor points must be eliminated in order to keep the degree of the divisor consistent with the genus of the curve. We claim that the final divisor is real, contained in the union of all the ovals and it is always possible to attribute exactly one divisor point in each finite oval and no divisor point in the infinite oval in this case too. In the simplest example (see Figure 34, case $\epsilon = 0$ and $\Psi_3 \neq c\Psi_1$, $c \neq 0$), \mathcal{G}_0 contains only one edge, two trivalent white vertices and bounds two distinct faces, f_1 and f_2 . The network divisor numbers at the vertices V_1 and V_2 coincide with the coordinates of the corresponding points on the components Γ_1 and Γ_2 and the divisor points on Γ are trivial by definition. Contrary to the case of zero edge vectors of type 1, we cannot extend analytically the wave function to include the edge carrying the zero vector. Therefore we eliminate such edge from the network and we merge the two faces f_1, f_2 into a single one f_{12} eliminating the corresponding double point and face from Γ . We also eliminate one divisor point so to have only one divisor point in the face Ω_{12} : for instance we eliminate the divisor point on Γ_1 and keep that on Γ_2 in the Figure, but we could also do the opposite.

REFERENCES

- [1] S. Abenda, *On a family of KP multi-line solitons associated to rational degenerations of real hyperelliptic curves and to the finite non-periodic Toda hierarchy*, J.Geom.Phys. **119** (2017) 112–138.
- [2] S. Abenda, *On some properties of KP-II soliton divisors in $Gr^{TP}(2, 4)$* , Ric. Mat. **68**, Issue 1, (2019), 75–90
- [3] S. Abenda, P.G. Grinevich, *Rational degenerations of M-curves, totally positive Grassmannians and KP-solitons*, Commun. Math. Phys. **361** Issue 3 (2018) 1029–1081.
- [4] S. Abenda, P.G. Grinevich *Real soliton lattices of the Kadomtsev-Petviashvili II equation and desingularization of spectral curves corresponding to $Gr^{TP}(2, 4)$* . (Russian) English version published in Proc. Steklov Inst. Math. **302** (2018), no. 1, 1–15. Tr. Mat. Inst. Steklova **302** (2018), Topologiya i Fizika, 7–22.

- [5] S. Abenda, P.G. Grinevich, *Reducible M -curves for Le -networks in the totally-nonnegative Grassmannian and KP -II multilines solitons*, Sel. Math. New Ser. **25**, no. 3 (2019) 25:43.
- [6] S. Abenda, P.G. Grinevich, *KP theory, plabic networks in the disk and rational degenerations of M -curves*, arXiv:1801.00208.
- [7] S. Abenda, P.G. Grinevich, *Edge vectors on plabic networks in the disk and amalgamation of totally non-negative Grassmannians*, arXiv:1908.07437.
- [8] Affolter, N., M. Glick, P. Pylyavskyy, and S. Ramassamy, *Vector-relation configurations and plabic graphs* arXiv:1908.06959v1.
- [9] E. Arbarello, M. Cornalba, P.A. Griffiths, *Geometry of algebraic curves. Volume II. With a contribution by Joseph Daniel Harris*, Grundlehren der Mathematischen Wissenschaften 268, Springer, Heidelberg, (2011) xxx+963 pp.
- [10] N. Arkani-Hamed, J.L. Bourjaily, F. Cachazo, A.B. Goncharov, A. Postnikov, J. Trnka, *Scattering Amplitudes and the Positive Grassmannian*, arXiv:1212.5605.
- [11] N. Arkani-Hamed, J.L. Bourjaily, F. Cachazo, A.B. Goncharov, A. Postnikov, J. Trnka, *Grassmannian geometry of scattering amplitudes*, Cambridge University Press, Cambridge, (2016), ix+194 pp.
- [12] M. Atiyah, M. Dunajski, L.J. Mason, *Twistor theory at fifty: from contour integrals to twistor strings*, Proc. A. **473** (2017), 20170530, 33 pp.
- [13] G. Biondini, Yu. Kodama, *On a family of solutions of the Kadomtsev-Petviashvili equation which also satisfy the Toda lattice hierarchy*, Journal of Phys. A: Math. Gen. **36** (2003) 10519–10536.
- [14] M. Boiti, F. Pempinelli, A.K. Pogrebkov, B. Prinari, *Towards an inverse scattering theory for non-decaying potentials of the heat equation*, Inverse Problems **17** (2001) 937–957.
- [15] V. Buchstaber, A. Glutsyuk, *Total positivity, Grassmannian and modified Bessel functions*, arXiv:1708.02154.
- [16] S. Chakravarty, Y. Kodama, *Soliton solutions of the KP equation and application to shallow water waves*. Stud. Appl. Math. **123** (2009) 83–151.
- [17] S. Corteel, L.K. Williams, *Tableaux combinatorics for the asymmetric exclusion process*, Adv. in Appl. Math. **39** (3) (2007) 293–310.
- [18] L.A. Dickey, *Soliton equations and Hamiltonian systems*. Second edition. Advanced Series in Mathematical Physics, 26. World Scientific Publishing Co., Inc., River Edge, NJ, 2003. xii+408 pp.
- [19] A. Dimakis, F. Müller-Hoissen, *KP line solitons and Tamari lattices*, J. Phys. A **44** (2011), no. 2, 025203, 49 pp.
- [20] B.A. Dubrovin, *Theta functions and non-linear equations*, Russian Math. Surveys, **36**:2 (1981), 11–92.
- [21] B.A. Dubrovin, I.M. Krichever, S.P. Novikov, *Integrable systems*. Dynamical systems, IV, 177–332, Encyclopaedia Math. Sci., 4, Springer, Berlin, (2001).
- [22] B. A. Dubrovin, S.M. Natanzon, *Real theta-function solutions of the Kadomtsev-Petviashvili equation*. Izv. Akad. Nauk SSSR Ser. Mat. **52** (1988) 267–286.
- [23] V. Fock, A. Goncharov, *Moduli spaces of local systems and higher Teichmüller theory*, Publ. Math. I.H.E.S. **103** (2006), 1–211.
- [24] V.V. Fock, A. B. Goncharov, *Cluster \mathcal{X} -Varieties, Amalgamation and Poisson-Lie Groups*, in Algebraic Geometry and Number Theory, dedicated to Drinfeld’s 50th birthday, pp. 27–68, Progr. Math. **253**, Birkhauser, Boston, (2006)
- [25] S. Fomin. *Loop-erased walks and total positivity*, Transactions of the AMS, **353**:9 (2001), 3563–3583.
- [26] S. Fomin, P. Pylyavskyy, E. Shustin, *Morsifications and mutations*, arXiv:1711.10598 (2017).
- [27] S. Fomin, A. Zelevinsky, *Double Bruhat cells and total positivity*. J. Amer. Math. Soc. **12** (1999) 335–380.
- [28] S. Fomin, A. Zelevinsky, *Cluster algebras I: foundations*. J. Am. Math. Soc. **15** (2002) 497–529.
- [29] N.C. Freeman, J.J.C. Nimmo, *Soliton solutions of the Korteweg de Vries and the Kadomtsev-Petviashvili equations: the Wronskian technique*, Proc. R. Soc. Lond. A **389** (1983), 319–329.
- [30] F.R. Gantmacher, M.G. Krein, *Sur les matrices oscillatoires*. C.R. Acad. Sci. Paris **201** (1935) 577–579.
- [31] F.R. Gantmacher, M.G. Krein, *Oscillation Matrices and Kernels and Small Vibrations of Mechanical Systems*. (Russian), Gostekhizdat, Moscow- Leningrad, (1941), second edition (1950); German transl. as Oszillationsmatrizen, Oszillationskerne und kleine Schwingungen mechanischer Systeme, Akademie Verlag, Berlin, (1960); English transl. as Oscillation Matrices and Kernels and Small Vibrations of Mechanical Systems, USAEC, (1961), and also a revised English edition from AMS Chelsea Publ., (2002).
- [32] Gekhtman, M., M. Shapiro, and A. Vainshtein, *Cluster algebras and Poisson geometry*. Mathematical Surveys and Monographs, 167. American Mathematical Society, Providence, RI, (2010), xvi+246 pp.
- [33] I. M. Gel’fand, R. M. Goresky, R. D. MacPherson, V. V. Serganova, *Combinatorial geometries, convex polyhedra, and Schubert cells*. Adv. in Math. **63** (1987), no. 3, 301–316.

- [34] I.M. Gel'fand and V.V. Serganova, *Combinatorial geometries and torus strata on homogeneous compact manifolds*. Russian Mathematical Surveys, **42** (1987), no. 2, 133–168.
- [35] A.B. Goncharov, R. Kenyon, *Dimers and cluster integrable systems*, Ann. Sci. Éc. Norm. Supér. (4) **46** (2013), no. 5, 747–813.
- [36] A. Harnack, *Über die Vieltheiligkeit der ebenen algebraischen Curven*. Math. Ann. **10** (1876) 189–199.
- [37] R. Hirota, *The direct method in soliton theory*. Cambridge Tracts in Mathematics, 155. Cambridge University Press, Cambridge, 2004. xii+200 pp.
- [38] B.B. Kadomtsev, V.I. Petviashvili, *On the stability of solitary waves in weakly dispersive media*, Sov. Phys. Dokl. **15** (1970) 539–541.
- [39] S. Karlin, *Total Positivity, Vol. 1*. Stanford, 1968.
- [40] Y. Kodama, L.K. Williams, *The Deodhar decomposition of the Grassmannian and the regularity of KP solitons*. Adv. Math. **244** (2013) 979–1032.
- [41] Y. Kodama, L.K. Williams, *KP solitons and total positivity for the Grassmannian*. Invent. Math. **198** (2014) 637–699.
- [42] Yuji Kodama, Yuancheng Xie, *Space curves and solitons of the KP hierarchy: I. The l -th generalized KdV hierarchy*, arXiv:1912.06768 .
- [43] I.M. Krichever, *An algebraic-geometric construction of the Zakharov-Shabat equations and their periodic solutions*. (Russian) Dokl. Akad. Nauk SSSR **227** (1976) 291–294.
- [44] I.M. Krichever, *Integration of nonlinear equations by the methods of algebraic geometry*. (Russian) Funkcional. Anal. i Prilozhen. **11** (1977) 15–31, 96.
- [45] I.M. Krichever, *Spectral theory of finite-zone nonstationary Schrödinger operators. A nonstationary Peierls model*, Functional Analysis and Its Applications, **20:3** (1986), 203–214.
- [46] I.M. Krichever, *Spectral theory of two-dimensional periodic operators and its applications*, Russian Math. Surveys, **44:8** (1989), 146–225
- [47] I.M. Krichever, *The τ -function of the universal Whitham hierarchy, matrix models and topological field theories*, Comm. Pure Appl. Math., **47** (1994), 437–475.
- [48] I.M. Krichever, K.L. Vaninsky, *The periodic and open Toda lattice*, AMS/IP Stud. Adv. Math., **33**, Amer. Math. Soc., Providence, RI, (2002), 139–158.
- [49] T. Lam, *Dimers, webs, and positroids*, J. Lond. Math. Soc. (2) **92** (2015), no. 3, 633–656.
- [50] T. Lam, *Totally nonnegative Grassmannian and Grassmann polytopes*, Current developments in mathematics 2014, 51–152, Int. Press, Somerville, MA, (2016).
- [51] G. Lawler, *Intersections of random walks*, Birkhäuser, (1991).
- [52] G. Lusztig, *Total positivity in reductive groups*, Lie Theory and Geometry: in honor of B. Kostant, Progress in Mathematics **123**, Birkhäuser, Boston, (1994), 531–568.
- [53] G. Lusztig, *Total positivity in partial flag manifolds*, Representation Theory, **2** (1998), 70–78.
- [54] T.M. Malanyuk, *A class of exact solutions of the Kadomtsev-Petviashvili equation*. Russian Math. Surveys, **46:3** (1991), 225–227.
- [55] V.B. Matveev, *Some comments on the rational solutions of the Zakharov-Schabat equations*. Letters in Mathematical Physics, **3** (1979), 503–512.
- [56] T. Miwa, M. Jimbo, E. Date, *Solitons. Differential equations, symmetries and infinite-dimensional algebras*. Cambridge Tracts in Mathematics, 135. Cambridge University Press, Cambridge, 2000. x+108 pp.
- [57] A. Nakayashiki, *On Reducible Degeneration of Hyperelliptic Curves and Soliton Solutions*, SIGMA, **15** (2019), 009, 18 pages.
- [58] S.M. Natanzon, *Moduli of real algebraic surfaces, and their superanalogues. Differentials, spinors, and Jacobians of real curves*, Russian Mathematical Surveys, **54:6** (1999), 1091–1147.
- [59] S.P. Novikov, *The periodic problem for the Korteweg-de Vries equation*, Functional Analysis and Its Applications, **8:3** (1974), 236–246.
- [60] S. Oh, A. Postnikov, D.E. Speyer, *Weak separation and plabic graphs*, Proc. Lond. Math. Soc. (3) **110** (2015), no. 3, 721–754.
- [61] A. Postnikov, *Total positivity, Grassmannians, and networks*, arXiv:math/0609764 [math.CO].
- [62] A. Postnikov, *Positive Grassmannian and polyhedral subdivisions*, arXiv:1806.05307.
- [63] A. Postnikov, D. Speyer, L. Williams, *Matching polytopes, toric geometry, and the totally non-negative Grassmannian*. J. Algebraic Combin. **30** (2009), no. 2, 173–191.
- [64] M. Sato, *Soliton equations as dynamical systems on infinite-dimensional Grassmann manifold*. in: Nonlinear PDEs in Applied Sciences (US-Japan Seminar, Tokyo), P. Lax and H. Fujita eds., North-Holland, Amsterdam (1982) 259–271.

- [65] I. Schoenberg, *Über variationsvermindende lineare Transformationen*, Math. Zeit. **32**, (1930), 321-328.
- [66] J.S. Scott, *Grassmannians and cluster algebras*, Proc. London Math. Soc. **92** (2006), 345-380.
- [67] I.A. Taimanov, *Singular spectral curves in finite-gap integration*, Russian Mathematical Surveys, **66**:1 (2011), 107-144.
- [68] K. Talaska, *A Formula for Plücker Coordinates Associated with a Planar Network*, IMRN, **2008**, (2008), Article ID rnn081, 19 pages.
- [69] O. Ya. Viro, *Real plane algebraic curves: constructions with controlled topology* Leningrad Math. J. **1** (1990), no. 5, 1059-1134.
- [70] V.E. Zakharov, A. B. Shabat, *A scheme for integrating the nonlinear equations of mathematical physics by the method of the inverse scattering problem. I*, Funct. Anal. and Its Appl., **8** (1974), Issue 3, 226-235.

DIPARTIMENTO DI MATEMATICA, UNIVERSITÀ DI BOLOGNA, P.ZZA DI PORTA SAN DONATO 5, I-40126 BOLOGNA BO, ITALY

E-mail address: `simonetta.abenda@unibo.it`

STEKLOV MATHEMATICAL INSTITUTE OF RUSSIAN ACADEMY OF SCIENCES, 8 GUBKINA ST., MOSCOW, 199911, RUSSIA, AND L.D. LANDAU INSTITUTE FOR THEORETICAL PHYSICS, PR. AKADEMIKA SEMENOVA 1A, CHERNOGOLOVKA, 142432, RUSSIA, AND LOMONOSOV MOSCOW STATE UNIVERSITY, FACULTY OF MECHANICS AND MATHEMATICS, 1 LENINSKIYE GORY, MAIN BUILDING 119991, MOSCOW, GSP-1, RUSSIA.

E-mail address: `gg@landau.ac.ru`